Deltares

The long-term morphological response to sea level rise and different sediment strategies in the Western Scheldt estuary (The Netherlands)



The long-term morphological response to sea level rise and different sediment strategies in the Western Scheldt estuary (The Netherlands)

Authors
Björn R. Röbke
Hesham Elmilady
Mick van der Wegen
Marcel Taal

Partners
–

The long-term morphological response to sea level rise and different sediment strategies in the Western Scheldt estuary (The Netherlands)

Client	
Contact	Marcel Taal
Reference	1210301-009-ZKS-0009
Keywords	Sea level rise, dredging and dumping, beach nourishments, sediment budget, long-term morphodynamics, Western Scheldt, Flemish coast, Delft3D version 4.0

Document control	
Version	1.0
Date	2020-12-22
Project number	1210301-009
Document ID	–
Pages	100
Status	final

Author(s)		
	B.R. Röbke	Deltares

Doc. version	Author	Reviewer	Approver	Publish
1.0	B.R. Röbke	Z.B. Wang	T. Segeren	Deltares

Executive summary

The objective of this study is to gain insight into the relative impact of (extreme) sea level rise (SLR) and different sediment strategies, i.e. dredging and dumping and beach nourishments, on the hydro- and morphodynamic behaviour of the Western Scheldt estuary (The Netherlands) till the end of the 21st century. For this, a process-based numerical morphodynamic model (Delft3D version 4) is applied that accounts for continuously changing hydrodynamic boundary conditions associated with SLR as well as for different dredging and dumping strategies and beach nourishments.

The scenario simulation results for the period 2020–2100 indicate that both, SLR and the sediment strategies have a significant impact on the bed levels and on the sediment budget of the estuary. While increasing SLR causes an increasing sediment export from the Western Scheldt towards the mouth/sea, the sediment loss can be reduced by dumping a larger portion of dredged material in the more upstream parts of the estuary and by performing beach nourishments in the mouth area. This is an important finding with regard to the future management of the Western Scheldt estuary.

The increasing sediment export with SLR coincides with a significant decrease of the maximum flood flow velocities in the channels, which is larger than the decrease in the maximum ebb flow velocities, resulting in an increasing seaward residual sediment transport with SLR. Changes in the resonant behaviour by increasing the mean water depth and the resonance length of the Scheldt river with SLR is believed to have an important impact on the sediment budget of the estuary.

A morphological hindcast performed with the model of the current study, extensive sensitivity analyses as well as comparable results found in earlier studies support the robustness of our findings. Future work may explain in more detail the processes responsible for the indicated hydro- and morphodynamic effects of SLR. These include SLR studies investigating the role of the intertidal area and of the mud dynamics in more detail.

Uitgebreide Nederlandse samenvatting

Achtergrond en doel van het onderzoek
Nederland en Vlaanderen werken samen in beleid, beheer en kennisontwikkeling over het Schelde-estuarium en hebben dit vastgelegd in verdragen. Vastgesteld is dat er nog te weinig inzicht is in de reactie van het Schelde-estuarium op (versnelde en extreme) zeespiegelstijging. Als eerste stap om de onzekerheden hierom te verminderen heeft de Vlaamse overheid aan Deltares gevraagd een quick scan uit te voeren naar de effecten van extreme zeespiegelstijging in het Schelde-estuarium tot 2100. De opdracht is om niet alleen het effect van een veranderende zeespiegel, maar ook het effect van verschillende vormen van morfologisch beheer (baggeren, storten, kustsuppleties) te bestuderen. De enige methode om dit systematisch te onderzoeken is met numerieke modellen. Tegenwoordig is er de rekenkracht om dit goed te doen.

Aanpak
Er is iteratief en systematisch gewerkt. Vanwege de vraag om een quick scan is met een bestaand en goed gecalibreerd model voor het hele estuarium gestart. In een later stadium is een hindcast over 48 jaar uitgevoerd, waarbij de instellingen zijn gecontroleerd op gevoeligheid. De reproductie van de waterbeweging en sediment voorraden was goed en de reproductie van de grootschalige morfologische ontwikkeling was voldoende. Dit geeft vertrouwen voor het gebruik van het model voor uitspraken over de effecten van zeespiegelstijging en veranderingen in morfologisch beheer.

De opgave is een geleidelijke stijging van de zeespiegel te bestuderen en hoe verschillende vormen van morfologisch beheer samen daarmee de ontwikkeling van het estuarium bepaalt. Gekeken is naar verschillende snelheden van zeespiegelstijging (richtjaar 2100) en hoe de stijging verloopt (lineair of met toenemende snelheid). Om de invloed van het sedimentbeheer te onderzoeken (onder elk van de zeespiegelscenario's) zijn simulaties uitgevoerd waarin het kustbeheer (suppleties) of de stortstrategie in de Westerschelde varieerden. Onderhoudsstrategieën voor de Zeeschelde zijn niet onderzocht. Voor dit deel van het estuarium en deze vraagstelling zijn geen goede morfologische modellen beschikbaar.

Om goed aan te sluiten bij de mondiale scenario's van klimaatverandering zijn toekomstige waterstanden bij verschillende scenario's van zeespiegelstijging afgeleid van een mondiaal model. Zo wordt rekening gehouden met de verschillen in stijging van de zeespiegel tussen de Noordzee en het mondiale gemiddelde. De stijging in de Noordzee is kleiner zo lang als het afsmelten van het landijs op Antarctica een beperkte bijdrage geeft (huidige situatie). De zeespiegel in de Noordzee zal echter juist sneller stijgen als Antarctica de grootste bijdrage gaat leveren aan de zeespiegelstijging.

Het systematische karakter van het onderzoek betekende dat een groot aantal scenario's is onderzocht. Door steeds resultaten naast elkaar te leggen waarbij maar één aspect (snelheid van zeespiegelstijging of wijze van sedimentbeheer) verschilde kunnen uitspraken gedaan worden over de effecten zeespiegelstijging, ook in combinatie met strategieën voor sedimentbeheer van kust en estuarium. De analyse richt zich op de eindtoestand van het estuarium in 2100 en niet op het traject er naar toe.

Tijdens het onderzoek is niet alleen gekeken naar verschillende scenario's van zeespiegelstijging en sedimentbeheer (hier: stortstrategieën en strandsuppleties), maar ook naar de invloed van de complexiteit van het numerieke model. Het gaat hierbij in het bijzonder om het wel of niet meenemen van de invloed van golven en slib op het mor-

fologische gedrag van het estuarium. Of de effecten van golven en slib meegenomen moeten worden hangt af van het type te beantwoorden vragen. Golven en slib zijn van belang om uitspraken te doen over de evolutie van intergetijdengebieden. Ze zijn minder belangrijk voor de evolutie van de grootschalige waterbeweging, waaronder de verandering van het hoogwaterniveau en de getijslag.

Hypothesen en onderzoeksresultaten over het lange termijn gedrag van het estuarium

De kennis die het onderzoek heeft opgeleverd wordt gepresenteerd in drie delen. De zekerheid waarmee conclusies kunnen worden getrokken is daarin niet hetzelfde en neemt af in de volgorde (i) waterbeweging, (ii) sedimentvoorraden en (iii) bodemligging.

Voor de lange termijn evolutie is de relatie tussen veranderingen in de sedimentvoorraden en de getijslag van bijzonder belang. De getijslag is toegenomen in de afgelopen eeuwen en het is een indicator voor de mate waarin de zee binnendringt. De relatie tussen sedimentvoorraden en getijslag is uitvoerig beschreven in verschillende rapporten voor de Vlaams-Nederlandse Scheldecommissie (VNSC). Gerefereerd wordt in het bijzonder naar het syntheserapport van het V&T-onderzoek (Consortium Deltares-IMDC-Svašek-Arcadis (2013), Synthese en conceptueel model (G-13); beschikbaar via https://www.vnsc.eu/uploads/2014/02/g-13-synthese-en-conceptueelmodel-v2-0.pdf).

Waterbeweging

De bestaande kennis doet verwachten dat de hoogwaterstand in het estuarium de veranderingen op zee zal volgen. Deze theorie geldt voor waterstandvariaties als gevolg van de getijbeweging en niet tijdens een individuele storm. De theorie is bevestigd met de modelresultaten. De hoogwaterstanden stijgen langs het gehele estuarium vrijwel lineair mee met de zeespiegel. Hier bovenop is er nog een extra toename door getijslag. Die is verwaarloosbaar bij Vlissingen, maar niet meer verderop in het estuarium. Er is 0,25 m extra stijging van het hoog water bij Schelle in het meest extreme scenario van 3 m zeespiegelstijging.

De laagwaterstanden stijgen ook mee met de zeespiegel, maar minder sterk. Dit volgt ook uit de bestaande theorie. Ook hier is er een extra effect in stroomopwaartse richting. Het laagwater stijgt op de Zeeschelde nog iets minder mee met de zeespiegel. Dit is de belangrijkste component in het toenemen van de getijslag. De extra toename van de getijslag nabij Schelle ten opzichte van Vlissingen is bijna 1 m, bij het meest extreme scenario van 3 m zeespiegelstijging. De toename van de getijslag kan verklaard worden via de toegenomen waterdiepte. De lengte van het systeem benadert nu de resonantielengte.

Uit het modelonderzoek blijkt dat met een andere verdeling van baggerspecie of meer kustsuppleties nauwelijks invloed op de waterstanden in het estuarium kan worden bereikt in een situatie met sterke zeespiegelstijging. Belangrijke wijzigingen in de verdeling van sediment in de langsrichting van de Westerschelde (zie hieronder) hebben dan ook geen significant effect op de getijslag. Ook dit sluit aan bij bestaande hypothesen en proceskennis. De toename in waterdiepte is, zeker bij de extremere zeespiegelstijging, zo groot dat een andere herverdeling van sediment binnen het estuarium nauwelijks significant meer is. Dit is een belangrijk verschil met de situatie van de laatste vijftig jaar. In die periode heeft het sedimentbeheer sterke invloed gehad op de gemiddelde diepte van de geulen, in het bijzonder in het gedeelte stroomopwaarts van Hansweert. Dit leidde tot toename van de amplificatie van de getijslag.

Residueel transport en getijasymmetrie
De scenario's laten zien dat bij zeespiegelstijging het estuarium meer sediment exporteert (als zeewaartse begrenzing is hierbij de lijn Vlissingen-Breskens gehanteerd). De Westerschelde is nu vloed-dominant en dat neemt af bij zeespiegelstijging, vooral in de westelijke delen. Dit wordt verklaard doordat de maximum snelheden tijdens vloed sterker afnemen dan tijdens eb, waardoor de residuale sedimenttransport richting zee sterker wordt.

Sedimentvoorraden
Het estuarium heeft in de afgelopen eeuwen veel sediment verloren, wat een belangrijke oorzaak is geweest van de toename in getijslag. De oorzaak van de afname ligt zowel in een langjarige ontwikkeling, die waarschijnlijk samenhangt met ingrepen en gebeurtenissen uit het verdere verleden (doorbraak Honte-Zeeschelde, bedijkingen, inundaties), de stortstrategie en de zandwinning in de afgelopen halve eeuw. Het behoud van sediment in het estuarium is een doelstelling die onder de VNSC is afgesproken.

Het staat vast dat op dit moment de menselijke invloed op de netto transporten van sediment veel groter is dan de invloed van de huidige zeespiegelstijging. Sedimentbalansen berekenen een netto transport over de grens Vlissingen-Breskens in de orde van $1 * 10^6$ m^3 per jaar of minder. Het netto transport door baggeren en storten kan daarentegen oplopen tot het tienvoudige, zijnde het jaarlijkse baggerbezwaar. De stortstrategie is dan ook een dominante factor geweest in de evolutie van het estuarium tot nu toe. Bij een grotere zeespiegelstijging wordt de invloed ervan op de netto sedimenttransporten ook groter.

Het estuarium is de afgelopen eeuwen dieper geworden. Die diepte zal toenemen door zeespiegelstijging, wat ook geldt voor de monding. De resultaten van alle scenario's laten consequent zien dat er meer netto transport vanuit de Westerschelde naar zee optreedt. De scenariostudies suggereren dat dit sediment in het mondingsgebied terechtkomt. Op de omvang van dit netto transport kan het sedimentbeheer wel invloed uitoefenen. Zowel zandsuppleties in het aanliggende kustgebied als een strategie waarbij meer gestort wordt in het oosten van het estuarium leiden tot minder export voorbij de lijn Vlissingen-Breskens. Ook is te zien dat het behoud van sediment in het oostelijke deel de toenemende verdieping van dat deel vermindert.

De toename van de export van sediment bij (snellere) zeespiegelstijging is niet alleen een zeer consistent resultaat in de modelresultaten van dit project, maar volgde ook uit eerdere studies met een semi-empirisch model gebaseerd op morfologisch evenwicht (ESTMORF).

Bodemligging
De (versnelde) zeespiegelstijging doet de gemiddelde diepte van het estuarium toenemen. De verwachting is dat hierdoor ook de morfologie van het estuarium verandert, omdat geulen en platen zich hieraan aanpassen. De huidige hypothese is dat de stortstrategie significante invloed uitoefent op de morfologie van geulen en platen. Die invloed van de stortstrategie over 80 jaar is modelmatig niet te reproduceren. Hiervoor moeten andere instrumenten worden ingezet.

Wat wel onderzocht kan worden is de invloed van sedimentbeheer en zeespiegel op de 'gemiddelde' morfologie van het estuarium. Dat kan bereikt worden door te kijken naar de hypsometrische curve. Hieruit komen enkele interessante observaties. De hypsometrische curves zijn ook gemaakt voor de simulaties met en zonder slib. De

resultaten laten zien dat de veranderingen op de intergetijdengebieden voor een belangrijk deel door slib worden veroorzaakt. De intergetijdengebieden groeien onder invloed van zeespiegelstijging, maar kunnen de stijging niet zonder meer bijhouden. Dit betekent een afname van het areaal. Deze afname kan zeer substantieel zijn en tientallen procenten bedragen bij de hogere zeespiegelstijging scenario's. De veranderingen in de geulen zijn grotendeels door verplaatsing van zand. Ze verdiepen onder invloed van zeespiegelstijging. Dit verklaart een deel van het netto transport van sediment dat over de grens Vlissingen-Breskens wordt berekend. Omdat een strategie waarbij meer gestort wordt in het oosten de toenemende verdieping in dat deel van het estuarium vermindert, is de verwachting dat deze stortstrategie op lange termijn een positief effect heeft op de omvang van de intergetijdengebieden. De onzekerheden in de morfologische modellering zijn echter te groot om met de berekende hypsometrische curves deze hypothese te bevestigen. Tevens gaat het om relatief kleine arealen in relatie tot de estuarium-brede scope van de studie. Opgemerkt wordt dat het Land van Saeftinghe uiteraard geen klein gebied is, maar dat dit een schorgebied is en minder gevoelig voor veranderingen rond de interactie tussen platen en geulen.

Op basis van deze studie en bestaande kennis kunnen ook voorzichtige uitspraken gedaan worden over de ontwikkeling van de grootschalige morfologie. Er is een trend tot verstarring van het plaatgeulsysteem in de laatste decennia waarneembaar. Deze lijkt in alle scenario's evenredig door te zetten. Grootschalige migratie van geulen blijft beperkt. De toegenomen waterdiepte en het sedimentverlies lijken, zeker bij snellere zeespiegelstijging, de kans te verminderen dat geulen die nu stelselmatig verondiepen, zoals het Middelgat, gaan verdwijnen. Hiervoor is simpelweg geen sediment beschikbaar en het is zelfs mogelijk dat de debietverdeling tussen de geulen zal veranderen.

Invloed op baggerbezwaar

De kosten van vaarwegonderhoud zijn zeer belangrijk in het beheer van het estuarium. Het is echter niet mogelijk op basis van het uitgevoerde modelonderzoek hier andere uitspraken over te doen dan wat via de geaccepteerde, gangbare denkmodellen kan gebeuren. Het lijkt evident dat bij een hogere gemiddelde waterstand in combinatie met een toename van de export van sediment uit het estuarium de waterdiepte zal toenemen. Voor de waterstanden bij laag water is die toename in waterdiepte wel minder groot dan de zeespiegelstijging. Dit is hiervoor uitgelegd bij de getijslag. Een tweede evidente aanname is dat ook in de toekomst de sedimentstrategie lokaal veel invloed zal hebben, onder meer op het tempo van aanzanding van drempels. Het is echter niet mogelijk om met enig morfologisch model lokale bodemontwikkelingen over 80 jaar te voorspellen. We bestuderen immers een watersysteem waar voortdurend ingegrepen wordt.

Hoofdconclusies voor beleid en beheer

- Bij snellere zeespiegelstijging wordt er netto meer zand het estuarium uit geëxporteerd en minder slib het estuarium in geïmporteerd.
- De hoogwaterstanden stijgen mee met de zeespiegel. Hier bovenop is er in de meer stroomopwaartse delen van het estuarium een extra toename van maximaal 10 %. Berekend is 0,25 m extra stijging bij Schelle, bij een mondiale zeespiegelstijging van 3 m.
- Onder invloed van zeespiegelstijging nemen de maximale snelheden tijdens vloed sterker af dan de maximale snelheden tijdens eb. Hierdoor neemt het residuale sedimenttransport richting zee toe.

- De intergetijdengebieden groeien alleen gedeeltelijk mee met de zeespiegel. Het areaal neemt daarom in absolute zin af. De waterstanden stijgen sneller dan de platen in hoogte toenemen.
- Met sedimentbeheer kan invloed uitgeoefend worden op de verdeling van het sediment over het estuarium. Bij extreme zeespiegelstijging heeft dit beheer een te beperkt effect om de getijslag significant te beïnvloeden.
- Het beleidsdoel 'behoud van meergeulenstelsel' moet onder snellere zeespiegelstijging niet langer geïnterpreteerd als een zorg voor behoud van de configuratie van nevengeulen. De zorgen moeten gekoppeld zijn aan de verandering in de waterstanden en het areaal intergetijdengebieden. Hieraan zijn veel gebruiksfuncties gekoppeld.

De conclusies over de evolutie van waterstanden bij extreme zeespiegelstijging lijken robuust, evenals de constatering dat de mogelijkheden om hier met sedimentbeheer op in te spelen (binnen de huidige scope ervan) beperkt zijn. Bij de huidige, beperkte, zeespiegelstijging is de invloed van het sediment juist wel groot.

Resterende onzekerheden

Dit onderzoek had als doel via modelonderzoek inzicht te krijgen in het effect van extreme zeespiegelstijging op een estuarium waarin veel sedimentbeheer plaatsvindt. Hierbij is rekening gehouden met de onzekerheden die het zwaarst wegen, in de context dat de kans op (extreme) zeespiegelstijging meer in beschouwing wordt genomen bij besluiten.

Op basis van dit onderzoek is het expert-oordeel dat de volgende onzekerheden nu nog het zwaarst doorwegen, waarbij de onzekerheden rond de eerste twee punten niet verkleind kunnen worden met het type onderzoek waarover dit rapport verslag doet:

- De snelheid van de zeespiegelstijging.
- De veranderingen in sedimentbeheer in 80 jaar (en uiteraard ook ander beleid en economische ontwikkeling).
- De betrouwbaarheid van de voorspelde morfologische ontwikkeling op lange termijn, in het bijzonder op het niveau van intergetijdengebieden.
- De invloed van slib en driedimensionale residuele stroming.
- De effecten op de Zeeschelde en mogelijkheden van morfologisch beheer daarop. Deze waren niet in de studie meegenomen.

About Deltares

Deltares is an independent institute for applied research in the field of water and subsurface. Throughout the world, we work on smart solutions, innovations and applications for people, environment and society. Our main focus is on deltas, coastal regions and river basins. Managing these densely populated and vulnerable areas is complex, which is why we work closely with governments, businesses, other research institutes and universities at home and abroad. Our motto is 'Enabling Delta Life'.

As an applied research institute, the success of Deltares can be measured in the extent to which our expert knowledge can be used in and for society. As Deltares we aim at excellence in our expertise and advice, where we always take the consequences of our results for environment and society into consideration.

All contracts and projects contribute to the consolidation of our knowledge base. We look from a long-term perspective at contributions to the solutions for now. We believe in openness and transparency, as is evident from the free availability of our software and models. Open source works, is our firm conviction.

Deltares is based in Delft and Utrecht, the Netherlands. We employ over 800 people who represent some 40 nationalities. We have branch and project offices in Australia, Indonesia, New Zealand, the Philippines, Singapore, the United Arab Emirates and Vietnam. In the USA Deltares also has an affiliated organization.

www.deltares.nl

Contents

	Executive summary	**4**
	About Deltares	**10**
	List of Figures	**12**
	List of Tables	**17**
1	**Introduction**	**18**
1.1	Background	18
1.2	Study aims and outline	18
2	**The study area**	**21**
3	**Methodology**	**23**
3.1	General approach and scenario overview	23
3.2	Model setup	26
3.3	Model calibration	30
4	**Results**	**33**
4.1	Morphological hindcast 1964–2012	33
4.1.1	Sediment budget	33
4.1.2	Morphodynamics	36
4.2	Scenario results	37
4.2.1	Hydrodynamics	39
4.2.2	Residual sediment transport	44
4.2.3	Sediment budget	47
4.2.4	Morphodynamics	54
5	**Discussion and conclusions**	**62**
A	**Appendix**	**66**
References		**97**

List of Figures

1.1 Satellite image and bathymetry of the Westernscheldt estuary including labels of the main morphological features. 19

3.1 Dumping locations according to the current DAD and future DAD strategies as well as beach nourishment locations in the Western Scheldt estuary, which are considered in the Delft3D-Scheldt-SLR Model in this study. 24

3.2 Model domain and computational flow grid of the Delft3D-Scheldt-SLR Model. 27

3.3 Water level time series for buoy station Westhinder based on a linear and non-linear sea level rise of 2.63 m SLR in the period 2020 to 2100. 28

4.1 Cumulative total sediment volume change (relative to 1964) in the Western Scheldt estuary between Vlissingen-Breskens and the Dutch-Belgian border in the period 1964–2012 according to data available in the literature and according to bed level changes in the hindcast simulations based on the three configurations of the Delft3D-Scheldt-SLR Model, i.e. the sand-only model, the sand-only wave model and the sand-mud wave model. 34

4.2 Sediment transport and budget for various defined cells in the Western Scheldt estuary in the hindcast period 1964–2012 based on measured bed levels and on the hindcast simulations performed with the sand-only model, the sand-only wave model and the sand-mud wave model configurations of the Delft3D-Scheldt-SLR Model. 35

4.3 Cumulative erosion and sedimentation in the Western Scheldt estuary in the period 1964–2012 according to measured bed levels and simulated bed levels based on the three configurations of the Delft3D-Scheldt-SLR Model, i.e. the sand-only model, the sand-only wave model and the sand-mud wave model. 36

4.4 Hypsometric curves of the Western Scheldt estuary between Vlissingen-Breskens and the Dutch-Belgian border according to the bed levels measured in 1964 and 2012 and simulated for 2012 based on the hindcast simulations performed with the sand-only model, the sand-only wave model and the sand-mud wave model configurations of the Delft3D-Scheldt-SLR Model. 38

4.5 Comparison of simulated mean low (MLW) and mean high water levels (MHW) without SLR correction and with SLR correction at various stations in the Western Scheldt estuary for the year 2020 (no SLR) and the year 2100 for various linear SLR scenarios for the current DAD strategy based on the sand-only model. 40

4.6 Comparison of simulated M2, S2 and M4 tidal amplitudes and simulated relative tidal phases $2*\varphi$M2$-\varphi$M4 at various stations in the Western Scheldt estuary for the year 2020 (no SLR) and the year 2100 for various linear SLR scenarios for the current DAD strategy based on the sand-only model. 41

4.7 Maximum flood and ebb flow velocities in the Western Scheldt estuary during spring tide in 2100 simulated with the sand-mud wave model configuration of the Delft3D-Scheldt-SLR Model for the 2.63 m linear SLR and the 0 m SLR scenarios based on the current dredging and dumping (DAD) strategy without beach nourishments but with wave forcing. 42

4.8 Maximum flood and ebb flow velocities in the Western Scheldt estuary during spring tide in 2100 simulated with the sand-mud Delft3D-Scheldt-SLR Model for the 2.63 m linear SLR and the 0 m SLR scenarios based on the future dredging and dumping (DAD) strategy. 43

4.9 Residual sediment (sand) transport in the Western Scheldt estuary during spring tide in 2100 simulated with the sand-mud wave model configuration of the Delft3D-Scheldt-SLR Model for the 0 m SLR and the 2.63 m linear SLR scenarios based on the current dredging and dumping (DAD) strategy without beach nourishments but with wave forcing. 45

4.10 Residual sediment (sand) transport in the Western Scheldt estuary during spring tide in 2100 simulated with the sand-mud wave model configuration of the Delft3D-Scheldt-SLR Model for the 0 m SLR and the 2.63 m linear SLR scenarios based on the future dredging and dumping (DAD) strategy without beach nourishments but with wave forcing. 46
4.11 Cumulative sediment transport (sand only) through cross-section Vlissingen-Breskens at the mouth of the Western Scheldt in the period 2020 to 2100 simulated for five linear SLR scenarios for the current and future dredging and dumping (DAD) strategy without beach nourishments and with beach nourishments based on the sand-only model configuration of the Delft3D-Scheldt-SLR Model. 48
4.12 Cumulative sediment transport (sand only) through cross-section Vlissingen-Breskens at the mouth of the Western Scheldt in the period 2020 to 2100 simulated for five linear SLR scenarios for the current and future dredging and dumping (DAD) strategy without beach nourishments and with beach nourishments based on the sand-only wave model configuration of the Delft3D-Scheldt-SLR Model. 49
4.13 Cumulative sediment transport (sand and mud; not corrected for porosity) through cross-section Vlissingen-Breskens at the mouth of the Western Scheldt in the period 2020 to 2100 simulated for five linear SLR scenarios for the current and future dredging and dumping (DAD) strategy based on the sand-mud wave model configuration of the Delft3D-Scheldt-SLR Model. 50
4.14 Sediment (sand only) transport and budget for various defined cells in the Western Scheldt estuary simulated with the sand-only model configuration of the Delft3D-Scheldt-SLR Model for five linear SLR scenarios for the current dredging and dumping (DAD) strategy. 51
4.15 Sediment (sand only) transport and budget for various defined cells in the Western Scheldt estuary simulated with the sand-only model configuration of the Delft3D-Scheldt-SLR Model for five linear SLR scenarios for the future dredging and dumping (DAD) strategy. 53
4.16 Bed level of the Western Scheldt estuary in 2020 (including 25 years spin-up time based on the current DAD strategy) and 2100 as simulated with the sand-only model configuration of the Delft3D-Scheldt-SLR Model for five linear SLR scenarios for the current DAD (dredging and dumping) strategy. 55
4.17 Cumulative erosion and sedimentation in the period 2020 to 2100 in the Western Scheldt as simulated with the sand-only model configuration of the Delft3D-Scheldt-SLR Model for five linear SLR scenarios for the current DAD (dredging and dumping) strategy. 56
4.18 Bed level of the Western Scheldt estuary in 2020 (including 25 years spin-up time based on the future DAD strategy) and 2100 as simulated with the sand-only model configuration of the Delft3D-Scheldt-SLR Model for five linear SLR scenarios for the future DAD (dredging and dumping) strategy. 57
4.19 Cumulative erosion and sedimentation in the period 2020 to 2100 in the Western Scheldt as simulated with the sand-only model configuration of the Delft3D-Scheldt-SLR Model for five linear SLR scenarios for the future DAD (dredging and dumping) strategy. 58
4.20 Thalweg (i.e. the line of lowest bed levels) of the main navigation channel in the Western Scheldt estuary, for which the depth profiles are shown in Fig. 4.21 and in Figs. A.25–A.27 in the Appendix. 58
4.21 Depth profiles of the thalweg (i.e. the line of lowest bed levels) of the main navigation channel in the Western Scheldt estuary as simulated with the sand-only model configuration of the Delft3D-Scheldt-SLR Model for various linear SLR scenarios based on the current and future DAD strategies. 59

4.22 Hypsometric curves of the Western Scheldt estuary between Vlissingen-Breskens and the Dutch-Belgian border as simulated with the sand-mud wave model configuration of the Delft3D-Scheldt-SLR Model for the 0 m SLR and for the 2.63 m linear SLR scenarios based on the current and future DAD strategies. 60
A.1 Comparison of simulated mean low (MLW) and mean high water levels (MHW) without SLR correction and with SLR correction at various stations in the Western Scheldt estuary for the year 2020 (no SLR) and the year 2100 for various linear SLR scenarios for the future DAD strategy based on the sand-only model. 67
A.2 Comparison of simulated M2, S2 and M4 tidal amplitudes and simulated relative tidal phases $2*\varphi M2-\varphi M4$ at various stations in the Western Scheldt estuary for the year 2020 (no SLR) and the year 2100 for various linear SLR scenarios for the future DAD strategy based on the sand-only model. 68
A.3 Sediment (sand only) transport and budget for various defined cells in the Western Scheldt estuary simulated with the sand-only model configuration of the Delft3D-Scheldt-SLR Model for five linear SLR scenarios for the current dredging and dumping (DAD) strategy including beach nourishments. 69
A.4 Sediment (sand only) transport and budget for various defined cells in the Western Scheldt estuary simulated with the sand-only model configuration of the Delft3D-Scheldt-SLR Model for five linear SLR scenarios for the future dredging and dumping (DAD) strategy including beach nourishments. 70
A.5 Sediment (sand only) transport and budget for various defined cells in the Western Scheldt estuary simulated with the sand-only wave model configuration of the Delft3D-Scheldt-SLR Model for five linear SLR scenarios for the current dredging and dumping (DAD) strategy. 71
A.6 Sediment (sand only) transport and budget for various defined cells in the Western Scheldt estuary simulated with the sand-only wave model configuration of the Delft3D-Scheldt-SLR Model for five linear SLR scenarios for the future dredging and dumping (DAD) strategy. 72
A.7 Sediment (sand only) transport and budget for various defined cells in the Western Scheldt estuary simulated with the sand-only wave model configuration of the Delft3D-Scheldt-SLR Model for five linear SLR scenarios for the current dredging and dumping (DAD) strategy including beach nourishments. 73
A.8 Sediment (sand only) transport and budget for various defined cells in the Western Scheldt estuary simulated with the sand-only wave model configuration of the Delft3D-Scheldt-SLR Model for five linear SLR scenarios for the future dredging and dumping (DAD) strategy including beach nourishments. 74
A.9 Bed level of the Western Scheldt estuary in 2020 (including 25 years spin-up time based on the current DAD strategy) and 2100 as simulated with the sand-only model configuration of the Delft3D-Scheldt-SLR Model for five linear SLR scenarios for the current DAD (dredging and dumping) strategy including beach nourishments. 75
A.10 Cumulative erosion and sedimentation in the period 2020 to 2100 in the Western Scheldt as simulated with the sand-only model configuration of the Delft3D-Scheldt-SLR Model for five linear SLR scenarios for the current DAD (dredging and dumping) strategy including. 76
A.11 Bed level of the Western Scheldt estuary in 2020 (including 25 years spin-up time based on the future DAD strategy) and 2100 as simulated with the sand-only model configuration of the Delft3D-Scheldt-SLR Model for five linear SLR scenarios for the future DAD (dredging and dumping) strategy including beach nourishments. 77

A.12 Cumulative erosion and sedimentation in the period 2020 to 2100 in the Western Scheldt as simulated with the sand-only model configuration of the Delft3D-Scheldt-SLR Model for five linear SLR scenarios for the future DAD (dredging and dumping) strategy including beach nourishments. 78
A.13 Bed level of the Western Scheldt estuary in 2020 (including 25 years spin-up time based on the current DAD strategy) and 2100 as simulated with the sand-only wave model configuration of the Delft3D-Scheldt-SLR Model for five linear SLR scenarios for the current DAD (dredging and dumping) strategy. 79
A.14 Cumulative erosion and sedimentation in the period 2020 to 2100 in the Western Scheldt as simulated with the sand-only wave model configuration of the Delft3D-Scheldt-SLR Model for five linear SLR scenarios for the current DAD (dredging and dumping) strategy. 80
A.15 Bed level of the Western Scheldt estuary in 2020 (including 25 years spin-up time based on the future DAD strategy) and 2100 as simulated with the sand-only wave model configuration of the Delft3D-Scheldt-SLR Model for five linear SLR scenarios for the future DAD (dredging and dumping) strategy. 81
A.16 Cumulative erosion and sedimentation in the period 2020 to 2100 in the Western Scheldt as simulated with the sand-only wave model configuration of the Delft3D-Scheldt-SLR Model for five linear SLR scenarios for the future DAD (dredging and dumping) strategy. 82
A.17 Bed level of the Western Scheldt estuary in 2020 (including 25 years spin-up time based on the current DAD strategy) and 2100 as simulated with the sand-only wave model configuration of the Delft3D-Scheldt-SLR Model for five linear SLR scenarios for the current DAD (dredging and dumping) strategy including beach nourishments. 83
A.18 Cumulative erosion and sedimentation in the period 2020 to 2100 in the Western Scheldt as simulated with the sand-only wave model configuration of the Delft3D-Scheldt-SLR Model for five linear SLR scenarios for the current DAD (dredging and dumping) strategy including beach nourishments. 84
A.19 Bed level of the Western Scheldt estuary in 2020 (including 25 years spin-up time based on the future DAD strategy) and 2100 as simulated with the sand-only wave model configuration of the Delft3D-Scheldt-SLR Model for five linear SLR scenarios for the future DAD (dredging and dumping) strategy including beach nourishments. 85
A.20 Cumulative erosion and sedimentation in the period 2020 to 2100 in the Western Scheldt as simulated with the sand-only wave model configuration of the Delft3D-Scheldt-SLR Model for five linear SLR scenarios for the future DAD (dredging and dumping) strategy including beach nourishments. 86
A.21 Bed level of the Western Scheldt estuary in 2020 (including 25 years spin-up time based on the current DAD strategy) and 2100 as simulated with the sand-mud wave model configuration of the Delft3D-Scheldt-SLR Model for five linear SLR scenarios for the current DAD (dredging and dumping) strategy. 87
A.22 Cumulative erosion and sedimentation in the period 2020 to 2100 in the Western Scheldt as simulated with the sand-mud wave model configuration of the Delft3D-Scheldt-SLR Model for five linear SLR scenarios for the current DAD (dredging and dumping) strategy. 88
A.23 Bed level of the Western Scheldt estuary in 2020 (including 25 years spin-up time based on the future DAD strategy) and 2100 as simulated with the sand-mud wave model configuration of the Delft3D-Scheldt-SLR Model for five linear SLR scenarios for the future DAD (dredging and dumping) strategy. 89
A.24 Cumulative erosion and sedimentation in the period 2020 to 2100 in the Western Scheldt as simulated with the sand-mud wave model configuration of the Delft3D-Scheldt-SLR Model for five linear SLR scenarios for the future DAD (dredging and dumping) strategy. 90

A.25 Depth profiles of the thalweg (i.e. the line of lowest bed levels) of the main navigation channel in the Western Scheldt estuary as simulated with the sand-only model configuration of the Delft3D-Scheldt-SLR Model for various linear SLR scenarios based on the current and future DAD strategies including beach nourishments. 91
A.26 Depth profiles of the thalweg (i.e. the line of lowest bed levels) of the main navigation channel in the Western Scheldt estuary as simulated with the sand-only wave model configuration of the Delft3D-Scheldt-SLR Model for various linear SLR scenarios based on the current and future DAD strategies. 92
A.27 Depth profiles of the thalweg (i.e. the line of lowest bed levels) of the main navigation channel in the Western Scheldt estuary as simulated with the sand-only wave model configuration of the Delft3D-Scheldt-SLR Model for various linear SLR scenarios based on the current and future DAD strategies including beach nourishments. 93
A.28 Depth profiles of the thalweg (i.e. the line of lowest bed levels) of the main navigation channel in the Western Scheldt estuary as simulated with the sand-mud wave model configuration of the Delft3D-Scheldt-SLR Model for various linear SLR scenarios based on the current and future DAD strategies. 94
A.29 Hypsometric curves of the Western Scheldt estuary between Vlissingen-Breskens and the Dutch-Belgian border as simulated with the sand-only model configuration of the Delft3D-Scheldt-SLR Model for the 0 m SLR and for the 2.63 m linear SLR scenarios based on the current and future DAD strategies. 95
A.30 Hypsometric curves of the Western Scheldt estuary between Vlissingen-Breskens and the Dutch-Belgian border as simulated with the sand-only wave model configuration of the Delft3D-Scheldt-SLR Model for the 0 m SLR and for the 2.63 m linear SLR scenarios based on the current and future DAD strategies. 96

List of Tables

3.1 Overview of the SLR scenarios based on the IPCC (Intergovernmental Panel on Climate Change) report by CHURCH and CLARK (2013) and the article by LE BARS *et al.* (2017), which are considered in this study to investigate the hydro- and morphodynamic effects of SLR in the Western Scheldt estuary in the period 2020–2100. 23

3.2 Overview of the basic set of the performed scenario simulations for the period 2020–2100 based on various SLR scenarios (0 m, 0.4 m, 0.96 m, 1.67 m and 2.63 m), two types of SLR (linear and non-linear), two DAD (dredging and dumping) strategies (current and future), beach nourishments ex-/included, waves ex-/included and mud ex-/included. 25

3.3 Average significant wave height, wave peak period, mean wave direction, wind speed and wind direction used for the forcing of the waves model in the form of a uniform and constant wave condition and wind field, respectively. 28

3.4 Overview of selected model parameter settings applied to the Delft3D-Scheldt-SLR Model. 31

1 Introduction

1.1 Background

Both the Netherlands and Belgium (more specifically Flanders) are facing uncertainties associated with climate change and (extreme) sea level rise (SLR). Both countries share the responsibility for policy and management of the Western Scheldt, the estuary of the Scheldt river located in the southwest of the Netherlands (Fig. 1.1). Besides the effects of SLR, there is uncertainty about the impact of the future sediment management. Two elements of sediment management are investigated in this study: beach nourishments near the mouth and the proposed new disposal or dumping strategy in the Western Scheldt in comparison to the present one. According to the new strategy, a larger portion of dredged sediment is disposed in the deep parts of the main channel and by this further upstream. As a result, the net human downstream sediment transport due to the dredging and dumping activities will be reduced. Other elements of sediment management such as deepening, setbacks of embankments and the construction of waterworks to increase sedimentation are not considered in this study.

Relatively little is known about the morphological response of estuaries to accelerated SLR. This is mainly due to the individual features of each estuary and delta and the specific interactions of the estuarine morphodynamics with human interventions. While several conceptual models exist that give indications on the hydro- and morphodynamic response of estuaries to SLR, there are hardly any process-based models available for this kind of study. Consequently, at this stage, research on the effects of SLR and sediment strategies on the hydro- and morphodynamic processes in the Western Scheldt is the most import measure in order to gain more insight into the system functioning. Such research to support joint policy and management of the Western Scheldt estuary is part of the *Treaty of Vlissingen* of the year 2005. In this context, the Flemish government asked Deltares to perform a quick scan study on the hydro- and morphodynamic effects of (extreme) SLR and of different sediment strategies in the Western Scheldt. This study was carried out in collaboration with the IHE Delft Institute for Water Education.

1.2 Study aims and outline

The main objective of the current study is to gain insight into the relative impact of (extreme) sea level rise (SLR) and of different sediment strategies, i.e. dredging and dumping and beach nourishments, on the hydro- and morphodynamic behaviour of the Western Scheldt estuary (The Netherlands) till the end of the 21st century. For this, we apply a process-based numerical morphodynamic model (Delft3D version 4) that accounts for continuously changing hydrodynamic boundary conditions associated with SLR as well as for different dredging and dumping (or disposal; DAD) strategies and beach nourishments. Based on this approach, the following aims can be drawn together:

- Translate global SLR scenarios to the local SLR scenarios for the study area. This is an important step since moderate SLR scenarios, in which the main contribution of SLR is related to ice melting in the Arctic, indicate a smaller SLR in the North Sea compared to the global average. In contrast, extreme SLR scenarios, in which ice melting in the Antarctic is the main contribution to SLR, imply a SLR

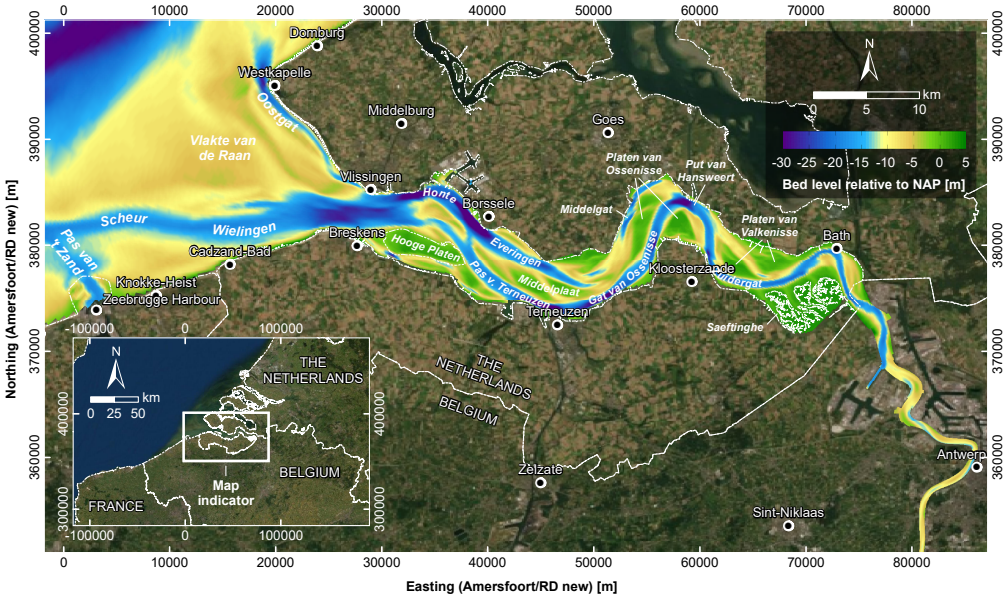

Figure 1.1 Satellite image and bathymetry of the Western Scheldt estuary including labels of the main morphological features. The bathymetry is based on the Vaklodingen and JARKUS datasets measured in 2012 as well as on GEBCO and EMODnet data from the years 2014 and 2013, respectively (IOC, IHO & UNESCO 2015).

in the North Sea above average (cf. Sec. 3.1).

- Apply the derived local SLR scenarios to a calibrated and validated process-based morphodynamic model of the study area that also allows to simulate different sediment strategies in the form of DAD and beach nourishments in the Western Scheldt.
- Perform multiple sensitivity analyses with the model by applying various model settings and by removing or adding complexity (in particular waves and multiple sediment fractions including cohesive sediment) in order to study the robustness of the model outcomes.
- Analyse the impact of SLR and sediment strategies on the simulated hyrdro- and morphodynamics in the Western Scheldt. Here, the focus rather lies on the differences between the various SLR scenarios and between the different sediment strategies than on the absolute model predictions.
- Perform a morphological hindcast for the period 1964 to 2012, in order to see how well the model predicts the sediment budget and the bed level changes in the estuary observed in this historical period.
- Draw conclusions on the general hydro- and morphodynamic effects of SLR and of the different sediment strategies in the Western Scheldt based on the model outcomes and to evaluate the reliability of the results and their applicability for policy and management of the estuary.

Based on these objectives, this project report continues with a concise presentation of the study area with a focus on the local geomorphology, tidal forcing and wave climate (Sec. 2). Section 3 deals with the general approach and scenario overview of the study as well as with the methodology of the model setup and model calibration. Subsequently, the results of the morphological hindcast are presented (Sec. 4.1), followed

by the description of the future scenario results (Sec. 4.2). For reasons of clarity and comprehensibility, we do not show the simulation results for the whole set of performed scenario runs but only for those which are relevant to the conclusions of this study. Moreover, a large part of the scenario results is shown in the Appendix. Finally, the results of the morphological hindcast and of the scenario simulations are discussed and evaluated in terms of the study aims including an outlook with regard to future research (Sec. 5).

2 The study area

The Western Scheldt is a funnel-shaped estuary with a length of about 70 km. It is characterised by a system of multiple meandering ebb channels and relatively straight flood channels intersected by several elongated intertidal shoals (Fig. 1.1; WANG *et al.* 2002; BOLLE *et al.* 2010). Dikes and bank protection measures form the lateral boundaries of the estuary. Despite anthropogenic deepening of the navigation channel of the Western Scheldt between 1970 and 1975, natural processes dominated the morphological development of the channel system until 1997 (WANG *et al.* 2002). Since then, increasing DAD activities associated with two following deepening phases (1995 and 2005) significantly influenced the morphodynamics.

The main navigation channel of the Western Scheldt is currently being dredged to a depth of 17.20 m NAP (Normaal Amsterdams Peil = Amsterdam Ordnance Datum $\approx$ mean sea level) up to harbour of Antwerp. The maximum depth of the channel of about -51.5 m below NAP can be found near the mouth between Borssele and Vlissingen. The maximum height of the intertidal shoals is about 2.5 m above NAP. The mouth of the Western Scheldt shows two major channels — the main navigation channel Wielingen-Scheur passing the harbour of Zeebrugge as well as the smaller Oostgat channel along the coast between Vlissingen and Westkapelle (Fig. 1.1). The two channels are separated by the shoal Vlakte van de Raan. Water depths in the mouth area are typically less than 10 m below NAP but reach almost 18 m below NAP in the channels. Onshore, land elevations usually do not exceed few metres except for the dune areas around Knokke-Heist with maximum heights of about 30 m above NAP.

Facing the south-western North-Sea, the Western Scheldt is exposed to wind, wave and tidal forces. The area is dominated by winds from the south-western sector, followed by winds from a north-eastern direction (BAEYE *et al.* 2010). In line with the wind climate, the main wave direction in the mouth is south-west although the highest waves are associated with the north-western sector, which is related to the longer fetch in this direction and the typical path of extratropical cyclones during the storm season (BAEYE *et al.* 2010; SPENCER *et al.* 2015).

The average significant wave height H_s offshore the mouth is of the order of 1.4 m with an associated peak period T_p of circa 6.5 s (RWS 2017). Tides mainly occur semi-diurnally and increase in an upstream direction up to Antwerp. The average tidal range and mean high water level at Vlissingen/Bath are 3.83 m/4.94 m and 2.07 m/2.75 m above NAP, respectively (Vlaamse Hydrografie 2011). The maximum storm surge level ever recorded at Vlissingen/Bath is 4.55 m/5.60 m above NAP, which was on 1st February 1953 (Vlaamse Hydrografie 2011).

The tidal prism of the Western Scheldt at Vlissingen is about 2.2*10^9 m^3, which is significantly larger than the average discharge per semi-diurnal tide of the Western Scheldt of approximately 5*10^6 m^3 (corresponds to an average instantaneous discharge of circa 120 m^{3}s^{-1}; VERLAAN 1998; WANG *et al.* 2002). The maximum depth-averaged flow velocities in the channels during ebb and flood are of the order of 1 m s^{-1} to 1.5 m s^{-1}.

Most of the incoming tide enters the estuary via the main navigation channel Scheur-Wielingen (VAN DER WEGEN *et al.* 2017). In wide parts of the estuary, the falling tide lasts longer than the rising tide (vertical tidal asymmetry). This flood dominance decreases downstream resulting in phase differences $(2\phi_2 - \phi_4)$ of the water levels of

the order of few degrees around zero (neither flood nor ebb dominant) at the mouth near Vlissingen (WANG *et al.* 2002; BOLLE *et al.* 2010). Further westwards, the coast between Zeebrugge harbour and Cadzand-Bad is generally flood dominated, although conditions are spatially highly variable and local ebb dominated areas can be observed (for further details on the regional hydrodynamics see BLIEK *et al.* 1998, TROUW *et al.* 2015).

The dominant sediment fraction in the channels of the Western Scheldt is fine sand with a grain size of about 200 μm, while mud (grain size $\leq 2\,\mu$m) is mainly found further upstream and in the area of the intertidal shoals (WANG *et al.* 2002). The mouth area is characterised by a mix of fine/medium sand and mud. Fine and medium sands in the study area mainly originate from the cliffs of Calais and the English Channel, while muddy material is mainly associated with (i) a Holocene source in the form of a submerged mudflat-marsh system in the area around Zeebrugge harbour, (ii) mud supply from the French and Belgian coasts as well as (iii) the sediment input by the Westernscheldt (FETTWEIS and VAN DEN EYNDE 2003; FETTWEIS *et al.* 2007; VAN LANCKER *et al.* 2012; VAN DER WEGEN *et al.* 2017).

3 Methodology

3.1 General approach and scenario overview

This study explores the hydro- and morphodynamic effects of SLR and different sediment strategies in the Western Scheldt by using a process-based numerical morphodynamic model, the so-called Delft3D-Scheldt-SLR Model. With this model, we investigate the long-term hydro- and morphodynamic effects of (i) five different SLR scenarios, of (ii) two different DAD strategies in the estuary and of (iii) four different beach nourishment strategies in the mouth area (the DAD strategies and beach nourishments are summarised as *sediment strategies*) in the period 2020–2100. The study particularly concentrates on the relative but not on the absolute impact of SLR and sediment strategies. We therefore rather focus on the differences between the various SLR scenarios and between the different sediment strategies than on the absolute model predictions.

Based on the IPCC (Intergovernmental Panel on Climate Change) report by CHURCH and CLARK (2013) and the article by LE BARS *et al.* (2017), we determined five different SLR scenarios between no (0 m) SLR and extreme (2.63 m) SLR for the period 2020–2100 (Table 3.1). In contrast to CHURCH and CLARK (2013), LE BARS *et al.* (2017) consider high-end estimates of the Antarctic ice sheet loss (cf. DECONTO and POLLARD 2016) resulting in significantly higher SLR projections than published earlier. Consequently, the chosen scenarios in Table 3.1 cover a large range of potential SLR in the Western Scheldt within the coming 80 years.

Due to, in particular, rotational effects, ocean circulation, glacio-hydro isostasy, freshwater inputs and gravitational pull of ice mass, the global SLR clearly differs from the local SLR in the study area (cf. left and central column of Table 3.1; CHURCH and CLARK 2013). In our numerical model, we do not apply the global temporally varying SLR as stated by CHURCH and CLARK (2013) and LE BARS *et al.* (2017) for the period 2005 to 2100, which — most probably — is not applicable for the study area. Instead, we consider continuous (i) linear and (ii) non-linear SLR for the period 2020–2100 (for further

Table 3.1 Overview of the SLR scenarios based on the IPCC (Intergovernmental Panel on Climate Change) report by CHURCH and CLARK (2013)* and the article by LE BARS *et al.* (2017)**, which are considered in this study to investigate the hydro- and morphodynamic effects of SLR in the Western Scheldt estuary in the period 2020–2100. Note that rotational effects, ocean circulation, glacio-hydro isostasy, freshwater inputs, gravitational pull of ice mass etc. cause significant differences between the global (left column) and local SLR (central column) (cf. CHURCH and CLARK 2013). The local SLR values are displayed for Westhinder station located almost 32 km offshore the Belgian coast (see Fig. 3.2) and were determined with the validated hydrodynamic Global Tide and Storm Surge Model (for details see Sec. 3.2).

Global SLR [m] 2020–2100	Local SLR [m] 2020–2100 at Westhinder station	Refers to original scenario
0	0	–
0.4	0.22	IPCC AR5 RCP2.6-SLR*
0.96	1.10	RCP4.5-SLR 50th perc.**
1.67	1.96	RCP8.5-SLR 50th perc.**
2.63	3.02	RCP8.5-SLR 95th perc.**

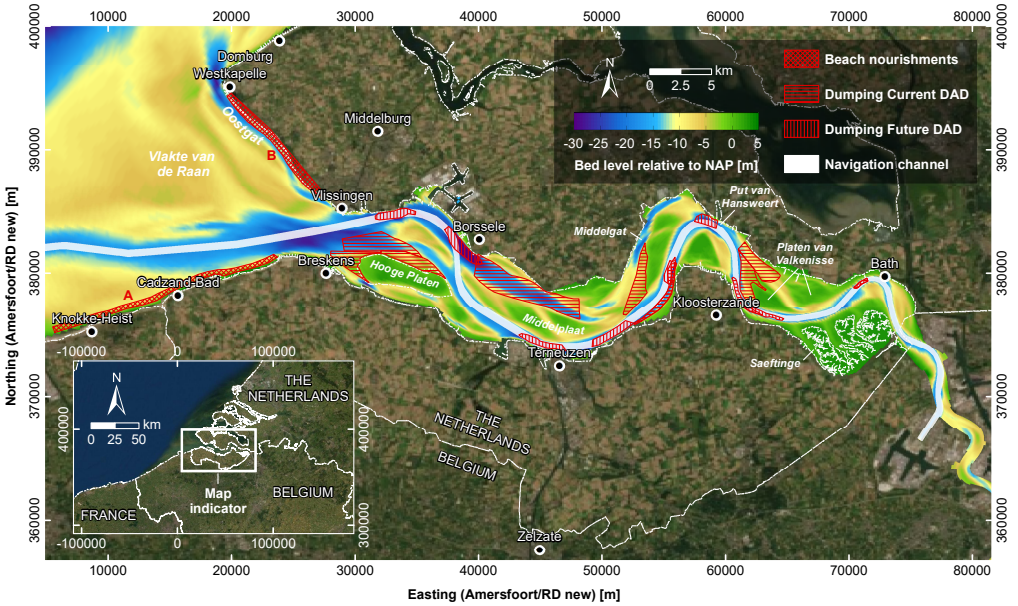

Figure 3.1 Dumping locations according to the current DAD (dredging and dumping) and future DAD strategies as well as beach nourishment locations (A = beaches between Zeebrugge Harbour and Breskens; B = beaches along Oostgat channel) in the Western Scheldt estuary, which are considered in the Delft3D-Scheldt-SLR Model in this study.

details see Sec. 3.2).

The two DAD strategies considered in this study are based (i) on the DAD strategy applied in the years 2013–2014 (referred to as *current DAD*; cf. VROOM and SCHRIJVERSHOF 2015) and (ii) on the DAD strategy which might be applied in the future (referred to as *future DAD*). While the dredging is the same for both strategies, the dumping of the dredged sediment clearly differs (Fig. 3.1). In case of the current DAD strategy, dredged sediment is partly dumped in the area of the shoals and partly in the area of the channels of the estuary. In contrast, dumping in the future DAD strategy is almost exclusively performed in the deep parts of the channels, i.e. the parts of the channels which are significantly deeper than the current dredging depth. Moreover, a larger portion of the dredged material is dumped in the more upstream part (upstream of Terneuzen) of the Western Scheldt in the future DAD strategy.

The four beach nourishment strategies are based on different combinations of nourishment volumes for the beaches between Zeebrugge Harbour and Breskens (A) and along the Oostgat channel (B) (Fig. 3.1). In the two base cases, we apply a yearly volume of 0 m^3 (i.e. no nourishments) as well as yearly volumes of 750,000 m^3 (area A) and 250,000 m^3 (area B) respectively, which approximate the volumes currently nourished at these beaches. We further consider increased nourishment volumes of 4,750,000 m^3 (area A)/250,000 m^3 (area B) and of 750,000 m^3 (area A)/4,250,000 m^3 (area B). Since the increased nourishment volumes rather had quantitative than qualitative impact on the simulated sediment budgets and morphology, in this report we only present the results for the two base cases.

In order to investigate the sensitivity of the long-term hydro- and morphodynamics to the different SLR scenarios and sediment strategies, each SLR scenario is simulated in combination with both DAD strategies as well as with the four nourishment strategies. The resulting scenarios are simulated based on three different model configurations, i.e. the (i) sand-only model without wave forcing, (ii) sand-only wave model with wave

Table 3.2 Overview of the basic set of the performed scenario simulations for the period 2020–2100 based on various SLR scenarios (0 m, 0.4 m, 0.96 m, 1.67 m and 2.63 m), two types of SLR (linear and non-linear), two DAD (dredging and dumping) strategies (current and future), beach nourishments ex-/included, waves ex-/included and mud ex-/included. *Note that the mud-sand simulations were only performed for the linear SLR scenarios excluding beach nourishments but including waves. The table does not show a large number of additional scenario and hindcast simulations performed for the model calibration and for sensitivity analyses to test the model's robustness (see Sec. 3.3).

Run ID	Global/local SLR 2020–2100 [m]	Type of SLR	DAD strategy	Beach nourish.	Waves incl.	Mud incl.*
SLR_{0}	0/0	Linear/ Non-linear	Current/ Future	No/Yes	No/Yes	No/Yes
$SLR_{0.4}$	0.4/0.22	Linear/ Non-linear	Current/ Future	No/Yes	No/Yes	No/Yes
$SLR_{0.96}$	0.96/1.10	Linear/ Non-linear	Current/ Future	No/Yes	No/Yes	No/Yes
$SLR_{1.67}$	1.67/1.96	Linear/ Non-linear	Current/ Future	No/Yes	No/Yes	No/Yes
$SLR_{2.63}$	2.63/3.02	Linear/ Non-linear	Current/ Future	No/Yes	No/Yes	No/Yes

forcing and (iii) sand-mud wave model with wave forcing (note that the mud-sand wave model was only applied for the linear SLR scenarios excluding beach nourishments but including waves). This was done to study the effects of waves and of cohesive sediment (mud) on the model outcomes and to test their robustness. While all simulations were performed in morphodynamic mode, i.e. with bed level updating during the simulation, the sand-only model was also ran in morphostatic mode, i.e. without bed level updating, in order to test whether the simulated bed level changes in the model have impact on the predicted trends with regard to SLR and the sediment strategies.

Table 3.2 summarises the basic set of the performed scenario simulations excluding additional scenario and hindcast simulations performed for the model calibration/sensitivity analyses described in Sec. 3.2. According to the objective of this study (see above and Sec. 1.2), the various combinations of different scenario simulations particularity allow a pairwise comparisons between the simulations and to study the relative hydro- and morphodynamic impact of SLR and of the sediment strategies on the Western Scheldt.

3.2 Model setup

The model of the current study, i.e. the Delft3D-Scheldt-SLR Model, is based on the flow (Delft3D-FLOW) and wave (Delft3D-WAVE) modules of the Delft3D modelling suite (version 4). The flow module solves the non-linear shallow water equations of unsteady flow and transport phenomena based on the Navier-Stokes equations for incompressible free surface flow (Deltares 2020a). The module is designed for flow phenomena where the horizontal spatial and temporal scales are much larger than the vertical scales, such as tidal waves, storm surges or tsunamis. In our application, the Delft3D-FLOW module takes account of sediment transport and associated morphodynamics and is coupled with the Delft3D-WAVE module (based on the second-generation wave model SWAN (Simulating WAves Nearshore), which allows to include the effects of short-crested waves on the simulated hydro- and morphodynamics (Deltares 2020b).

The Delft3D-Scheldt-SLR Model was created based on the calibrated and validated Delft3D-NeVla Hincast Model by VAN DER WEGEN *et al.* (2017), which was used to hindcast the morphological development of the Western Scheldt mouth in the period 1963–2011. The Delft3D-Scheldt-SLR Model comprises a coupled flow and waves model. The computational flow grid covers the Western Scheldt mouth and the entire Belgian coast up to 36 km offshore as well as the Scheldt river including all major tributaries (Fig. 3.2). The large model domain ensures that effects of SLR on the regional hydrodynamics (e.g. increase in tidal amplitudes in the estuary due to SLR) are accounted for by the model. The flow grid is based on the grid of the Delft3D-NeVla Hindcast Model by VAN DER WEGEN *et al.* (2017) but de-refined by factor two. The grid resolution increases from the north-western offshore boundary (circa 1000 m by 600 m) towards the tributaries (up to 30 m by 6 m). The typical resolution in the estuary is about 200 m by 100 m. In total, the flow grid comprises 55,316 grid cells. The waves grid corresponds to the flow grid but does not cover the Scheldt upstream the Dutch-Belgian border, since in this area, the morphodynamic effects of waves are limited. The waves grid comprises 29,670 grid cells.

The bathymetry of the Delft3D-Scheldt-SLR Model is based on the Vaklodingen (RWS 2011a; RWS 2012a) and JARKUS (RWS 2011b; RWS 2012b) datasets measured in 2011 and 2012 as well as on EMODnet (EMODnet 2016) and GEBCO (IOC, IHO & UNESCO 2015) data from the years 2016 and 2014, respectively (cf. Fig. 1.1). The historical bathymetry for the morphological hindcast (see below) was compiled from Vaklodingen datasets measured in the years 1963 and 1964 and, in more remote parts of the model domain (i.e. west of Cadzand), in the year 1969 (RWS 1963; RWS 1964; RWS 1969).

The Delft3D-Scheldt-SLR Model uses two types of open boundary conditions, i.e. water level conditions along the three offshore model boundaries and discharge conditions at the heads of the tributaries (Fig. 3.2). Both, the water level conditions and the discharge conditions were defined in the form of a one year time series. For the discharge conditions, the yearly averaged measured discharge of each tributary was determined and used as a constant value for the entire one year time series. The water level conditions were derived from the validated hydrodynamic Global Tide and Storm Surge Model (GTSM; MUIS *et al.* 2016). This model allows for the global simulation of various sea level scenarios and by this for taking account of regional differences of SLR as well as of the effects of a higher sea level on the tidal amplitudes and phases (cf. IRAZOQUI-APECECHEA *et al.* 2020).

For each of the five SLR scenarios considered in this study (see Table 3.1), a one year simulation was performed with the GTSM model, in which we applied the final

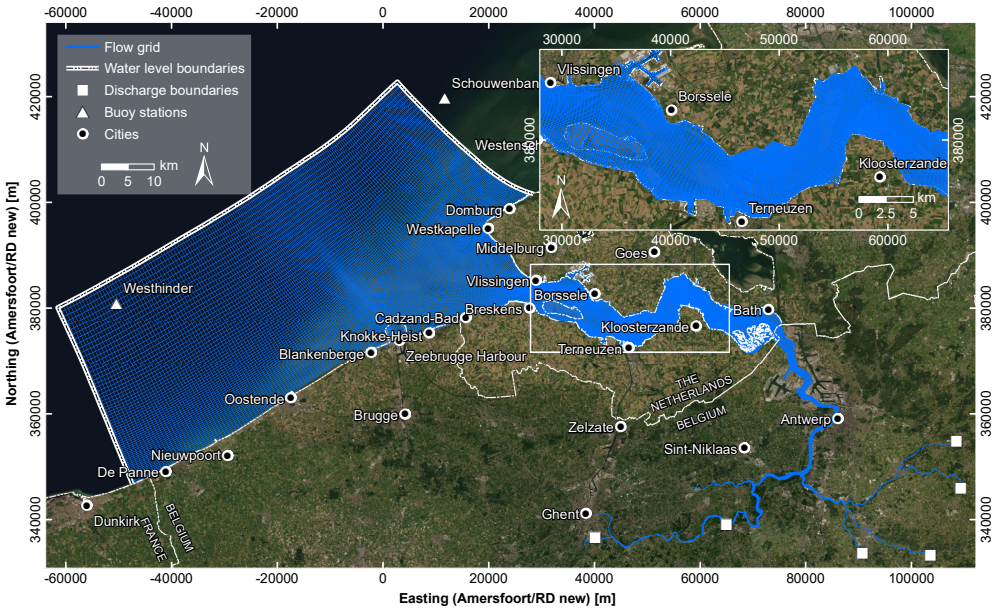

Figure 3.2 Model domain and computational flow grid of the Delft3D-Scheldt-SLR Model. The grid resolution increases from the north-western offshore boundary (circa 1000 m by 600 m) towards the tributaries (up to 30 m by 6 m). The typical resolution in the estuary is about 200 m by 100 m.

sea level reached at the end of each SLR scenario in the year 2100, i.e. 0 m, 0.4 m, 0.96 m, 1.67 m and 2.63 m. Using these simulations and the nesting method, the water level boundary conditions for the Delft3D-Scheldt-SLR Model for each sea level were determined. For an accurate reproduction of the tidal amplitudes and phases in the model domain, the water level boundary conditions as derived from the GTSM model had to be adjusted. This was done by lowering the amplitudes of 32 tidal components by about 20 % (which was the average deviation from the measured M2, M4 and S2 tidal amplitudes) for all offshore boundary sections (see also Sec. 3.3).

Based on the adjusted one year water level time series, for all SLR scenarios larger than 0 m, new one year time series were created. These time series start with the values of the 0 m SLR scenario and linearly/non-linearly (based on a sinusoidal function reflecting increasing SLR during the whole simulation period of 80 years) increase towards the values simulated for the final sea levels of 0.4 m, 0.96 m, 1.67 m and 2.63 m, respectively (Fig. 3.3). This allowed to simulate a continuous SLR with the Delft3D-Scheldt-SLR Model. All SLR scenarios (including the 0 m SLR scenario) were computed for a simulation time of 80 years (2020 to 2100) by using a morphological scale factor (so-called *morfac*) of 82.54. The morfac of 82.54 extends the one year (exact: 355 days) hydrodynamic simulation time (minus 1 day morphological spin-up time) and by this the SLR to a morphological simulation time of 80 years.

The waves model is forced with a uniform and constant wave condition along the offshore model boundaries based on the average significant wave height, wave peak period and mean wave direction measured at station Schouwenbank (just east of the eastern offshore model boundary, circa 24 km offshore the coastline; Fig. 3.2) in the period 1983 (2006 for wave directions) to 2014 (cf. VAN DER WEGEN *et al.* 2017). In line with the chosen wave condition also a uniform and constant wind field was applied. For this, the average wind speed and wind direction measured at Vlissingen (Fig. 3.2) in the period 2006 to 2014 were used.

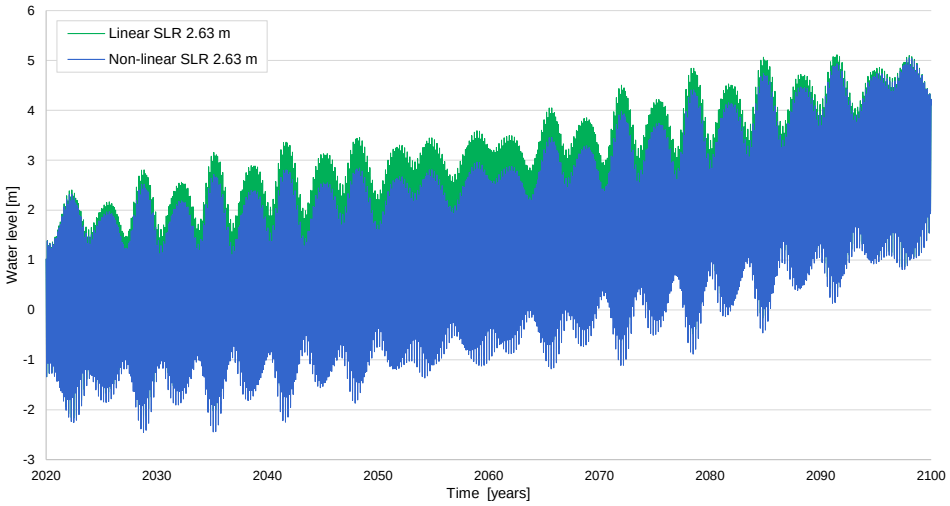

Figure 3.3 Water level time series for buoy station Westhinder (circa 32 km offshore the Belgian coast; Fig. 3.2) based on a linear (green curve) and non-linear (blue curve) sea level rise of 2.63 m in the period 2020 to 2100.

Three different configurations of the Delft3D-Scheldt-SLR Model are applied in this study, i.e. the (i) sand-only model without wave forcing, (ii) sand-only wave model with wave forcing and (iii) 3D sand-mud wave model with wave forcing (cf. Sec. 3.1). Both sand-only configurations (2DH, no salinity) consider a single sediment fraction in the form of fine sand with a median sediment diameter (D_{50}) of 200 μm, which is the dominant sediment fraction in the channels of the Western Scheldt (Sec. 2). The initial sediment thicknesses for fine sand were derived from measurements and estimations of the thickness of non-cohesive (i.e. easily erodible) sediment from the year 2012 (DAM 2013a; VAN DER WERF and BRIÈRE 2013). Starting with the 2012 sediment thicknesses and bathymetry as initial conditions, 25-year spin-up runs were performed for the two different DAD strategies (Fig. 3.1; Sec. 3.1) based on a SLR of 0 m and without beach nourishments. These spin-up runs allowed to determine model bathymetries and initial sediment thicknesses in better equilibrium with the model's hydrodynamics and DAD activities and by this to get a clearer picture of the hydro- and morphodynamic effects of SLR and of the sediment strategies. Non spun-up bathymetries and initial sediment thicknesses in the scenario simulations would result in a longer adaption of the model to the forcing and by this in more similarities between the different scenarios at the end

Table 3.3 Average significant wave height, wave peak period, mean wave direction (all parameters measured in the periods 1983/2006 to 2014 at buoy station Schouwenbank; Fig. 3.2), wind speed and wind direction (both measured between 2006 and 2014 at Vlissingen; Fig. 3.2) used for the forcing of the waves model in the form of a uniform and constant wave condition and wind field, respectively.

Parameter	Average value
Significant wave height H_s	1.41 m
Peak wave period T_p	6.5 s
Mean wave direction θ_m	292°
Wind speed V	5.5 m s^{-1}
Wind direction W	261°

of the simulations. All scenario runs therefore started based on the 25-year spun up sediment thicknesses and bathymetries determined for the two DAD strategies.

The sand-mud wave model takes account of fine sand ($D_{50} = 200\,\mu$m) and mud (cohesive sediment, $D_{50} \leq 63\,\mu$m), the latter being particularly present on the intertidal shoals and in the more upstream parts of the estuary (Chap. 2). The initial sediment thicknesses for the sand-mud wave model were determined following a similar approach as applied by VAN DER WEGEN *et al.* (2011) (San Pablo Bay, USA) and VAN MAREN *et al.* (2020) (Western Scheldt). Starting from the 2012 measured bathymetry, we performed a one year hydrodynamic simulation without bed updating. While the mud is initially not present in the model, it is entering the domain through the open model boundaries for which corresponding mud concentrations are imposed. During the simulation period, the mud distributes within the model domain based on the hydrodynamic conditions and sediment supply, until the available mud mass in the top active sediment layer approximates a dynamic equilibrium state. The mud percentage in the top layer was temporally averaged over the last 29.5 days of the simulation, which includes spring-neap tidal variations. We disregard cells at which notable sediment depletion occurred (e.g. in the channels) resulting in a low ($< 200\,\mathrm{kg\,m^2}$) sediment mass in the seabed. The generated percentage was imposed on the given 2012 sediment thicknesses to create the initial sand and mud thicknesses for the 25-year morphological spin-up simulations. Following that, the final conditions (e.g. hydrodynamics, bathymetry, sediment thicknesses, suspended sediment concentration and salinity) of the spin-up simulations were used to force the forecast simulations.

The mud transport in the sand-mud wave model is calculated according to the sediment transport formulation for cohesive sediment by PARTHENIADES (1965). We implement two mud fractions with a settling velocity (ws) of $0.5\,\mathrm{mm\,s^{-1}}$ and $2\,\mathrm{mm\,s^{-1}}$ along with a critical bed shear stress for erosion of mud ($TcrEro$) of $0.25\,\mathrm{N\,m^2}$, and an erosion parameter (M) of $1 * 10^{-4}\,\mathrm{kg\,m^{-2}\,s^{-1}}$. The bed stratigraphy consists of a top active (or transport) layer (0.5 m thick), which interacts with the water column, 4 underlayers (1 m thick each) and a base layer, which extends to the non-erodible bed. When deposition occurs, sediment is imported to the underlayers after mixing within the active layer. When erosion occurs, the active layer exports sediment to the water column, which is replenished from the below underlayer to maintain the active layer thickness.

The sand-mud wave model settings include a temporally constant mud suspended sediment concentration (SSC) at the model boundaries. A SSC of $100\,\mathrm{mg\,l^{-1}}$ and $50\,\mathrm{mg\,l^{-1}}$ is imposed at the shoreline at the south-western and north-eastern model boundaries, respectively (cf. Fig. 3.2). Further offshore, the SSC gradually decreases to $20\,\mathrm{mg\,l^{-1}}$. The concentrations at the seaward model boundaries are equally divided between the two mud fractions, while only the finer mud fraction ($ws = 0.5\,\mathrm{mm\,s^{-1}}$) is imposed at the riverine boundaries with a SSC of $200\,\mathrm{mg\,l^{-1}}$. Dredging (circa 2 m above NAP) is imposed starting from the riverine boundaries up to Rupelmonde in order to prevent exaggerated mud accumulation in the Scheldt and its tributaries.

The basic sand-mud wave model is a 3D model with 7 vertical sigma layers equally divided over the water column. Salinity effects are included by assigning a constant concentration of 32 psu and of 0 psu at the seaward and riverine boundaries, respectively. The model domain covers an area approximately equivalent to the sand-only (wave) model, albeit with a coarser horizontal grid resolution by a factor of about 4. The horizontal eddy diffusivity in the sand-mud wave model was increased to a value of $10\,\mathrm{m^2\,s^{-1}}$. Finally, the Scheldt tributaries, i.e. Zenne, Dijle, Kliene Nete, and Grote Nete are schematised as a single tributary.

For all three model configurations, a morphological hindcast for the period 1964 to 2012 was performed, in order to see how well the models predict the sediment budget and the bed level changes in the estuary observed in this historical period. In contrast to the scenario runs, the hindcast simulations do not start with spun up bathymetries and sediment thicknesses but use a historical bathymetry measured around the year 1964 (cf. Sec. 3.2). The historical sediment thicknesses for the year 1964 were determined by modifying the 2012 sediment thicknesses according to the observed bed level changes in the period 1964–2012. For this, the amount of erosion in metres recorded in this period was added to the initial sediment thickness observed in 2012 in order to obtain the approximate thicknesses for 1964. In the hindcast simulations, a morfac of 51.59 was applied.

3.3 Model calibration

Since the Delft3D-Scheldt-SLR Model is mainly based on the calibrated and validated Delft3D-NeVla Hincast Model by VAN DER WEGEN *et al.* (2017) and this study focuses on the relative but not on the absolute impact of SLR and sediment strategies on the estuary's hydro- and morphodynamics, no thorough model calibration was performed. For the hydrodynamic model calibration, the following steps were taken:

- For an accurate reproduction of the tidal amplitudes and phases (determined based on a classical tidal harmonic analysis according to PAWLOWICZ *et al.* (2002) for various water level stations in the model domain), the water level boundary conditions as derived from the GTSM model were adjusted by lowering the amplitudes of 32 tidal components by about 20 % (cf. Sec. 3.2).
- Spatially varying bottom friction (Manning's $n = 0.017\,\mathrm{s\,m^{-\frac{1}{3}}}$ to $0.025\,\mathrm{s\,m^{-\frac{1}{3}}}$) was tested against uniform bottom friction (Manning's $n = 0.023\,\mathrm{s\,m^{-\frac{1}{3}}}$).

The morphodynamic model calibration was mainly performed for the hindcast simulations and included

- tests with different values for the horizontal eddy diffusivity (between $1\,\mathrm{m^2\,s^{-1}}$ and $10\,\mathrm{m^2\,s^{-1}}$),
- tests with different sediment transport formulations for sand according to ENGELUND and HANSEN (1967) and VAN RIJN (1993, 2007),
- tests with different values for the current- and wave related suspended and bedload transport factors (Sus, Bed, SusW and BedW between 1 and 0.25),
- tests with different values for the critical bed shear stress for erosion of mud (TcrEro between $0.25\,\mathrm{N\,m^2}$ and $0.5\,\mathrm{N\,m^2}$), and
- tests with different discharges of the Scheldt river (average measured discharge of $120\,\mathrm{m^3 s^{-1}}$ against increased discharge of $360\,\mathrm{m^3 s^{-1}}$).

Additionally to the morphodynamic model calibration, sensitivity analyses based on the scenario simulations were performed for

- the different values for the horizontal eddy diffusivity,

Table 3.4 Overview of selected model parameter settings applied to the Delft3D-Scheldt-SLR Model. Parameters for which different settings were tested during the model calibration are listed in bold.

Parameter	Value/setting
Hydrodynamic simulation time	355 days
Time step	12 s
Wave communication interval	60 min
Wave computational mode	Stationary
Morphological scale factor (morfac)	82.54/51.59 [-]
Morphological simulation time	80 years
Dimensions	2D
Secondary flow	Switched on
Horizontal eddy viscosity	1 $m^2 s^{-1}$ (uniform)
Horizontal eddy diffusivity	1/10 $m^2 s^{-1}$ (uniform)
Bottom friction (Manning's n)	0.023 s $m^{-\frac{1}{3}}$ (uniform)
Total river discharge	120 $m^3 s^{-1}$
Median sand diameter (D50)	200 μm
Sediment transport formulation for sand	VAN RIJN (1993)
Sediment transport formulation for mud	PARTHENIADES (1965)
Current-related suspended and bedload transport factor (Sus, Bed)	0.5 [-]
Wave-related suspended and bedload transport factors (SusW, BedW)	0.3 [-]
Settling velocities for mud	0.0005 m s^{-1}/0.002 m s^{-1}
Erosion parameter for mud M	$1 * 10^{-4}$ kg m^{-2} s^{-1}
Critical bed shear stress for erosion of mud ($TcrEro$)	0.25 N m^2
Lateral bed slope factor (α_{bn})	100 [-]
Salinity	Not included

- the different bottom frictions,
- the different sediment transport formulations for sand,
- the different values for the current- and wave related suspended and bedload transport factors, and for
- different grain sizes for sand (200 μm against 250 μm and the combination of 120 μm and 250 μm),

in order to investigate the robustness of the scenario simulation results.

Table 3.4 gives an overview of the final specific physical and numerical parameter settings applied to the Delft3D-Scheldt-SLR Model. Parameters for which different settings were tested during the model calibration are listed in bold. For all remaining parameters available in the flow and waves modules, default values are taken according to Deltares (2019a,b).

4 Results

4.1 Morphological hindcast 1964–2012

4.1.1 Sediment budget

Figure 4.1 shows the cumulative total sediment volume changes (relative to 1964; excluding and including sand mining volumes) in the Western Scheldt estuary between Vlissingen-Breskens and the Dutch-Belgian border in the hindcast period 1964–2012 according to data in the literature (RWS 2012c) and according to simulated bed levels based on the three different configurations of the Delft3D-Scheldt-SLR Model. As described in Sec. 2, the hindcast period is characterised by three distinct deepening phases of the main navigation channel, i.e. between 1970 and 1975, 1995 and 2005. Especially since the second deepening phase of 1995, sediment dynamics in the Western Scheldt are being dominated by human interventions (cf. WANG *et al.* 2002). While the observed sediment volume of the Western Scheldt increased in the beginning of the hindcast period (grey solid curve in Fig. 4.1), it significantly decreased since 1970, i.e. simultaneously with the beginning of intensive sand mining (cf. grey solid and grey dotted curves), at an average yearly rate of about $2.7^{*}10^{6}$ m^3 until 2005. Since 2005 — the year of the third deepening phase — the sediment volume of the Western Scheldt was increasing again with about $1.65^{*}10^{6}$ m^3 per year on average. This increase, however, is at least not directly related to changes of the sand mining activities, since the sand mining volumes have even slightly increased in the period 2005–2012.

The cumulative total sediment volume changes simulated with the Delft3D-Scheldt-SLR Model are highly sensitive to the various model settings applied during the model calibration (Sec. 3.3). Figure 4.1 shows the volume changes simulated with the three different model configurations (i.e. the sand-only model, the sand-only wave model and the sand-mud wave model) based on the final model settings according to (cf. Tab. 3.4). The simulated volume changes show less variation in the short-term than the observed volume changes. This is mainly related to the constant sand mining volumes (average volume in the entire period) and the more constant DAD activities (continuous DAD after each time step based on three fixed dredging depth levels) in the model compared to reality. While both sand-only model configurations (solid beige and green curves) overestimate the observed volumes changes by almost factor 2, there is a close match in case of the sand-mud wave model (solid blue curve). The reduced volume loss in the sand-mud wave model compared to both sand-only models mainly is a result of (i) the import of mud into the estuary, (ii) the 3D modelling approach and (iii) a reduced sand export due to the sand being protected from erosion associated with the presence of mud in the model. The above mentioned three phases of the observed volume changes are not clearly reproduced by the model, which is partly caused by implementation of sand mining and DAD in the model (see above). Nevertheless, all model configurations, especially the sand-mud wave model, indicate an increased volumes loss in the period between ca. 1975 and ca. 2000 and a decrease of volume loss after ca. 2000.

The sediment volume change of the Western Scheldt in the hindcast period can also be illustrated in the form of yearly average volume changes for various defined cells in the estuary. Figure 4.2 shows these average volume changes or sediment budgets per cell (numbers 1 to 8) for the period 1964–2012 based on measured bed levels (A) and on the hindcast simulations performed with the three configurations of the Delft3D-Scheldt-SLR Model (B–D). According to the measured bed levels, cells 1, 2 and 4 are characterised by a positive average sediment budget (between $2.69^{*}10^{5}$ m^3 and

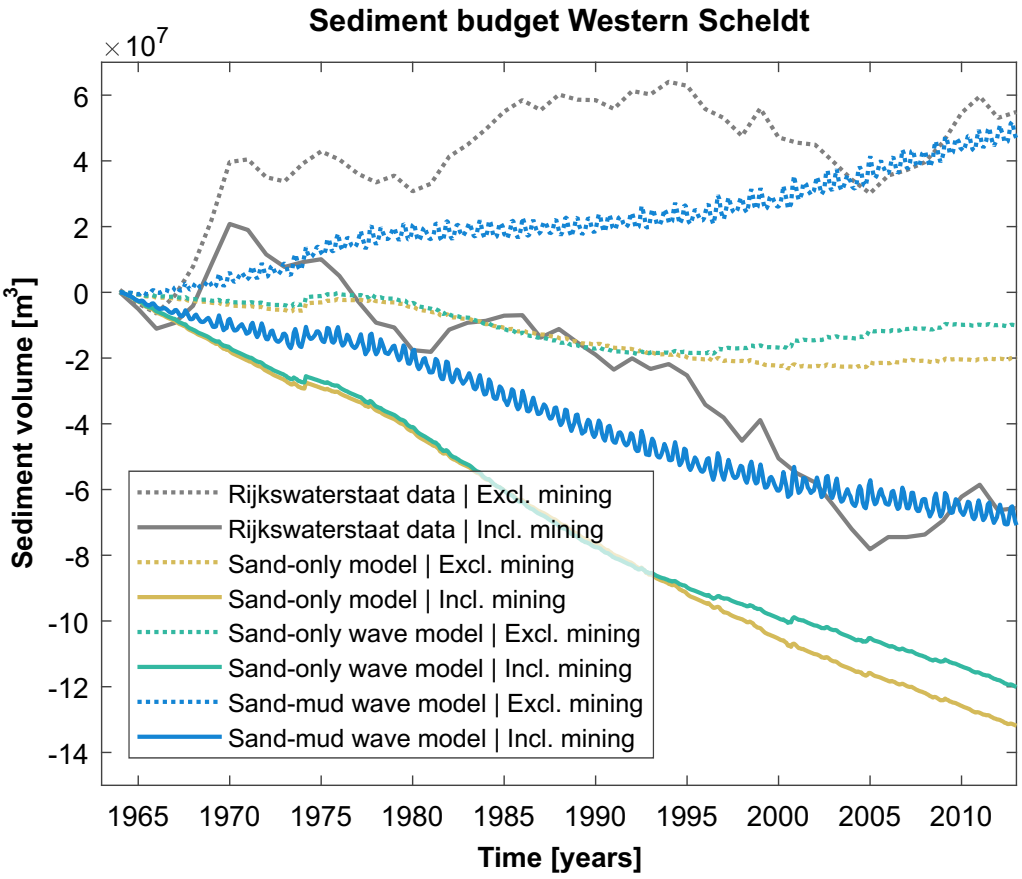

Figure 4.1 Cumulative total sediment volume change (relative to 1964) in the Western Scheldt estuary between Vlissingen-Breskens and the Dutch-Belgian border in the period 1964–2012 according to data available in the literature (RWS 2012c; grey curves) and according to bed level changes in the hindcast simulations based on the three configurations of the Delft3D-Scheldt-SLR Model, i.e. the sand-only model (beige curves), the sand-only wave model (green curves) and the sand-mud wave model (blue curves). Note that for reasons of comparability, the results of the 2D version of the sand-mud wave model are displayed. The dotted/solid curves show the sediment volume change excluding/including the sand mining volumes.

$5.86^{*}10^{5}$ m^3 per year), while a negative budget is recorded for cells 3 and 4–7 (between $-2.25^{*}10^{5}$ m^3 and $-5.54^{*}10^{5}$ m^3 per year). Consequently, the western estuary usually shows an increase in sediment volume, while there is a significant volume loss in the easternmost estuary in the period 1964–2012. Summing up the average sediment budgets for all cells results in an overall negative sediment budget in accordance with the grey solid line in Fig. 4.1. The observed patterns of the negative/positive sediment volume changes (blue to red patches) are usually well reproduced by all three model configurations, but particularly by the sand-mud wave model (Fig. 4.2 B–D). Both the sand-only model (B) and the sand-mud wave model (D) reproduce the observed positive average sediment budgets for cells 1, 2 and 4 and the observed negative average sediment budget for cells 3 and 4–7. The sand-only wave model (C) predicts the same budgets except for cell 2 (negative instead of positive). The magnitude of the average sediment budgets are generally overestimated in both sand-only cases (B, C), while there is a better match for the sand-mud wave model (D). Due to the coarser grid resolution and the higher diffusivity of the sand-mud wave model, the patterns of the width-averaged volume changes are spatially less variable compared to the sand-only model configurations, which, however, is not believed to have a qualitative impact on the results. Altogether, the sand-mud wave model yields the best reproduction of the sediment budgets of the various cells in the Western Scheldt in the hindcast period

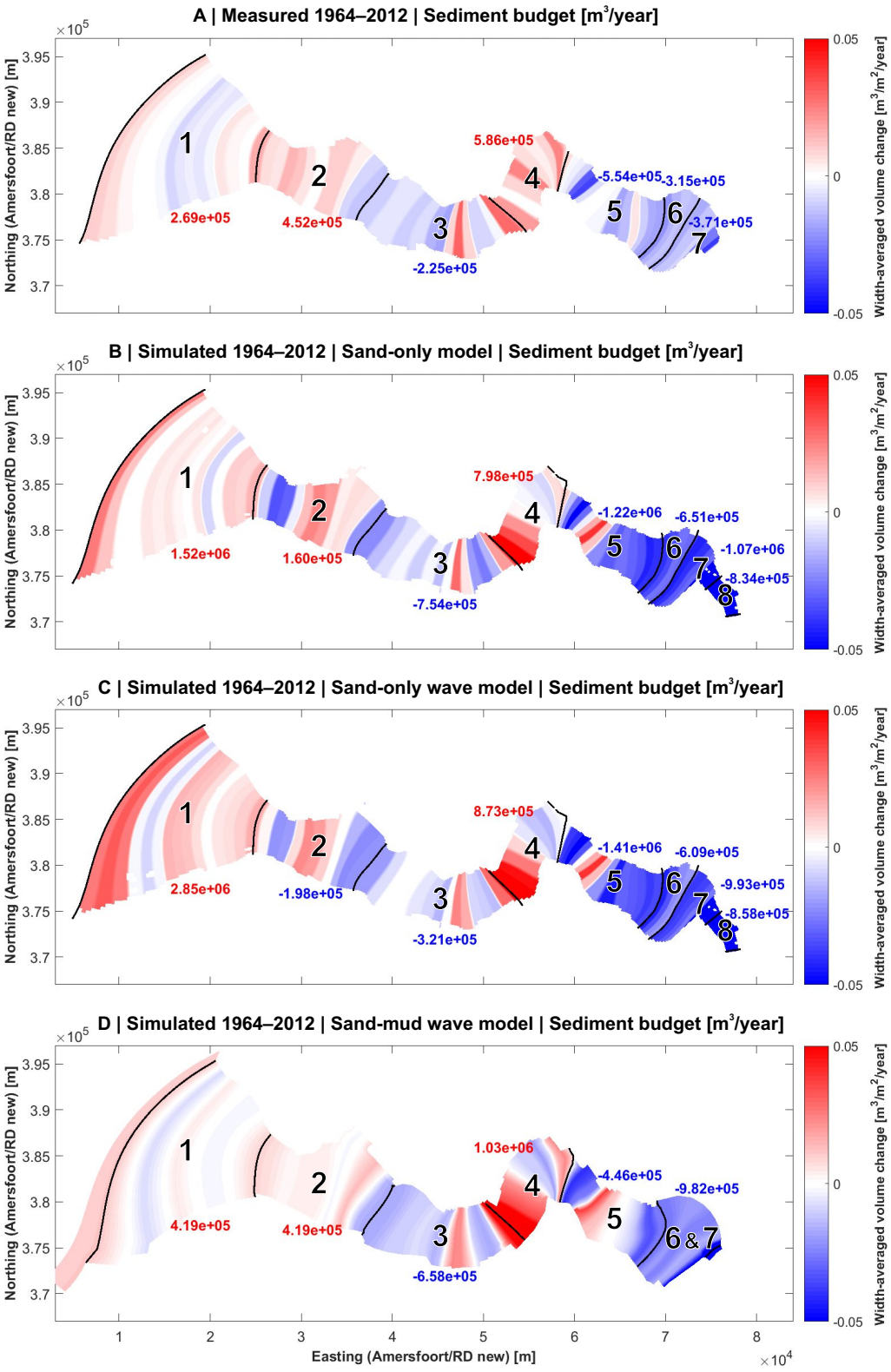

Figure 4.2 Sediment transport and budget for various defined cells (numbers 1 to 8) in the Western Scheldt estuary in the hindcast period 1964–2012 based on measured bed levels (A) and on the hindcast simulations performed with the sand-only model (B), the sand-only wave model (C) and the sand-mud wave model (D) configurations of the Delft3D-Scheldt-SLR Model (cf. Sec. 3.2). Numbers in blue/red indicate the averaged yearly negative/positive sediment budget per cell. Blue/red patches show areas of net negative/positive sediment volumes changes averaged over the width of the computational grid. Note that the boundaries of the cells in the sand-mud wave model slightly differ from those in the two sand-only model configurations due to the coarser grid resolution.

1964–2012, as was also found for the total sediment volume change presented above.

4.1.2 Morphodynamics

Figure 4.3 shows the cumulative erosion and sedimentation in the Western Scheldt estuary in the hindcast period 1964–2012 according to measured bed levels (A) and simulated bed levels based on the three configurations of the Delft3D-Scheldt-SLR Model (B–D). The observed bed level changes indicate significant deepening of the main navigation channel by up to 15 m during the hindcast period (Fig. 4.3 A), particularly in the upstream part of the Western Scheldt as well as between Terneuzen and Borssele (for the labels see Fig. 1.1). Sedimentation is most pronounced (up to 15 m) in the Middelgat and Eveningen channels located in the central Western Scheldt and — to a smaller amount and partly related to dumping of dredged material — in the area of the shoals Platen van Valkenisse, Platen van Ossenisse and Hooge Plaaten. The mouth area itself was comparably less dynamic in the hindcast period with bed level changes of between -5 m to 5 m.

In contrast to the sediment volume changes, the large-scale bed level changes simulated with the Delft3D-Scheldt-SLR Model were relatively little sensitive to the various model settings applied during the model calibration (Sec. 3.3) and model configurations (Fig. 4.3 B–D). In both sand-only cases (B, C), the absolute bed level changes (both erosion and sedimentation) are mostly overpredicted, especially in the western estuary and mouth. In case of the sand-mud wave model (D), however, the magnitude of bed level changes is clearly reduced (due to the 3D modelling approach and to the presence of mud in the model which protects the sand from being eroded too strong; see above) and thus in better agreement with the measurements. All three model configurations reproduce well the observed deepening of the main navigation channel as well as the sedimentation in the Middelgat and Eveningen channels. Dumping of sediment results in too pronounced sedimentation in all models (see e.g. dumping location north

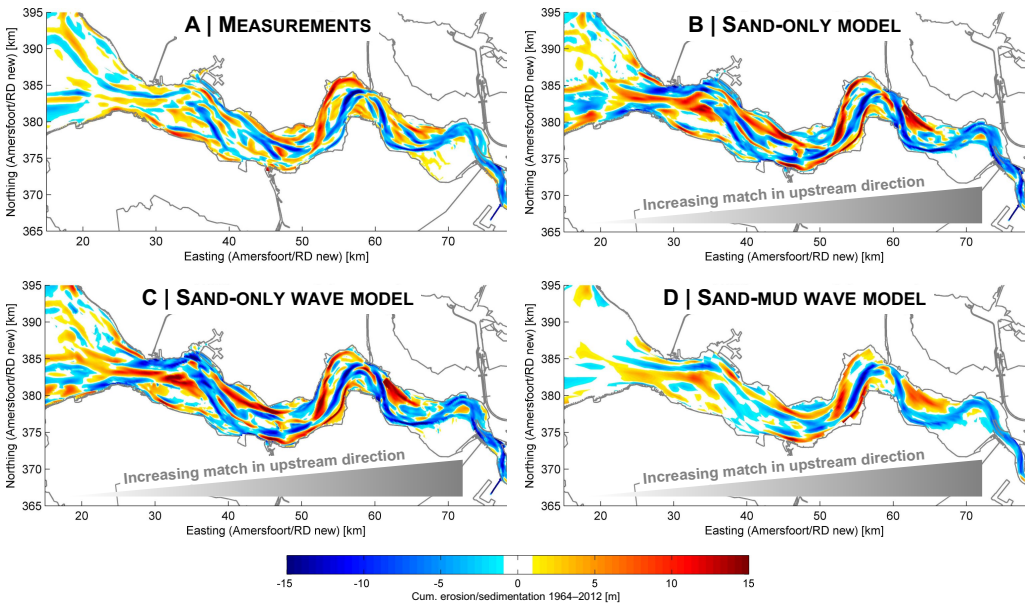

Figure 4.3 Cumulative erosion and sedimentation in the Western Scheldt estuary in the period 1964–2012 according to measured bed levels (A) and simulated bed levels based on the three configurations of the Delft3D-Scheldt-SLR Model, i.e. the sand-only model (B), the sand-only wave model (C) and the sand-mud wave model (D). Generally, the match between observed and simulated bed level changes increases upstream, where human interventions (in particular dredging, dumping and sand mining) dominate the estuarine morphodynamics to larger degree.

of the Platen van Valkenisse and around the Hooge Plaaten; cf. Fig. 3.1). This is due to dumping being realised in the models by releasing the dredged sediment directly at the bed but not at the water surface as it is happening in reality, which causes stronger spreading of the dumped sediment. While the mouth area and downstream part of the Western Scheldt show larger discrepancies between observed and simulated bed level changes, the match generally increases upstream, where human interventions such as dredging, dumping and sand mining dominate the estuarine morphodynamics to a larger degree. Including waves in the sand-only model mainly results in increased bed dynamics in the downstream and mouth area but does not clearly improve the simulated bed level changes (cf. Fig. 4.3 B–C). In contrast, the inclusion of mud and the 3D modelling approach are particularly relevant to achieve more realistic erosion-sedimentation patterns in the western estuary and, as mentioned before, to avoid an overestimation of the bed level changes (Fig. 4.3 D). Altogether, the sand-mud wave model therefore shows the best match with the measurements, as was observed for the total sediment volume change and the sediment budgets per cell (cf. Sec. 4.1.1). In general, the patterns of the predicted bed level changes are comparable with the results produced for similar hindcast periods by DAM 2013b (Fig. 4 therein) using a FINDEL2d model and by VAN DER WEGEN *et al.* 2017 (Fig. 4.5 therein) using the Delft3D-NeVla Hincast Model, i.e. the base for the Delft3D-Scheldt-SLR Model of the current study.

The hypsometric curves displayed in Fig. 4.4 give a summary view of the bed level changes of the Western Scheldt in the hindcast period 1964–2012 according to the measured (A) and simulated bed levels (B–D). The comparison of the 1964 (black dashed) and the 2012 (blue) curves in Fig. 4.4 A demonstrates that the intertidal area (circa above -2.5 m NAP) significantly rose as did the deep channels below -20 m NAP. In contrast, the area of the intermediate depths, i.e. between circa -2.5 m NAP and -20 m NAP, became lower. These trends are generally well predicted by all three model configurations (B–D), although the rise of intertidal area is underestimated while the subsidence of the area of the intermediate depths is overestimated by all three models.

4.2 Scenario results

This section deals with the simulation results — divided in hydrodynamics, residual sediment transport, sediment budget and morphodynamics — gained with the Delft3D-Scheldt-SLR Model based on the various scenarios listed in Table 3.2. Since the Delft3D-Scheldt-SLR Model was particularly created to investigate the relative but not the absolute impact of SLR and sediment strategies, in the following, we rather focus on the differences between the various SLR scenarios and between the different sediment strategies than the absolute model predictions (cf. Sec. 3.1). For reasons of clarity and comprehensibility, we do not show the simulation results for the whole set of performed scenarios runs but only for those which are relevant to the conclusions of this study. In particular we exclude the results of the non-linear SLR scenarios (cf. Sec. 3.2), the results based on the two alternative beach nourishment strategies and the results of the morphostatic simulations (cf. Sec. 3.1). In case of the non-linear SLR scenarios it could be observed that these simulations resulted in the same trends with regard to SLR and the sediment strategies as the simulations based on the linear SLR, although the morphological development at the end of the simulations in the 2100 was less advanced (for further details see Sec. 5). Concerning the two alternative beach nourishments, only minor quantitative but no qualitative impact on the hydro- and morphodynamic simulations results were found. Despite quantitative differences, the morphostatic simulations indicated the same trends regarding the sediment transport and budget as the morphodynamic simulations.

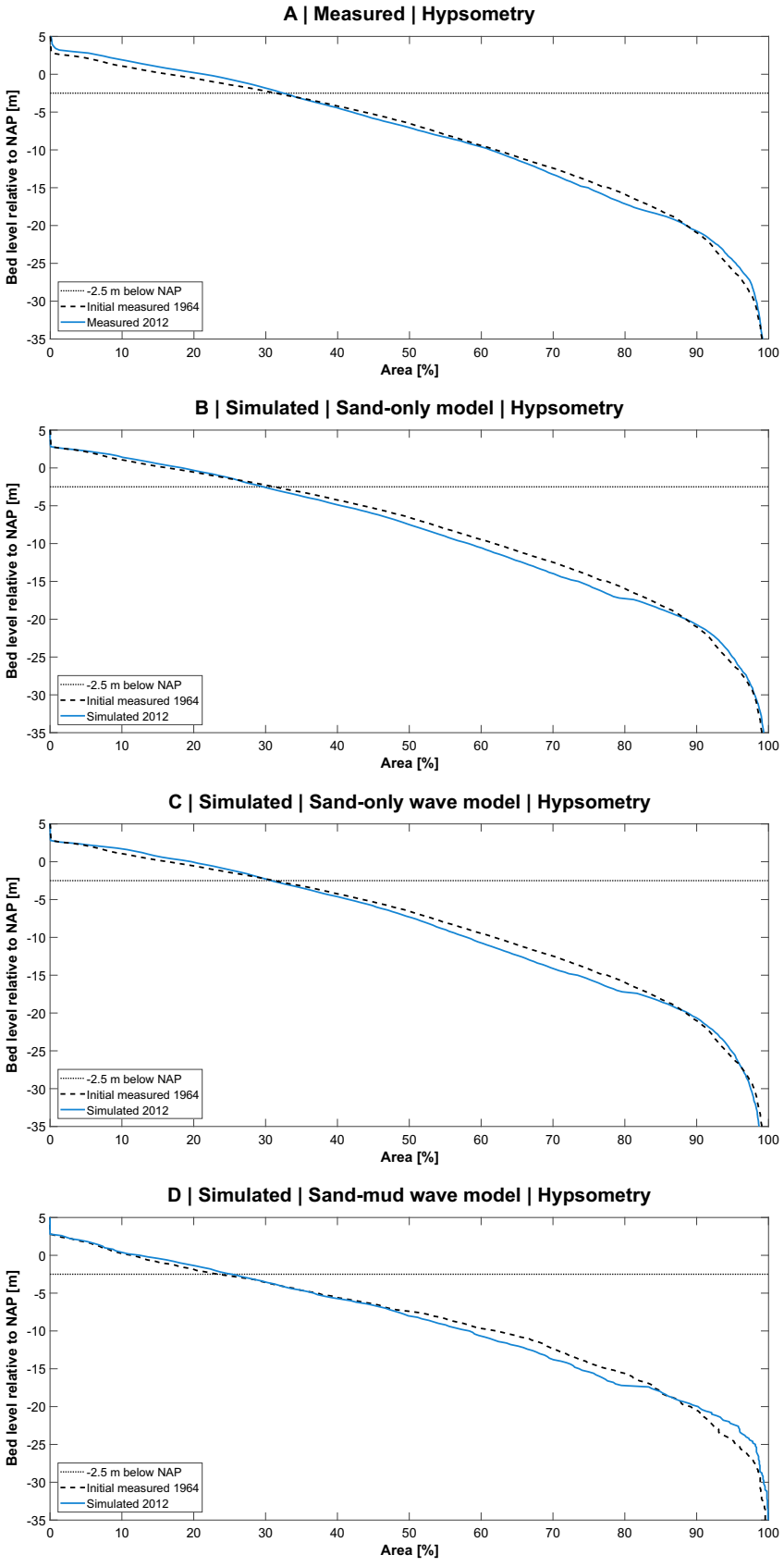

Figure 4.4 Hypsometric curves of the Western Scheldt estuary between Vlissingen-Breskens and the Dutch-Belgian border according to the bed levels measured in 1964 and 2012 (A) and simulated for 2012 based on the hindcast simulations performed with the sand-only model (B), the sand-only wave model (C) and the sand-mud wave model (D) configurations of the Delft3D-Scheldt-SLR Model. The -2.5 m NAP mark (black dotted line) indicates the approximate lower limit of the intertidal area.

4.2.1 Hydrodynamics

In this section, we present the hydrodynamics in the Western Scheldt as simulated separately based on the 2020 initial model bathymetry, current sea level (0 m SLR) and corresponding boundary conditions as well as based on the 2100 predicted bathymetries, 2100 sea levels and corresponding boundary conditions according to Table 3.1. In particular, we show the following hydrodynamic parameters: (i) the mean low (MLW) and mean high water levels (MHW), (ii) the amplitudes of the tidal components M2, S2 and M4, (iii) the relative tidal phases $2 * \varphi M2 - \varphi M4$ and (iv) the maximum flood and ebb flow velocities. These parameters show a significant sensitivity to the magnitude of SLR, while the observed trends are little influenced by the type of SLR (linear or non-linear), different DAD strategies, beach nourishments as well as by the presence of waves and mud in the Delft3D-Scheldt-SLR Model. Therefore, we focus on the hydrodynamics simulated in the different linear SLR scenarios based on the current DAD strategy without the inclusion of beach nourishments, which are representative for the corresponding other scenarios.

The top panel of Fig. 4.5 shows the simulated MLW and MHW for the years 2020 and 2100 for the linear SLR scenarios based on the current DAD strategy. The 2020 MLW and MHW closely correspond with the 2100 MLW and MHW in the 0 m SLR and 0.4 m SLR scenarios. Consequently, the simulated bed level changes after 80 years hardly influence the water levels. In the 0.96 m SLR, 1.67 m SLR and 2.63 m SLR scenarios, both, the MLW and MHW increase by about 1 m, 2 m and 3 m, respectively. The small differences in the water levels for the 0 m SLR and 0.4 m SLR scenarios compared to the large differences for the 0.96 m SLR, 1.67 m SLR and 2.63 m SLR directly reflect the differences between the global and the local SLR listed in Table 3.1. The table shows that a global SLR of 0.4 m results in a local SLR in the study area in the model by only 0.22 m, while a global SLR of 0.96 m, 1.67 m and 2.63 m results in a larger local SLR of 1.10 m, 1.96 m and 3.02 m respectively, for the reasons mentioned in Sec. 3.1.

In the bottom panel of Fig. 4.5, the corresponding simulated MLW and MHW for the years 2020 and 2100 corrected for the local SLR are illustrated. Consequently, the differences between the curves can directly be ascribed (i) to SLR related effects on the tides (in particular the tidal range) and (ii) to changes of the bathymetries within the 80 year simulation period in each SLR scenario. With increasing SLR, the MLW rises relatively less in the model. While the SLR corrected MLW at Vlissingen rises by about 0.12 m less in the 2.63 m SLR scenario compared to the 0 m SLR scenario, the difference is 0.37 m at Schelle. This means that the MLW is rising less in an upstream direction. In contrast to the MLW, the MHW rises relatively more with increasing SLR (except for the 0.4 m SLR scenario) and in an upstream direction (ca. 0.03 m more in the 2.63 m SLR scenario compared to the 0 m SLR scenario at Vlissingen, but 0.25 m more at Schelle). Consequently, the MLW rises less with SLR then the MHW does, resulting in an increase of the tidal range of 0.15 m at Vlissingen and of 0.62 m at Schelle in the 2.63 m scenario.

Figure A.1 in the Appendix shows the MLW and MHW (not corrected and corrected for SLR) simulated based on the future DAD strategy. As can be seen, both the MLW and MHW are almost the same at all gauge stations and therefore show the same trends as observed in the case of the current DAD strategy.

The observed changes of the simulated MLW, MHW and tidal range are closely related to the changes of the simulated amplitudes of the tidal components M2, S2 and M4 depicted in the upper panel of Fig. 4.6 for the current DAD strategy. In line with the increase in tidal range, the M2 and S2 amplitudes become significantly larger with increasing SLR in the model. This effect increases in an upstream direction. For the M2

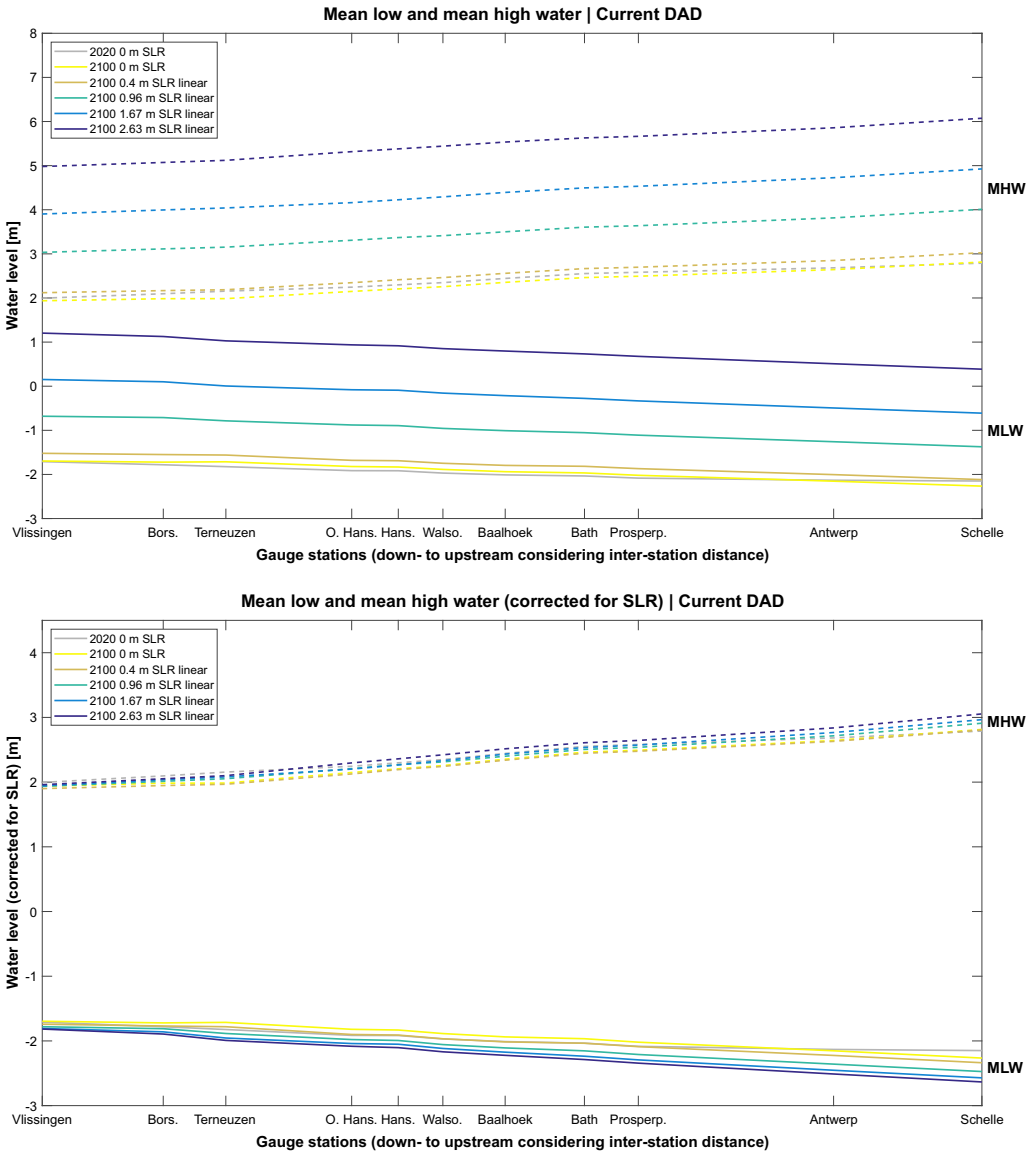

Figure 4.5 Comparison of simulated mean low (MLW) and mean high water levels (MHW) without SLR correction (top) and with SLR correction (based on the local SLR listed in Table 3.1; bottom) at various stations in the Western Scheldt estuary for the year 2020 (no SLR) and the year 2100 for various linear SLR scenarios for the current DAD strategy based on the sand-only model (cf. Table 3.2). MLW and MHW were derived from hydrodynamic simulation runs based (i) on the 2020 initial model bathymetry and 0 m SLR boundary conditions for the 2020 curves and (ii) on the 2100 predicted bathymetries and 2100 SLR boundary conditions associated with each SLR scenario for the 2100 curves. Based on the applied correction for SLR, differences between the curves in the bottom panel can directly be ascribed (i) to SLR related effects on the tides (amplitudes and phases) and (ii) to changes of the bathymetries within the 80 year simulation period in each SLR scenario.

tidal amplitude, the difference between the 0 m SLR and 2.63 m SLR scenarios is ca. 0.26 m at Vlissingen, while it is 0.56 m at Schelle. In contrast to M2 and S2, the M4 tidal amplitudes slightly decrease with increasing SLR. However, the absolute differences between the SLR scenarios are comparatively small. The future DAD strategy results in the same trends as described above for the case of the current DAD strategy (cf. Fig. A.2 in the Appendix).

The bottom panel of Fig. 4.6 shows the simulated relative tidal phases $2 * \varphi M2 - \varphi M4$

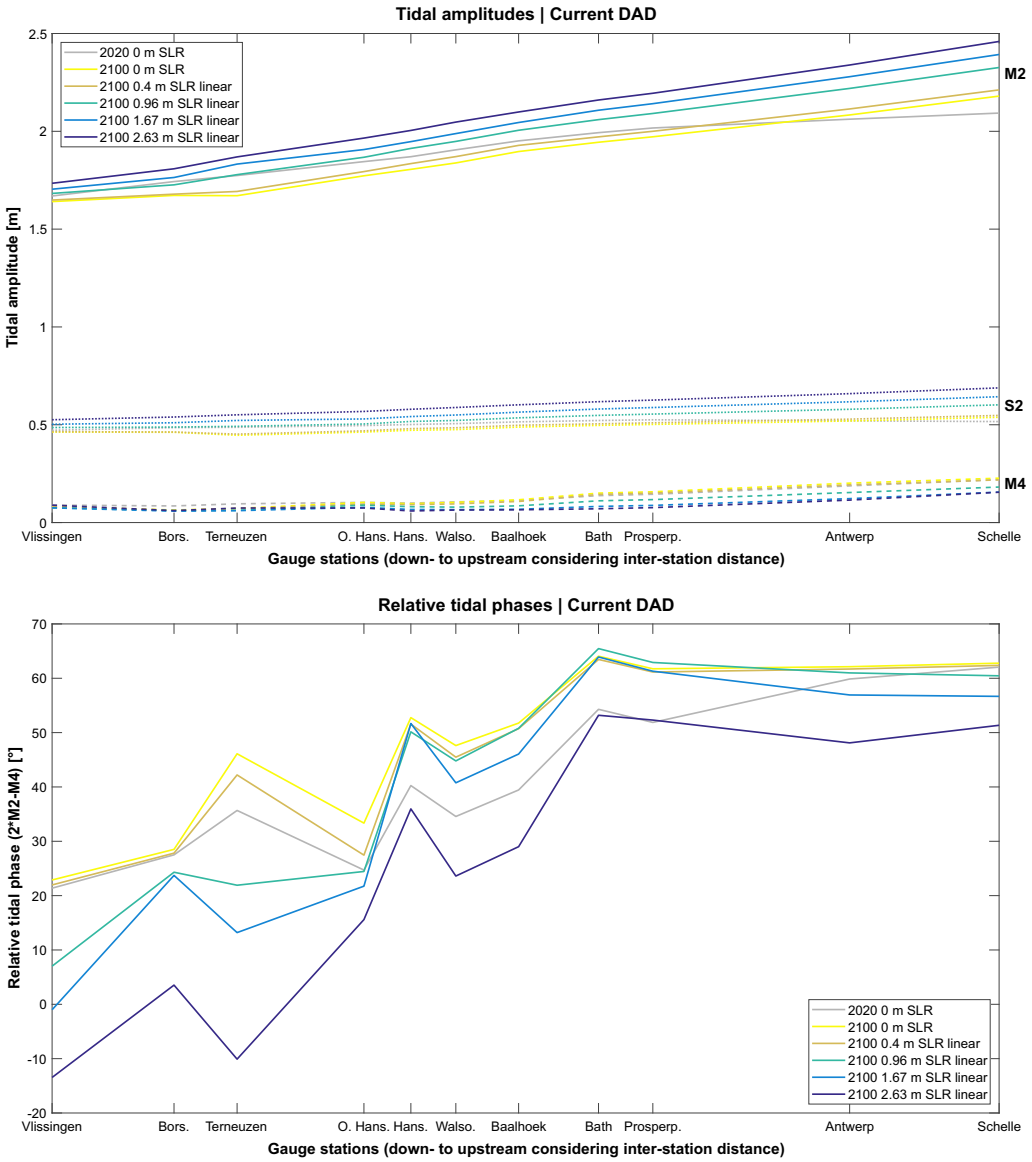

Figure 4.6 Comparison of simulated M2, S2 and M4 tidal amplitudes (top) and simulated relative tidal phases $2*\varphi M2-\varphi M4$ (bottom) at various stations in the Western Scheldt estuary for the year 2020 (no SLR) and the year 2100 for various linear SLR scenarios for the current DAD strategy based on the sand-only model (cf. Table 3.2). All parameters are derived from hydrodynamic simulation runs based (i) on the 2020 initial model bathymetry and 0 m SLR boundary conditions for the 2020 curves and (ii) on the 2100 predicted bathymetries and 2100 SLR boundary conditions associated with each SLR scenario for the 2100 curves. Differences between the curves can directly be ascribed (i) to SLR related effects on the tides (amplitudes and phases) and (ii) to changes of the bathymetries within the 80 year simulation period in each SLR scenario.

for the different SLR scenarios. The relative tidal phase expresses the vertical tidal asymmetry of a tidal basin and by this indicates where the basin is ebb dominant (falling tide lasts longer than the rising tide; $0° > 2*\varphi M2-\varphi M4 > -180°$) and where it is flood dominant (rising tide lasts longer than the falling tide; $0° < 2*\varphi M2-\varphi M4 < 180°$). The tidal asymmetry is an important parameter affecting the residual sediment transport in a basin (cf. e.g. BOLLE *et al.* 2010; WANG *et al.* 2002; GUO *et al.* 2018). The 2020 curve in Fig. 4.6 shows that the Western Scheldt is entirely flood dominant based on the initial model bathymetry and 0 m SLR boundary conditions. This flood dominance increases upstream. With increasing SLR, however, the system becomes less flood dominant,

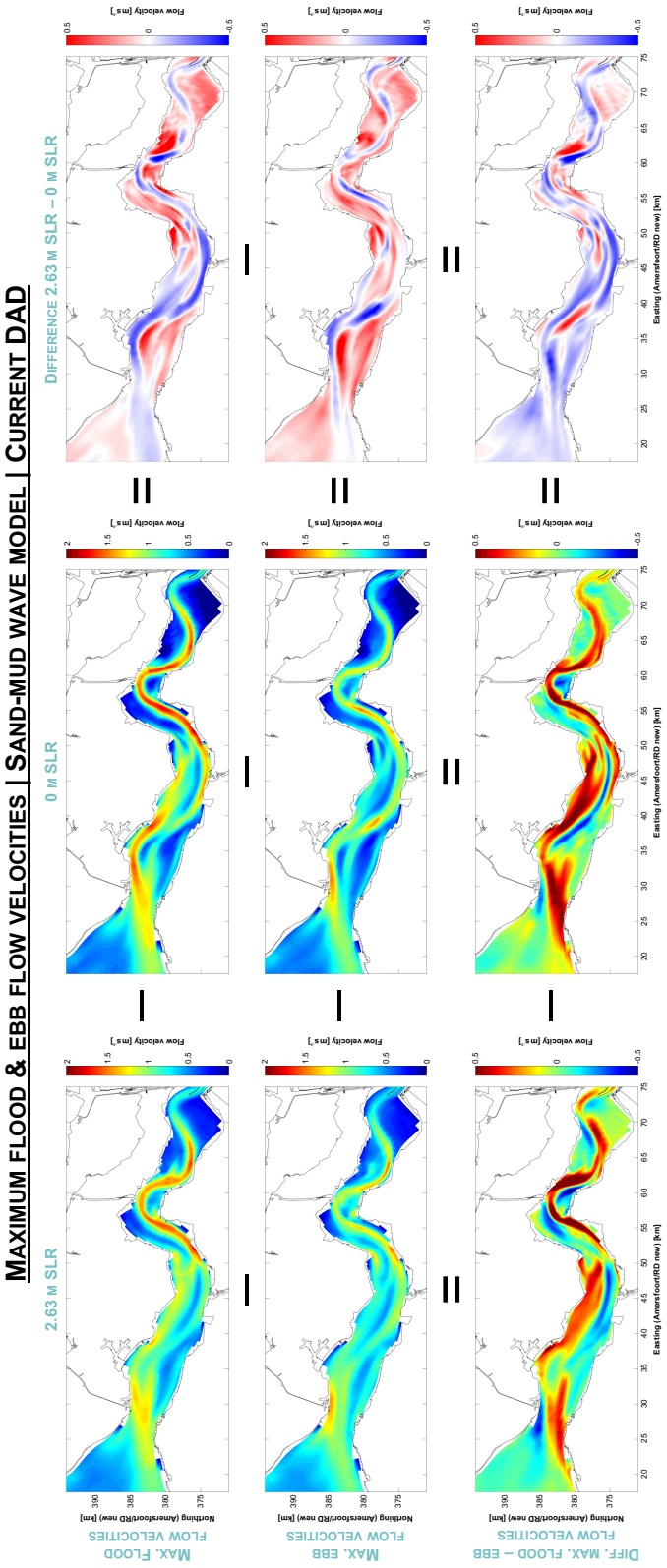

Figure 4.7 Maximum flood (top row) and ebb (central row) flow velocities in the Western Scheldt estuary during spring tide in 2100 simulated with the sand-mud wave model configuration of the Delft3D-Scheldt-SLR Model for the 2.63 m linear SLR (left column) and the 0 m SLR (central column) scenarios based on the current dredging and dumping (DAD) strategy without beach nourishments but with wave forcing (cf. Table 3.2). The illustrated flow velocities are derived from the bottom two layers of the (3D) sand-mud wave model, which are representative for the depth-averaged flow velocities. The bottom panels show the differences between the maximum flood and ebb flow velocities, with blue/yellow to red patches indicating lower/higher flood velocities compared to the ebb velocities. The panels of the right column display the differences in the maximum flood and ebb flow velocities between the 2.63 m SLR and the 0 m SLR scenarios, with blue/red patches indicating lower/higher flow velocities in case of the 2.63 m SLR scenario.

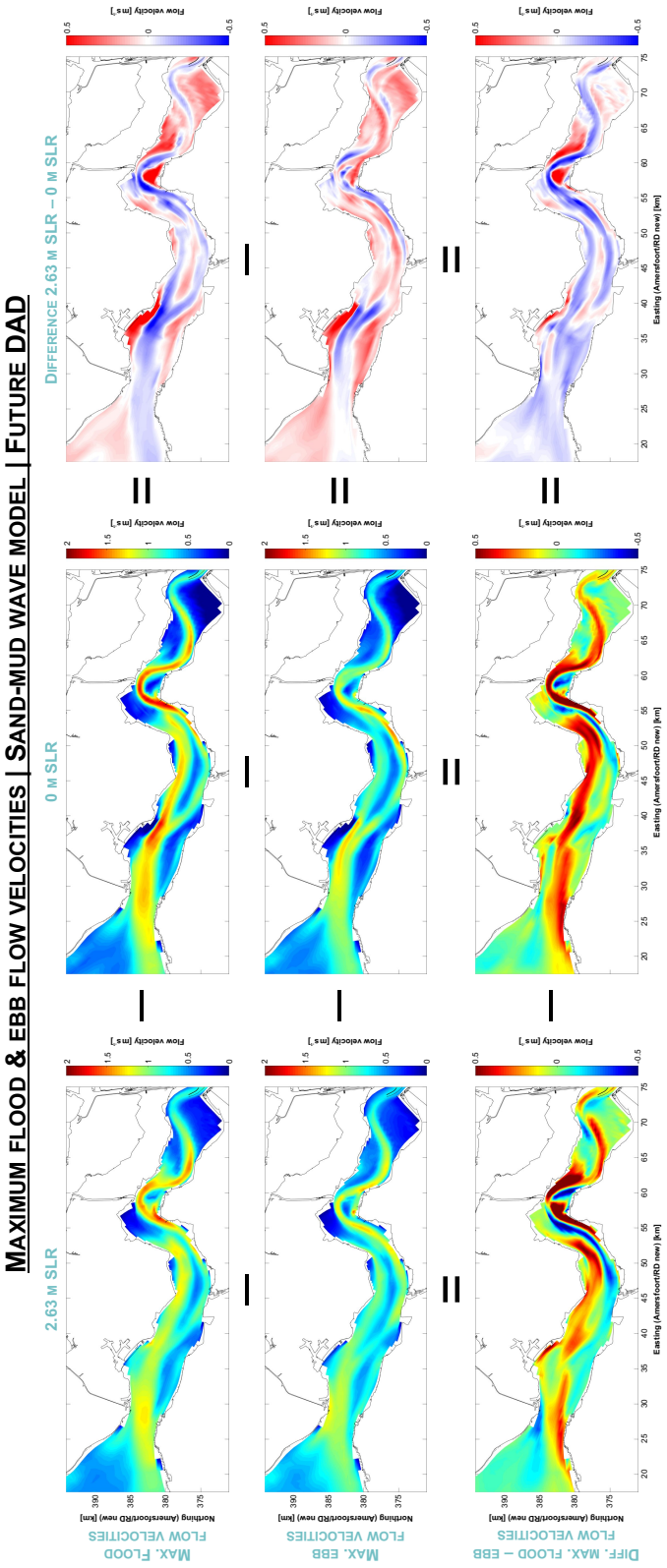

Figure 4.8 Maximum flood (top row) and ebb (central row) flow velocities in the Western Scheldt estuary during spring tide in 2100 simulated with the sand-mud Delft3D-Scheldt-SLR Model for the 2.63 m linear SLR (left column) and the 0 m SLR (central column) scenarios based on the future dredging and dumping (DAD) strategy (cf. Table 3.2). The illustrated flow velocities are derived from the bottom two layers of the (3D) sand-mud wave model, which are representative for the depth-averaged flow velocities. The bottom panels show the differences between the maximum flood and ebb flow velocities, with blue/yellow to red patches indicating lower/higher flood velocities compared to the ebb velocities. The panels of the right column display the differences in the maximum flood and ebb flow velocities between the 2.63 m SLR and the 0 m SLR scenarios, with blue/red patches indicating lower/higher flow velocities in case of the 2.63 m SLR scenario.

particularly in the downstream part of the estuary. In the most extreme scenario, i.e. the 2.63 m SLR scenario, the estuary turns even ebb dominant downstream of Terneuzen. Although the absolute relative tidal phases slightly differ, the same observations can be made for the case of the future DAD strategy (cf. Fig. A.2 in the Appendix).

The tidal asymmetry of a tidal basin is reflected by the asymmetry in maximum flood and ebb flow velocities (also called peak current asymmetry — PCA; cf. GUO *et al.* 2018). In Fig. 4.7, the maximum flood (top row) and ebb (central row) flow velocities in the Western Scheldt estuary during spring tide in 2100 simulated with the sand-mud wave model based on the current DAD strategy are illustrated. The results are only shown for the 2.63 m linear SLR (left column) and the 0 m SLR (central column) scenarios in order to visualise the maximum effects of SLR on the peak current asymmetry, while the effects are the same for the other SLR scenarios although less pronounced. The highest maximum flood and ebb flow velocities occur in the channels of the estuary. The maximum flood flow velocities are usually larger (up to $2\,m\,s^{-1}$) than the maximum ebb flow velocities (up to $1.5\,m\,s^{-1}$), reflecting the general flood dominance of the estuary (cf. Fig. 4.6). In the area of the channels, both the maximum flood and ebb flow velocities are mostly larger in the 0 m SLR than in the 2.63 m SLR scenario (see blue patches in the difference plots in the right column of Fig. 4.7), while it is the opposite in the shallow waters of the estuary. This is a direct result of the higher sea level in the 2.63 m SLR scenario: due to the increase in water depth with SLR, the flow velocities in the deep channels decrease (larger cross-sectional area), while they increase in shallow water (reduced bottom friction for surface flow) and there is more flow across the intertidal area (increasing inundation with increasing water depth).

The comparison of the upper two difference plots in the right column of Fig. 4.7 makes clear that the maximum flood flow velocities in the channels decrease more than the maximum ebb flow velocities in the 2.63 m SLR compared to the 0 m SLR scenario. As a consequence, the difference between the maximum flood and ebb flow velocities in the channels become smaller in the case of the 2.63 m SLR scenario, particularly in the western estuary (cf. difference plots at the bottom of Fig. 4.7). This means that the peak ebb flow becomes relatively more dominant, which is in line with the observed decrease of the flood dominance in the estuary with SLR (cf. Fig. 4.6). The maximum flood and ebb flow velocities simulated based on the future DAD strategy (Fig. 4.8) show the same trends as described for the case of the current DAD strategy above, although the flow patterns look different since the predicted locations and depths of the channels and shoals in the year 2100 differ for both DAD strategies (see Sec. 4.2.4).

4.2.2 Residual sediment transport

The residual sediment transport is an important parameter controlling the morphological changes and sediment budget of a tidal basin. The residual sediment transport is closely related to the tidal asymmetry/the peak current asymmetry of a basin (see Sec. 4.2.1 and below). Figure 4.9 shows the residual sediment (sand) transport in the Western Scheldt estuary during spring tide simulated based on the predicted 2100 bed levels with the sand-mud wave model applying the current DAD strategy. The results are only shown for the 0 m SLR (top) and the 2.63 m linear SLR (centre) scenarios in order to visualise the maximum effects of SLR on the residual sediment transport, while the effects are the same for the other SLR scenarios although less pronounced.

In both the 0 m SLR and the 2.63 m scenarios, the patterns of the residual sediment transport closely correspond to the patterns of the differences between the maximum flood and ebb flow velocities (cf. Sec. 4.2.1). Consequently, areas where the maximum flood flow velocities are higher than the maximum ebb flow velocities (yellow to red patches in the bottom panels of the left and central column in Fig. 4.7) coincide with

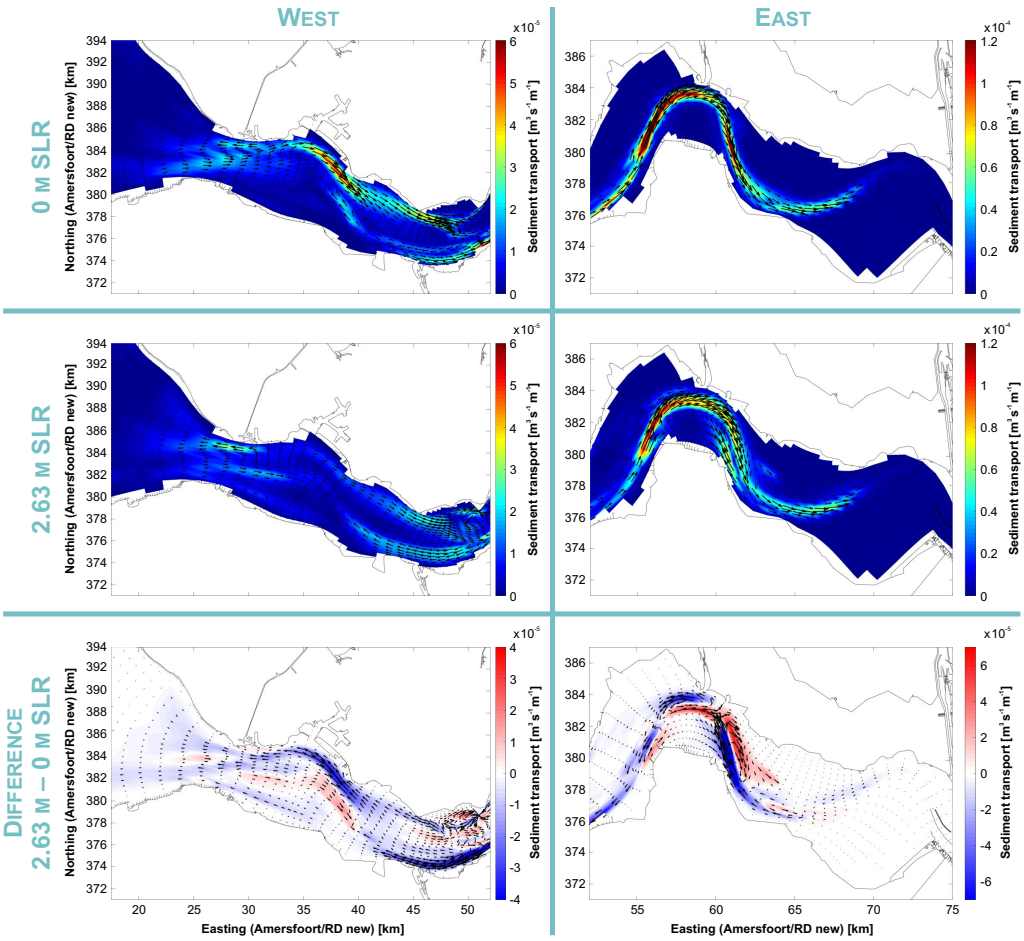

Figure 4.9 Residual sediment (sand) transport in the Western Scheldt estuary during spring tide in 2100 simulated with the sand-mud wave model configuration of the Delft3D-Scheldt-SLR Model for the 0 m SLR (top) and the 2.63 m linear SLR (centre) scenarios based on the current dredging and dumping (DAD) strategy without beach nourishments but with wave forcing (cf. Table 3.2). The bottom panels show the differences in residual sediment transport between the 2.63 m SLR and the 0 m SLR scenarios, with blue/red patches indicating a larger seaward/landward sediment transport in case of the 2.63 m SLR scenario.

landward residual sediment transport and vice versa. This demonstrates that the peak current asymmetry is the dominant factor determining the residual sediment transport in the Western Scheldt. As a result, the changes of the peak current asymmetry due to SLR described in Sec. 4.2.1 are directly reflected by the changes of the residual sediment transport due to SLR. This means that, in most parts of the estuary, especially in the west, the landward residual sediment transport decreases with SLR while the seaward residual sediment transport increases (see dominant blue patches in the bottom panels of Fig. 4.9). More specifically, the following observations can be made:

- At the entrance to the estuary between Vlissingen and Breskens, the seaward/landward residual sediment transport along the northern/southern bank clearly increases/decreases in the 2.63 m SLR compared to the 0 m SLR scenario.
- The landward residual sediment transport in the Everingen channel (for labels see Fig. 1.1) strongly decreases in the 2.63 m SLR compared to the 0 m SLR

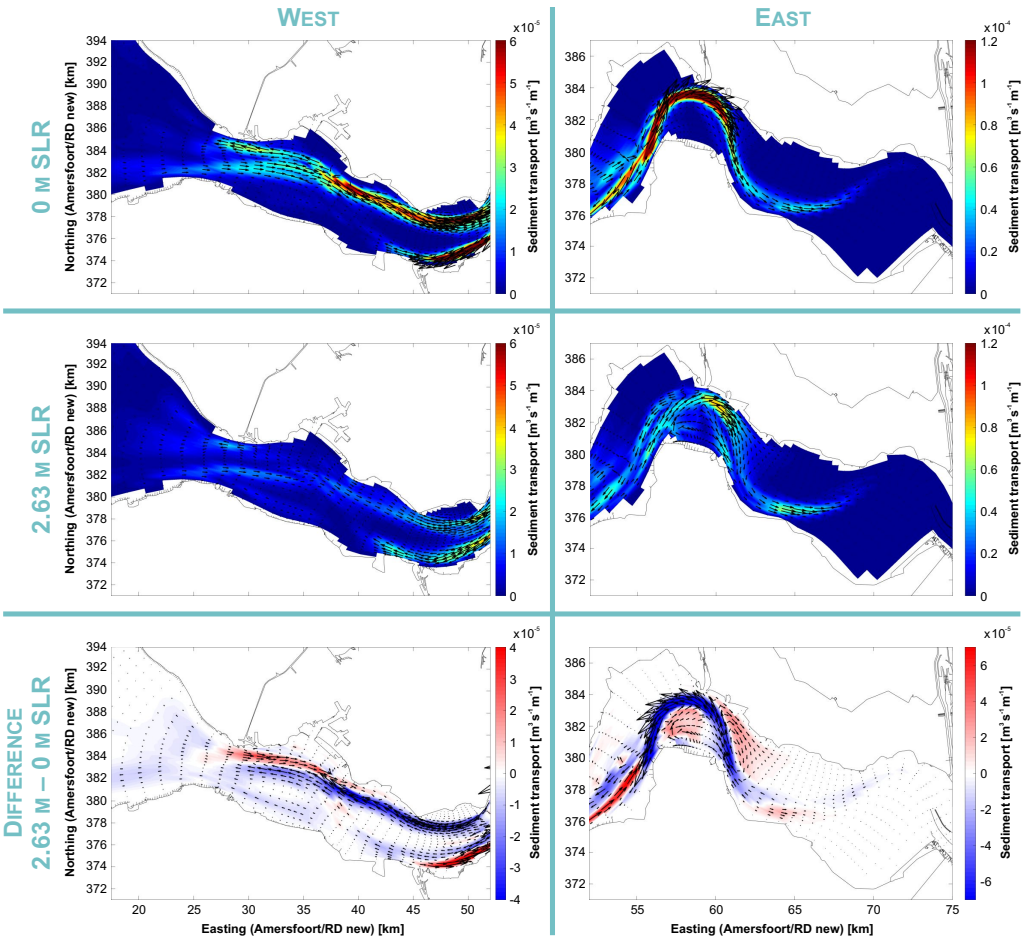

Figure 4.10 Residual sediment (sand) transport in the Western Scheldt estuary during spring tide in 2100 simulated with the sand-mud wave model configuration of the Delft3D-Scheldt-SLR Model for the 0 m SLR (top) and the 2.63 m linear SLR (centre) scenarios based on the current dredging and dumping (DAD) strategy without beach nourishments but with wave forcing (cf. Table 3.2). The bottom panels show the differences in residual sediment transport between the 2.63 m SLR and the 0 m SLR scenarios, with blue/red patches indicating a larger seaward/landward sediment transport in case of the 2.63 m SLR scenario.

scenario, while the seaward residual sediment transport in the channel Pas van Terneuzen becomes more pronounced.

- Also in the channels Gat van Ossenisse and Put van Hansweert, the landward residual sediment transport decreases in the 2.63 m SLR compared to the 0 m SLR scenario, although the decrease is less pronounced than in the other channels mentioned above. At the same time, a seaward residual sediment transport emerges in the downstream part of the Zuidergat channel.
- Upstream of the Zuidergat, the impact of SLR on the residual sediment transport in the Western Scheldt clearly diminishes.

Figure 4.10 shows the residual sediment (sand) transport in the Western Scheldt estuary for the case of the future DAD strategy. Also in this case, there is a close agreement with the patterns observed for the peak current asymmetry (cf. Fig. 4.8). Consequently, the SLR causes a general decrease/increase of the landward/seaward residual sediment transport. Nevertheless, there are several differences and shifts in the patterns of

the landward and seaward residual sediment transports since the predicted locations and depths of the channels and shoals in the year 2100 differ for both DAD strategies (see Sec. 4.2.4).

4.2.3 Sediment budget

An essential parameter to evaluate the long-term morphological development of the Western Scheldt estuary under SLR is the sediment budget. It is the sum of (i) the sediment transport through the cross-sections at Vlissingen-Breskens and the Dutch-Belgian border, (ii) the DAD across these cross-sections as well as (iii) the sand mining (the scenario runs do not consider sand mining). The sediment transport through the cross-section Vlissingen-Breskens — situated at the seaward border of the estuary — is of particular interest to assess the impact of SLR on the sediment budget of the Western Scheldt, since the sea is the most relevant natural sediment source for the Western Scheldt.

Figure 4.11 shows the simulated cumulative sediment transport through cross-section Vlissingen-Breskens in the period 2020 to 2100 for the different linear SLR scenarios and sediment strategies based on the sand-only model configuration of the Delft3D-Scheldt-SLR Model (cf. Table 3.2). The four figure panels indicate that in most scenarios sediment export is dominating during most of the simulation time. The impact of SLR on the sediment transport can — independent of the applied sediment strategy — be summarised as follows: (i) the export of sediment increases with SLR, (ii) there is a small difference in sediment transport between the 0 m and 0.4 m SLR scenarios but a significant difference onwards from 0.96 m, resulting in a maximum difference between the 0 m and 2.63 m SLR scenarios in 2100 of about $11 * 10^7$ m^3. Besides SLR, the DAD strategies have a clear impact on the sediment transport. Independent of the SLR scenario and the beach nourishments, the sediment export is significantly smaller or even turns into sediment import in case of the future DAD strategy compared to the current DAD strategy, with an absolute difference between both in 2100 of up to $4 * 10^7$ m^3. Similar to the future DAD strategy, also beach nourishments in the mouth of the Western Scheldt result in less sediment export or even sediment import, although this effect is comparatively small (maximum difference in 2100: $1 * 10^7$ m$^3 \widehat{=} 12.5\,\%$ of the total nourishment volume). Altogether, the current DAD strategy in combination with no beach nourishments result in the maximum sediment export at Vlissingen-Breskens in all five SLR scenarios, while the minimum sediment export can be observed in case of the future DAD strategy in combination with beach nourishments.

The cumulative sediment transport simulated based on the sand-only wave model (Fig. 4.12) show the same trends as described above for the case without wave forcing. However, the wave forcing results in less sediment export/more sediment import in all scenarios. This is due to the wave related sediment transport from the mouth into the estuary as a result of the prevailing west-south-westerly wave and wind direction in combination with the shallow waters in the mouth. Generally, the cumulative sediment transport shows larger variations over time compared to the case without wave forcing (cf. Fig. 4.11). This is a result of the increased bed dynamics and migration of morphological features in the area of cross-section Vlissingen-Breskens due to the presence of waves in the model (cf. Sec. 4.2.4).

In Fig. 4.13, the cumulative sediment transport (divided by sand and mud) through cross-section Vlissingen-Breskens is illustrated based on the sand-mud wave model configuration of the Delft3D-Scheldt-SLR Model. While mud is being imported, the cumulative transport of sand is significantly reduced compared to Figs. 4.11 and 4.12. This is due to the 3D modelling approach and the mud protecting the sand from erosion in the model (sand and mud are homogeneously mixed in the model, although

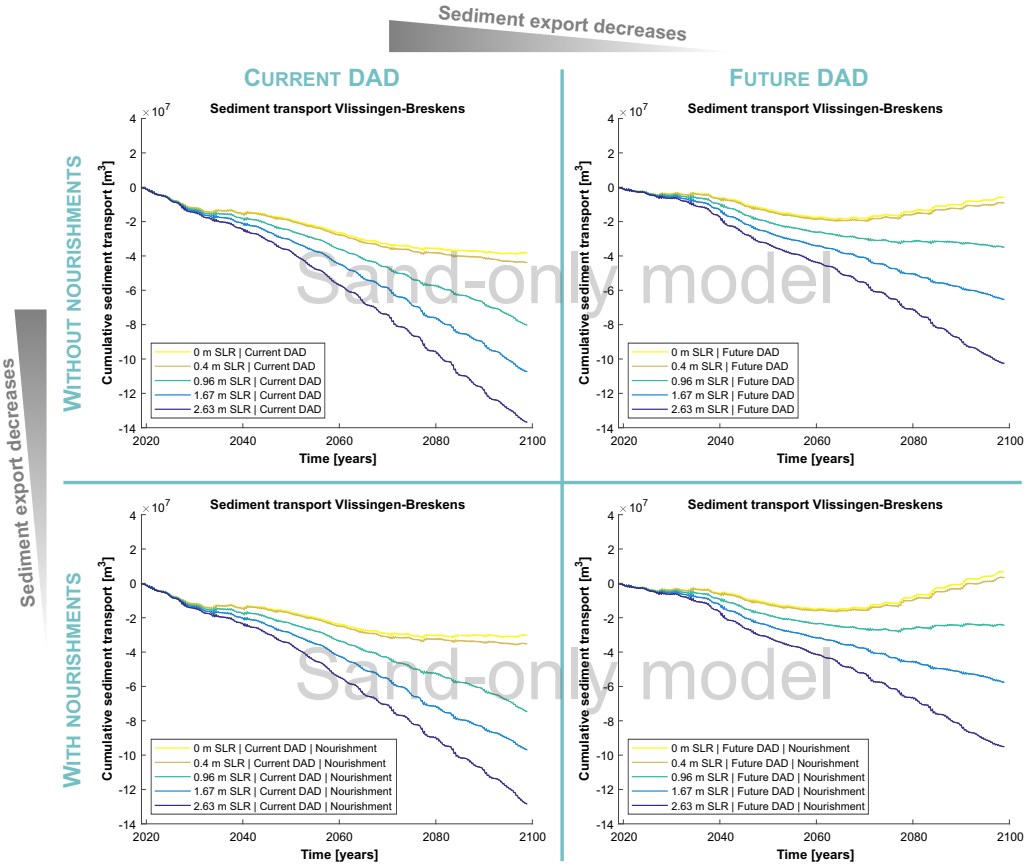

Figure 4.11 Cumulative sediment transport (sand only) through cross-section Vlissingen-Breskens at the mouth of the Western Scheldt in the period 2020 to 2100 simulated for five linear SLR scenarios for the current (left panels) and future (right panels) dredging and dumping (DAD) strategy without beach nourishments (top panels) and with beach nourishments (bottom panels) based on the sand-only model configuration of the Delft3D-Scheldt-SLR Model (cf. Table 3.2). Negative/positive values indicates seaward/landward sediment transport, i.e. sediment export/import. Both, in case of the future DAD strategy and in case of beach nourishments, the sediment export from the Western Scheldt to the mouth is reduced or even turns into sediment import.

with different spatial availability; cf. Sec. 3.2). In general, the inclusion of mud does not change the trends observed for the sand-only cases without/with waves. Consequently, increasing SLR still results in increasing sediment export/decreasing sediment import and there is less sediment export/more sediment import in case of the future DAD strategy (beach nourishments are not considered here).

Figure 4.14 shows the sediment (sand only) transport and budget for various defined cells (numbers 1 to 8) in the Western Scheldt estuary simulated for the five linear SLR scenarios and the current DAD strategy based on the sand-only model (cf. Table 3.2). Altogether, the following observations can be made:

- **Sediment transport volumes:** In all scenarios, most of the cross-sections show an landward sediment transport, while cross-section Vlissingen-Breskens (i.e. the boundary between Cells 1 and 2) shows a considerable seaward sediment transport (i.e. sediment export). The yearly averaged sediment transport/export through cross-section Vlissingen-Breskens increases with increasing SLR (from $4.65 * 10^5$ m^3/year in the 0 m SLR scenario to $1.66 * 10^6$ m^3/year in the 2.63 m SLR scenario), as was observed based on the cumulative sediment transport

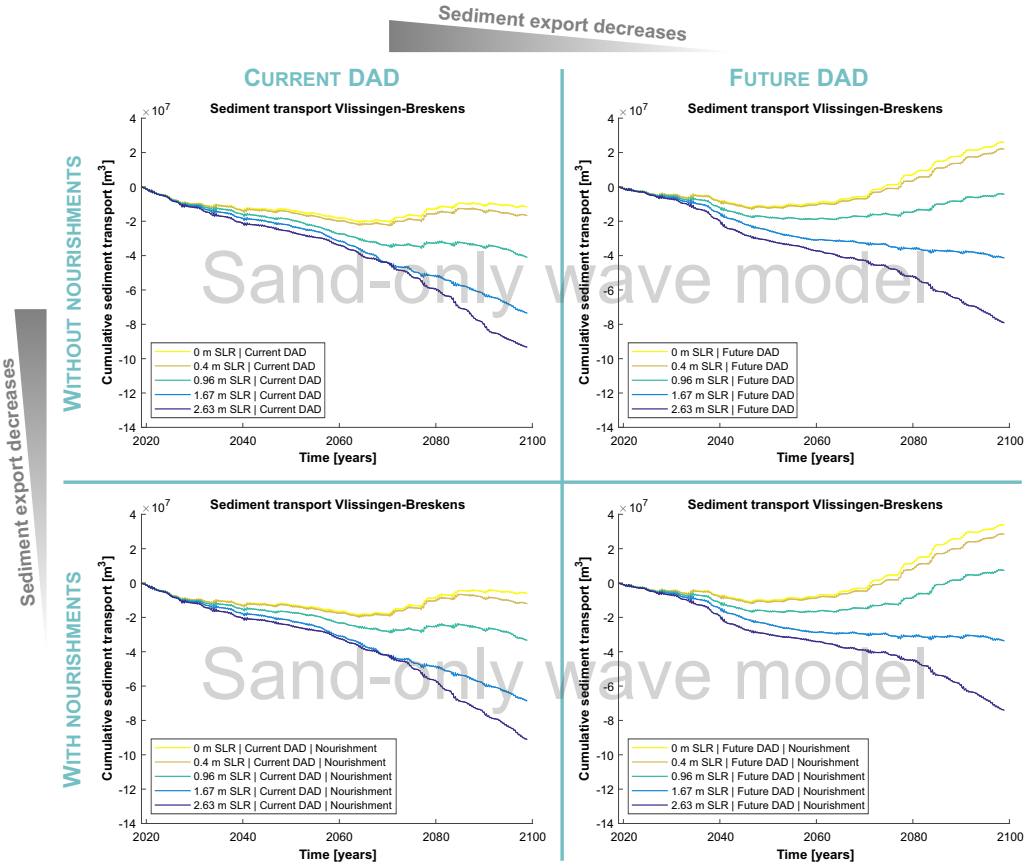

Figure 4.12 Cumulative sediment transport (sand only) through cross-section Vlissingen-Breskens at the mouth of the Western Scheldt in the period 2020 to 2100 simulated for five linear SLR scenarios for the current (left panels) and future (right panels) dredging and dumping (DAD) strategy without beach nourishments (top panels) and with beach nourishments (bottom panels) based on the sand-only wave model configuration of the Delft3D-Scheldt-SLR Model (cf. Table 3.2). Negative/positive values indicates seaward/landward sediment transport, i.e. sediment export/import. Both, in case of the future DAD strategy and in case of beach nourishments, the sediment export from the Western Scheldt to the mouth is reduced or even turns into sediment import.

(see above). At the same time, the landward sediment transport at the other cross-sections decreases with SLR or even turns into seaward sediment transport in case of the 1.67 m and 2.63 m SLR scenarios. This also holds true for the most upstream cross-section at the Dutch-Belgian border. However, the magnitude of sediment transport at this cross-section is negligibly small and therefore has minor impact on the total sediment budget of the estuary.

- **Sediment volume budgets:** Generally, the cells in the eastern part of the Western Scheldt show a negative sediment volume budget in all scenarios while the cells in the western part mostly show a positive budget. This is mainly related to the applied current DAD strategy according to which dredged material from the eastern part is dumped on the shoals in the western part of the estuary. The dumping volumes across the cross-sections are not accounted for in the sediment transport volumes through the cross-sections. This explains why the cells in the eastern/western estuary show a negative/positive budget although there is net sediment input/export into/from those cells through the cross-sections. The dumping in the western estuary causes areas of pronounced sediment accumulation (see red patches) in Cells 2 and 3. Particularly in Cell 3, this accumulation decreases with increasing SLR as a result of decreasing DAD volumes due to

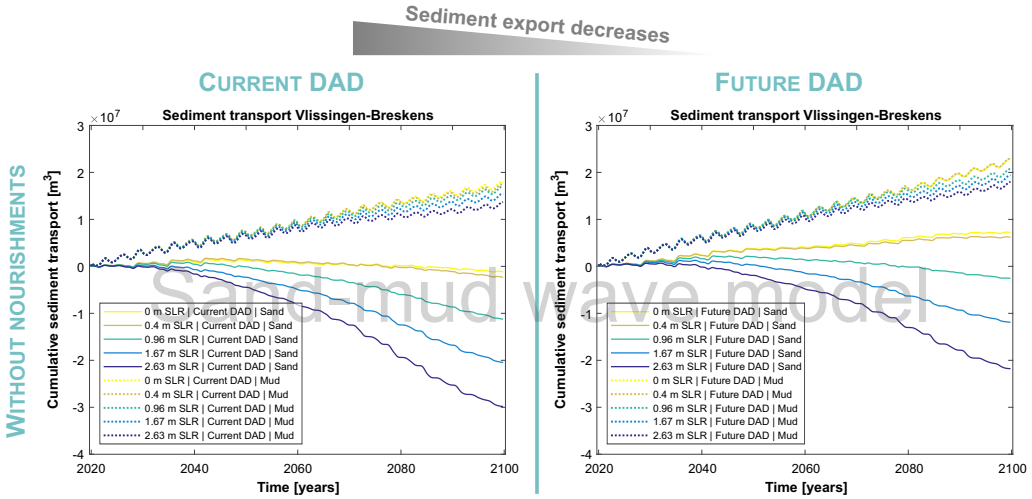

Figure 4.13 Cumulative sediment transport (sand and mud; not corrected for porosity) through cross-section Vlissingen-Breskens at the mouth of the Western Scheldt in the period 2020 to 2100 simulated for five linear SLR scenarios for the current (left panel) and future (right panel) dredging and dumping (DAD) strategy based on the sand-mud wave model configuration of the Delft3D-Scheldt-SLR Model (cf. Table 3.2). Negative/positive values indicates seaward/landward sediment transport, i.e. sediment export/import. In case of the future DAD strategy there is less sediment export from the Western Scheldt to the mouth/more sediment import from the mouth to the Western Scheldt. Note that the order of cumulative sand transport is significantly smaller than of the cumulative sand transport displayed in Figs. 4.11 and 4.12. This is due to the mud protecting the sand from erosion in the model (sand and mud are homogeneously mixed in the model, although with different spatial availability) as well as to the different configuration of the sand-mud wave model (3D mode, coarser resolution; cf. Sec. 3.2).

increasing water depths with SLR. In contrast to Cell 3, Cell 1 — situated in the mouth and therefore not directly being affected by dumping — shows an increasing sediment accumulation and by this an increasing positive sediment budget with increasing SLR.

Based on the considerable sediment export through cross-section Vlissingen-Breskens, the negligible sediment transport volumes through the cross-section at the Dutch-Belgian border and the relatively small sediment volume being imported/exported into/from the estuary due to DAD (see balances between *Dredge Output* and *Dredge Input*), the estuary is loosing sediment in the simulation period 2020–2100 and it is loosing more with increasing SLR. Judging by the directions of sediment transport, the sediment budgets and volume changes in Cells 1 to 3, most of the sediment being exported at Vlissingen-Breskens originates from the westernmost part of Cell 2 (see blue coloured patches) and accumulates in Cell 1, i.e. the mouth area.

The simulated sediment transports and budgets for the future DAD strategy (Fig. 4.15) show several similarities but also significant differences compared to the results based on the current DAD strategy:

- **Sediment transport volumes:** Also in case of the future DAD strategy there is an landward sediment transport through most of the cross-sections in all scenarios, while cross-section Vlissingen-Breskens indicates a seaward sediment transport. The latter, however, is significantly smaller than in case of the current DAD strategy, reflecting the observations made for the cumulative sediment transport (see above). As observed for the current DAD strategy, the yearly av-

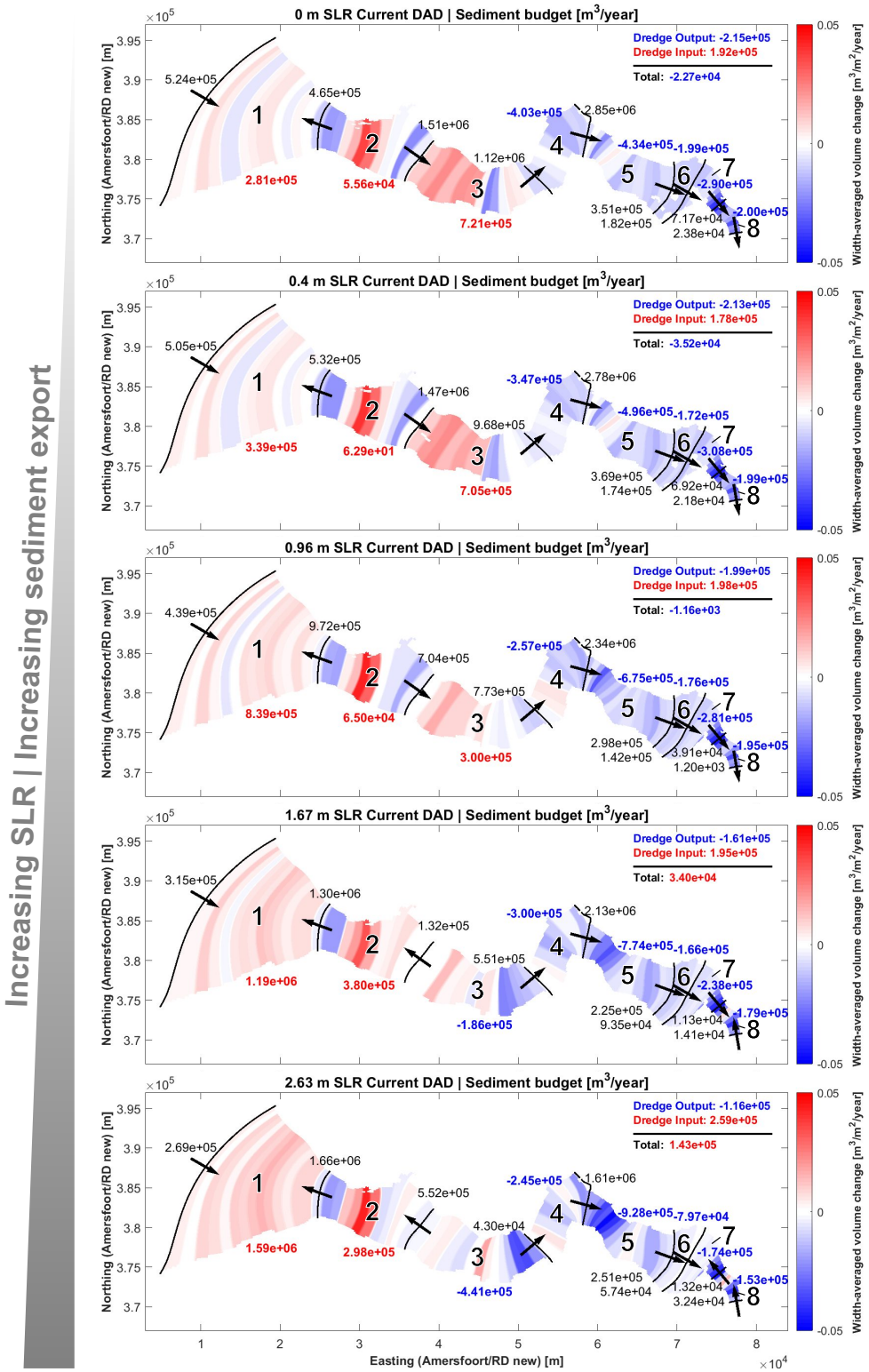

Figure 4.14 Sediment (sand only) transport and budget for various defined cells (numbers 1 to 8) in the Western Scheldt estuary simulated with the sand-only model configuration of the Delft3D-Scheldt-SLR Model for five linear SLR scenarios for the current dredging and dumping (DAD) strategy (cf. Table 3.2). Numbers in black indicate the yearly sediment transport through each cross-section in the direction of the arrows based on the average transport in the period 2020–2100. Dumping of sediment across the cross-sections is not accounted for in the sediment transport volumes. Numbers in blue/red indicate the averaged yearly negative/positive sediment budget per cell. Blue/red patches show areas of net negative/positive sediment volumes changes averaged over the width of the computational grid. *Dredge Output*/*Dredge Input* refer to the amount of dredged sediment that is dumped outside/inside the estuary from inside/outside the estuary. The *Total* gives the balance of both volumes. Generally, the sediment export through cross-section Vlissingen-Breskens increases with increasing SLR.

eraged sediment transport/export through cross-section Vlissingen-Breskens increases with increasing SLR (from $7.32*10^4$ m^3/year in the 0 m SLR scenario to $1.24*10^6$ m^3/year in the 2.63 m SLR scenario). At the same time, the landward sediment transport at the other cross-sections decrease with SLR or even turn into seaward sediment transport in case of the 1.67 m and 2.63 m SLR scenarios. This also holds true for the most upstream cross-section at the Dutch-Belgian border. However, the magnitude of sediment transport at this cross-section is negligibly small and therefore has minor impact on the total sediment budget of the estuary.

- **Sediment volume budgets:** In contrast to the current DAD strategy, the future DAD strategy results in considerably smaller sediment volume changes per cell due to the dumping in the nearby channels and less dumping across the cells. Consequently, the sediment budgets in the western and eastern part of the estuary show smaller discrepancies, although the eastern part still looses more sediment than the western part. With increasing SLR, however, also the sediment loss in the western estuary clearly increases. As is the case in the current DAD strategy, the mouth area (Cell 1) is characterised by an increasing sediment volume with SLR.

Owing to the reduced sediment export through cross-section Vlissingen-Breskens, the future DAD strategy causes the estuary to loose significantly less sediment in the simulation period 2020–2100 compared to the current DAD strategy. Nevertheless, the loss of sediment increases with SLR and the main source of the exported sediment stays the westernmost part of Cell 2. As observed in case of the current DAD strategy, the exported sediment accumulates in the mouth (Cell 1) although the volume is less due to the reduced sediment export at Vlissingen-Breskens.

Beach nourishments in the Western Scheldt mouth generally do not change the trends of sediment transport and sediment budgets described above for the various SLR scenarios and DAD strategies. However, the following effects of nourishments can be observed independent of the SLR and DAD strategies in all scenarios (Figs. A.3, A.4 in the Appendix):

- The beach nourishments increase the positive sediment budget of the mouth (Cell 1) by about $7*10^5$ m^3/year to $8*10^5$ m^3/year which corresponds to 70 % to 80 % of the nourishment volumes ($1*10^6$ m^3/year in total).
- There is less sediment export or even sediment import through cross-section Vlissingen-Breskens in case of beach nourishments. This effect, however, decreases with increasing SLR (from $1.29*10^5$ m^3/year less export in the 0 m SLR scenario to $0.1*10^5$ m^3/year less export in the 2.63 m SLR scenario in case of the current DAD strategy and from $1.54*10^5$ m^3/year less export in the 0 m SLR scenario to $0.9*10^5$ m^3/year less export in the 2.63 m SLR scenario in case of the future DAD strategy).
- Most of the Cells 2 to 8 show a larger positive sediment budget in case of beach nourishments. This effect, however, decreases in an upstream direction and with increasing SLR.

Figures A.5 to A.8 in the Appendix show the sediment (sand only) transport and budget simulated for all SLR scenarios and all sediment strategies (i.e. DAD and nourishments strategies) with wave forcing. Although, the inclusion of waves does not have impact

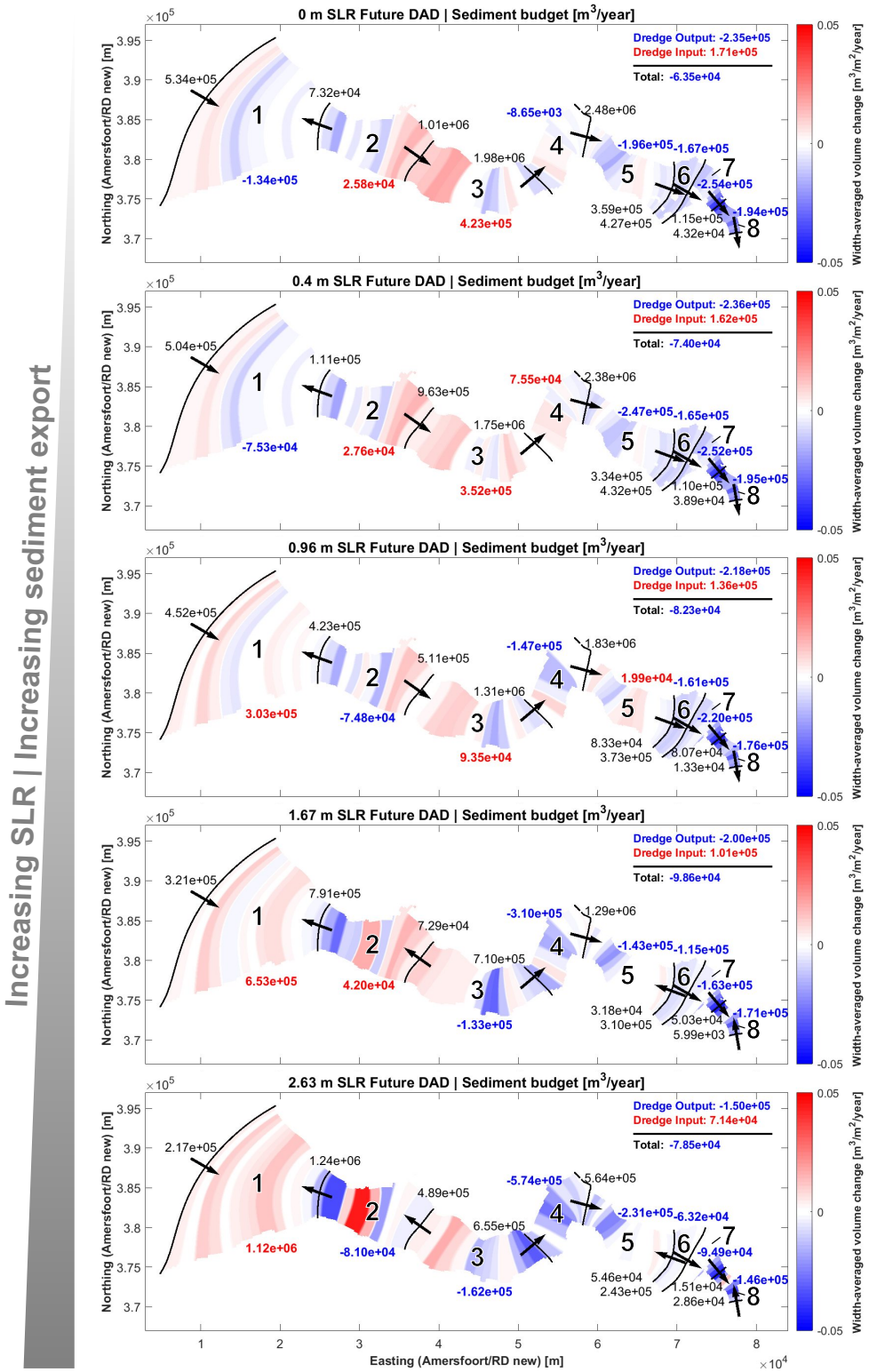

Figure 4.15 Sediment (sand only) transport and budget for various defined cells (numbers 1 to 8) in the Western Scheldt estuary simulated with the sand-only model configuration of the Delft3D-Scheldt-SLR Model for five linear SLR scenarios for the future dredging and dumping (DAD) strategy (cf. Table 3.2). Numbers in black indicate the yearly sediment transport through each cross-section in the direction of the arrows based on the average transport in the period 2020–2100. Dumping of sediment across the cross-sections is not accounted for in the sediment transport volumes. Numbers in blue/red indicate the averaged yearly negative/positive sediment budget per cell. Blue/red patches show areas of net negative/positive sediment volumes changes averaged over the width of the computational grid. *Dredge Output*/*Dredge Input* refer to the amount of dredged sediment that is dumped outside/inside the estuary from inside/outside the estuary. The *Total* gives the balance of both volumes. Generally, the sediment export through cross-section Vlissingen-Breskens increases with increasing SLR.

on the general trends observed above for the cases without wave forcing, the following differences can be summarised:

- The mouth (Cell 1) receives more sediment from the sea.
- There is less export/more import of sediment through cross-section Vlissingen-Breskens.
- The sediment transport and budget are stronger affected in the western than in the eastern estuary due to the decreasing impact of waves upstream.
- Despite the same overall trends, the wave driven migration of morphological features in the western estuary (cf. Sec. 4.2.4) causes a different sediment transport direction and budget for specific cross-sections and cells respectively.

In summary, the inclusion of waves causes more sediment transport from the sea into the mouth and from there more transport into the estuary resulting in less sediment export/more sediment input through cross-section Vlissingen-Breskens.

4.2.4 Morphodynamics

Figure 4.16 displays the 2020 initial model bed level of the Western Scheldt estuary and the 2100 bed levels simulated for the five SLR scenarios based on the current DAD strategy and the sand-only model configuration of the Delft3D-Scheldt-SLR Model. In Fig.4.17, the corresponding bed level changes in the simulation period 2020 to 2100 are shown. The maximum bed level changes in the simulation period amount to plus/minus 20 m (associated with channel migration), independent of the SLR scenario. Generally, the bed level changes are more intense in the western part of the estuary (significant erosion and sedimentation) than in the eastern part (mainly erosion). Indicated by the black arrows in Fig. 4.16, a general seaward/landward migration of the channel-shoal pattern can be observed at the mouth. Forced by the dredging, the course of the main navigation channel is stable while several secondary channels evolve. The area around the intertidal shoal Hooge Platen (for labels see Fig. 1.1) shows significant accumulation due to dumping activities. The Middelplaat shows a strong lateral migration in all scenarios, while the Platen van Valkenisse and particularly the intertidal area of Saeftinghe are comparably less active. While the SLR causes significant differences in the simulated 2100 bed levels on a micro- to meso-scale, three general, large-scale effects of SLR in the model can be observed:

- Generally, SLR has a stronger impact on the morphodynamics in the western than in the eastern estuary.
- The seaward/landward migration of the channel-shoal pattern at the mouth becomes more/less pronounced with increasing SLR (see sizes of the corresponding arrows in Figure 4.16).
- With increasing SLR, the bed level changes in the eastern estuary become slightly more pronounced.

The morphodynamics simulated for the various SLR scenarios based on the future DAD strategy (without nourishments and without waves; Figs. 4.18, 4.19) clearly differ from the case of the current DAD strategy. While the maximum bed level changes in the entire estuary still amount to plus/minus 20 m (independent of the SLR scenario), the future DAD strategy generally results in less pronounced bed level changes in the

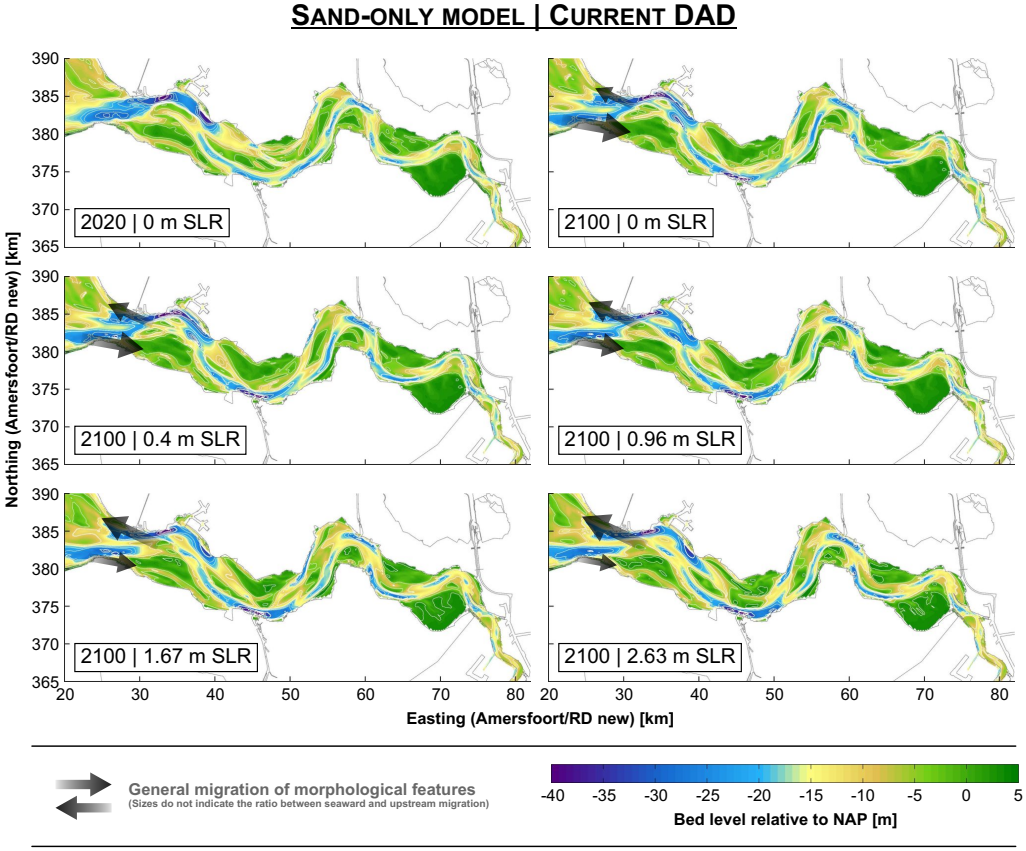

Figure 4.16 Bed level of the Western Scheldt estuary in 2020 (including 25 years spin-up time based on the current DAD strategy) and 2100 as simulated with the sand-only model configuration of the Delft3D-Scheldt-SLR Model for five linear SLR scenarios for the current DAD (dredging and dumping) strategy (cf. Table 3.2). For reasons of comparability, the reference level in all bed level plots is the current sea level (0 m NAP).

western estuary. In the eastern estuary, the magnitude of bed level changes is comparable to the case of the current DAD strategy, although larger areas of sedimentation can be observed. The deep parts of the main navigation channel are filled up in all SLR scenarios as a result of dumping. The area of the Hooge Platen (for labels see Fig. 1.1) hardly shows sedimentation since no dumping is performed here. Similar to the case of the current DAD strategy, also with the future DAD strategy, the Middelplaat shows strong lateral migration although the pattern clearly differs. The Platen van Valkenisse are characterised by significant sedimentation despite the absence of dumping activities. In spite of the differences in bed level changes between the current and the future DAD strategies, the following general large-scale effects of SLR on the morphodynamics remain the same: (i) the increase/decrease of the seaward/landward migration of the channel-shoal pattern at the mouth with increasing SLR and (ii) the amplification of the bed level changes in the eastern estuary with SLR. As an important difference, however, SLR seems to effect equally the western and eastern estuary in case of the future DAD strategy, while it had a stronger impact on the western estuary in case of the current DAD strategy (see above).

Figures A.9–A.12 in the Appendix show that beach nourishments in the mouth area do not change the general impact of SLR on the bed level changes in the estuary (see above), however, there is a significant effect on the micro- to meso-scale morphodynamics. This effect decreases with increasing distance from the location of the nourishments from the western to the eastern estuary.

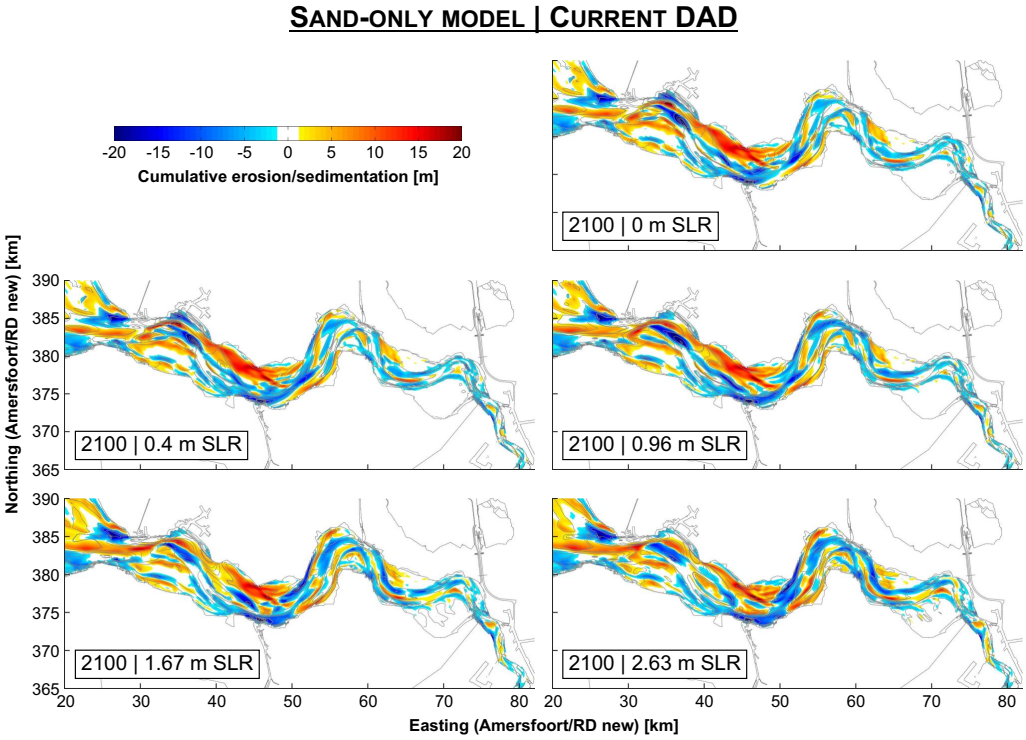

Figure 4.17 Cumulative erosion and sedimentation in the period 2020 to 2100 in the Western Scheldt as simulated with the sand-only model configuration of the Delft3D-Scheldt-SLR Model for five linear SLR scenarios for the current DAD (dredging and dumping) strategy (cf. Table 3.2).

The inclusion of waves in the Delft3D-Scheldt-SLR Model has a large impact on the estuarine morphodynamcis (Figs. A.13–A.20 in the Appendix). This is especially obvious from the western and central estuary, where the position and shape of the shoals and secondary channels in 2100 clearly differ from the case without waves. At the mouth, wave driven migration of morphological features during the simulation period causes larger temporal variations of the cumulative sediment transport at cross-section Vlissingen-Breskens compared to the case without wave forcing (cf. Sec. 4.2.3). Due to decreasing wave heights, the morphological effects of the waves decrease in an upstream direction. As a result, the final bed levels upstream of Kloosterzande (for labels see Fig. 1.1) are mostly comparable to the scenarios without wave forcing. Despite the large effects of waves on the simulated bed level changes, the above described general impact of SLR remains unchanged. This holds true for all applied sediment strategies.

Figures A.21–A.24 in the Appendix show the simulated estuarine morphodynamics based on the sand-mud wave model. Due to the coarser grid resolution and the higher diffusivity of the sand-mud wave model, the bed levels and erosion-sedimentation patterns are spatially less variable compared to the sand-only cases. Furthermore, the bed level changes predicted by the sand-mud wave model are less intense (mostly plus/minus 10 m; due to the 3D modelling approach and the mud protecting the sand from erosion in the model; cf. Sec. 4.2.3) and their patterns fundamentally differ from those predicted by the sand-only (wave) model. However, the morphodynamics remain more intense in the western compared to the eastern estuary and, indicated by the black arrows in Figs. A.21–A.23, a general seaward/landward migration of the channel-shoal pattern can still be observed at the mouth. In contrast to the sand-only cases, there is clearly less erosion and larger areas of sedimentation (due to the mud supply) in the eastern estuary. As observed before, the DAD strategies have a clear impact on the position shape of the shoals and secondary channels in 2100. The general impact

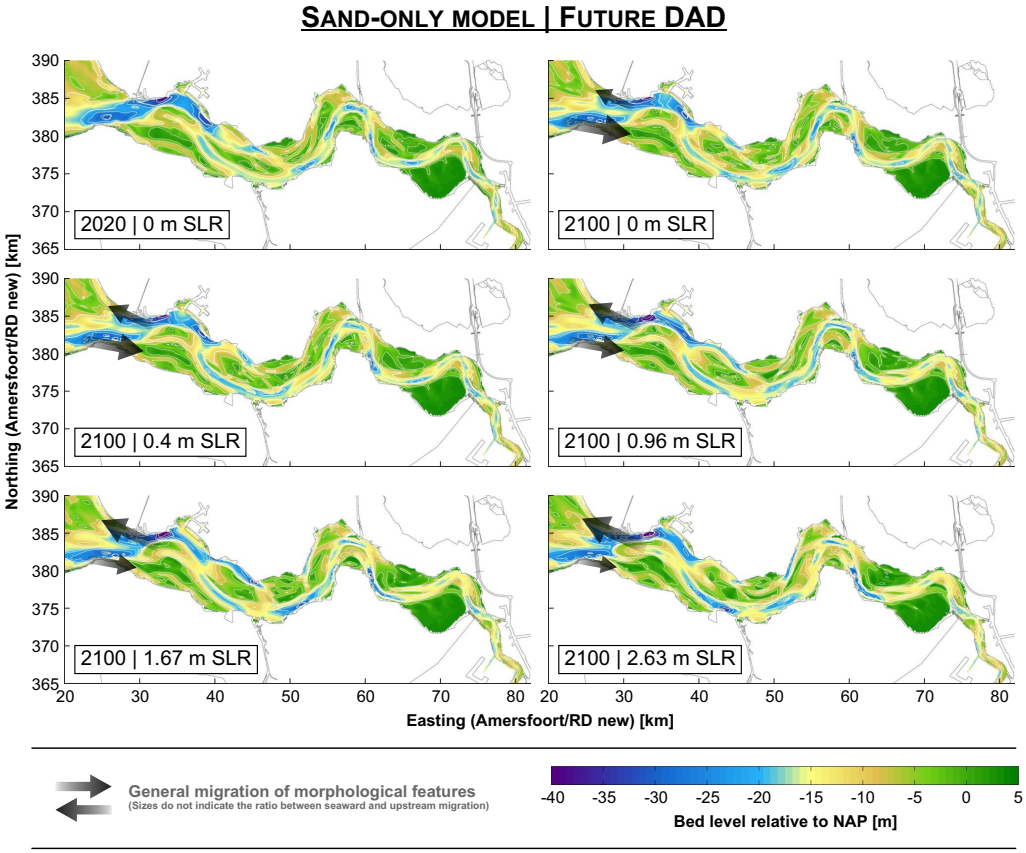

Figure 4.18 Bed level of the Western Scheldt estuary in 2020 (including 25 years spin-up time based on the future DAD strategy) and 2100 as simulated with the sand-only model configuration of the Delft3D-Scheldt-SLR Model for five linear SLR scenarios for the future DAD (dredging and dumping) strategy (cf. Table 3.2). For reasons of comparability, the reference level in all bed level plots is the current sea level (0 m NAP).

of SLR can be summarised as follows:

- Generally, SLR has a stronger impact on the morphodynamics in the western than in the eastern estuary.
- The seaward/landward migration of the bed at the mouth becomes more/less pronounced with increasing SLR.
- While the magnitude of bed level changes in the western estuary decreases with SLR, it increases in the eastern estuary.
- The intertidal area of Saeftinghe is rising with SLR, particularly in the extreme SLR scenarios.

Consequently, SLR mainly has mostly similar effects in the sand-mud wave model as was observed in both sand-only cases.

Figure 4.20 shows the thalweg (i.e. the line of lowest bed levels) of the main navigation channel in the Western Scheldt, for which the bed levels (relative to the current sea level, i.e. 0 m NAP) simulated for the five SLR scenarios and both DAD strategies (sand-only model) are displayed in Fig. 4.21. In case of the current DAD strategy (top panel

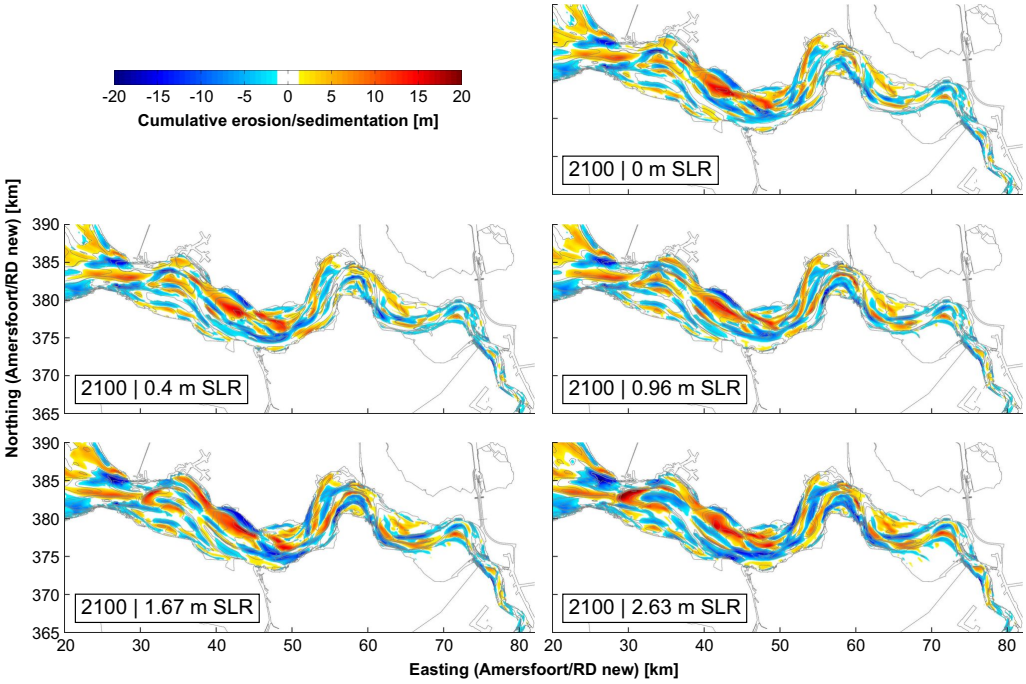

Figure 4.19 Cumulative erosion and sedimentation in the period 2020 to 2100 in the Western Scheldt as simulated with the sand-only model configuration of the Delft3D-Scheldt-SLR Model for five linear SLR scenarios for the future DAD (dredging and dumping) strategy (cf. Table 3.2).

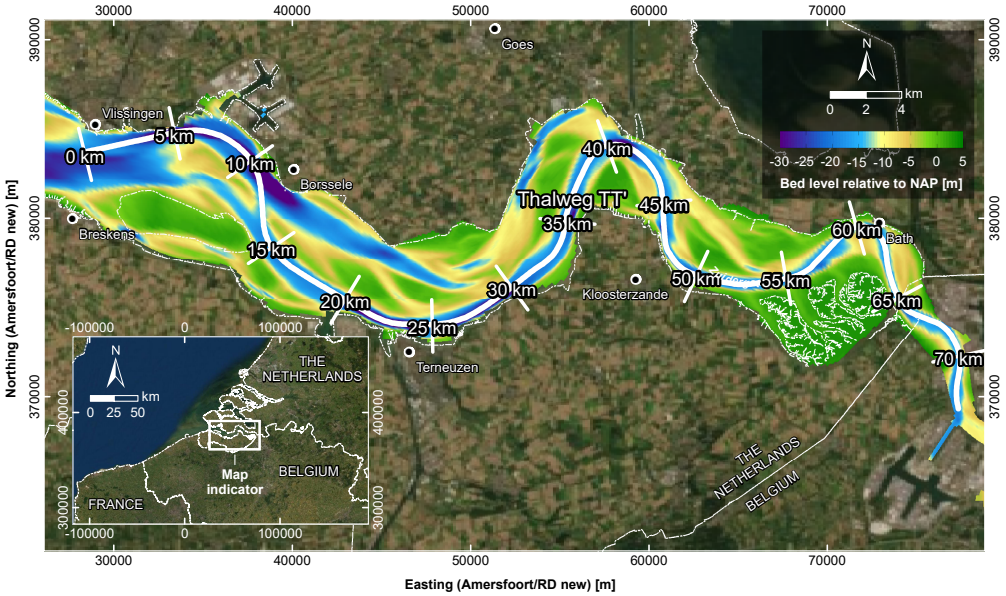

Figure 4.20 Thalweg (i.e. the line of lowest bed levels) of the main navigation channel in the Western Scheldt estuary, for which the depth profiles are shown in Fig. 4.21 and in Figs. A.25–A.27 in the Appendix.

of Fig. 4.21), the average bed level of the thalweg lowers in the simulation period 2020–2100 in all SLR scenarios. Especially the channels Honte, Pas van Terneuzen, Put van Hansweert and Zuidergat (for labels see Fig. 1.1) experience significant deepening. While in the western and central estuary, the bed level changes of the thalweg do not show a clear relation to the rate of SLR, they are clearly rising with increasing SLR

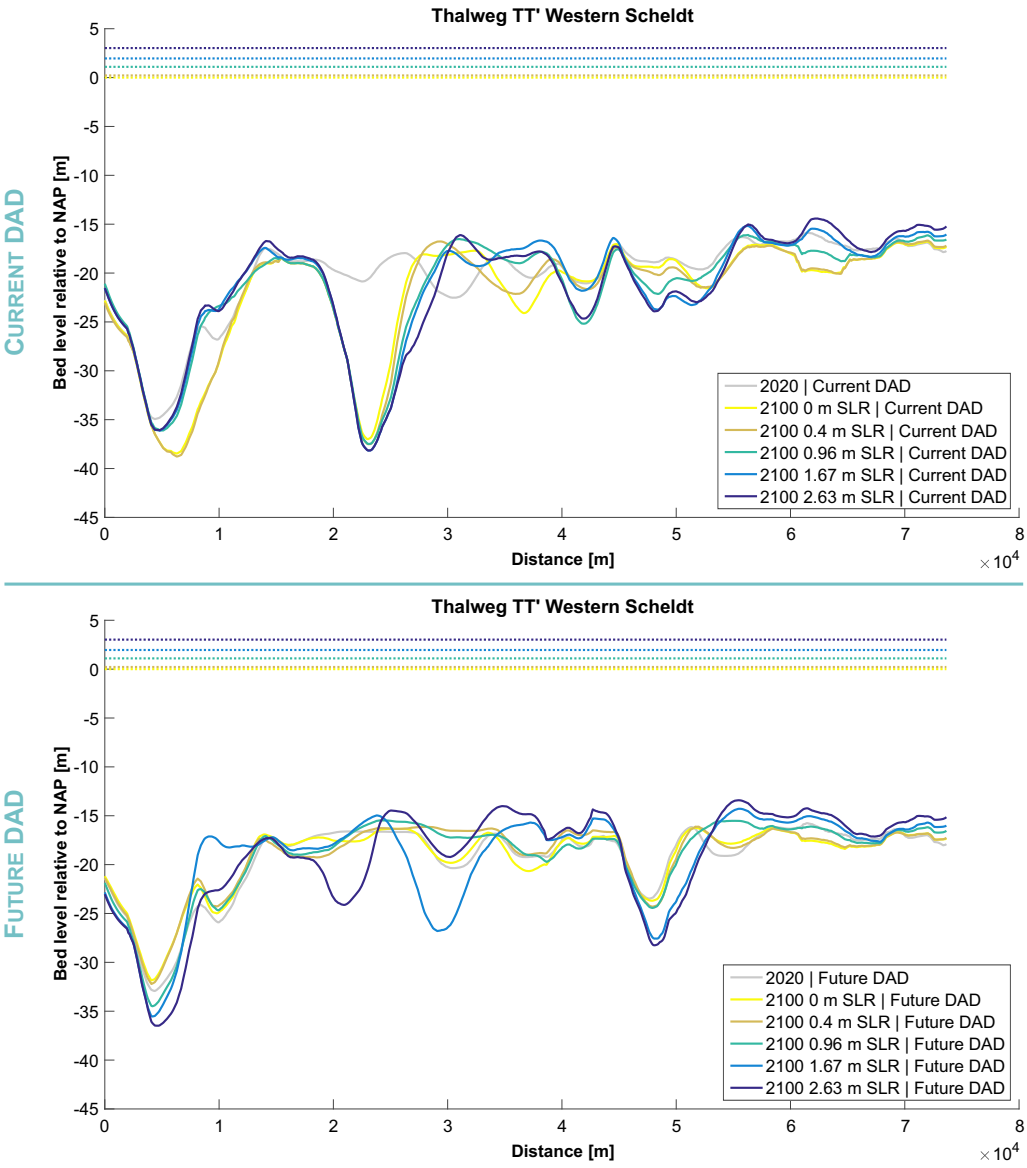

Figure 4.21 Depth profiles of the thalweg (i.e. the line of lowest bed levels) of the main navigation channel in the Western Scheldt estuary as simulated with the sand-only model configuration of the Delft3D-Scheldt-SLR Model for various linear SLR scenarios based on the current (top) and future (bottom) DAD strategies (cf. Table 3.2). For reasons of comparability, the same thalweg line is applied for all scenarios and the reference level of all depth profiles is the current sea level (0 m NAP). Dotted lines show the 2100 sea levels for all SLR scenarios. The course of the thalweg including distance marks is displayed in Fig. 4.20.

in the easternmost part of the estuary. This is partly related to the fact that the bed levels in this area are close to the dredging levels and that the dredging levels rise with increasing SLR.

In contrast to the current DAD strategy, the future DAD strategy does not result in an average deepening of the thalweg but instead, the deep parts are filled up due to dumping. Except for the deepening of the channels Honte and Zuidergat (for labels see Fig. 1.1) in the more extreme SLR scenarios (0.96 m, 1.67 m and 2.63 m SLR), no general trends associated with SLR can be observed in the western and central estuary. The eastern estuary, however, shows — similar to the case of the current DAD strategy — a clear

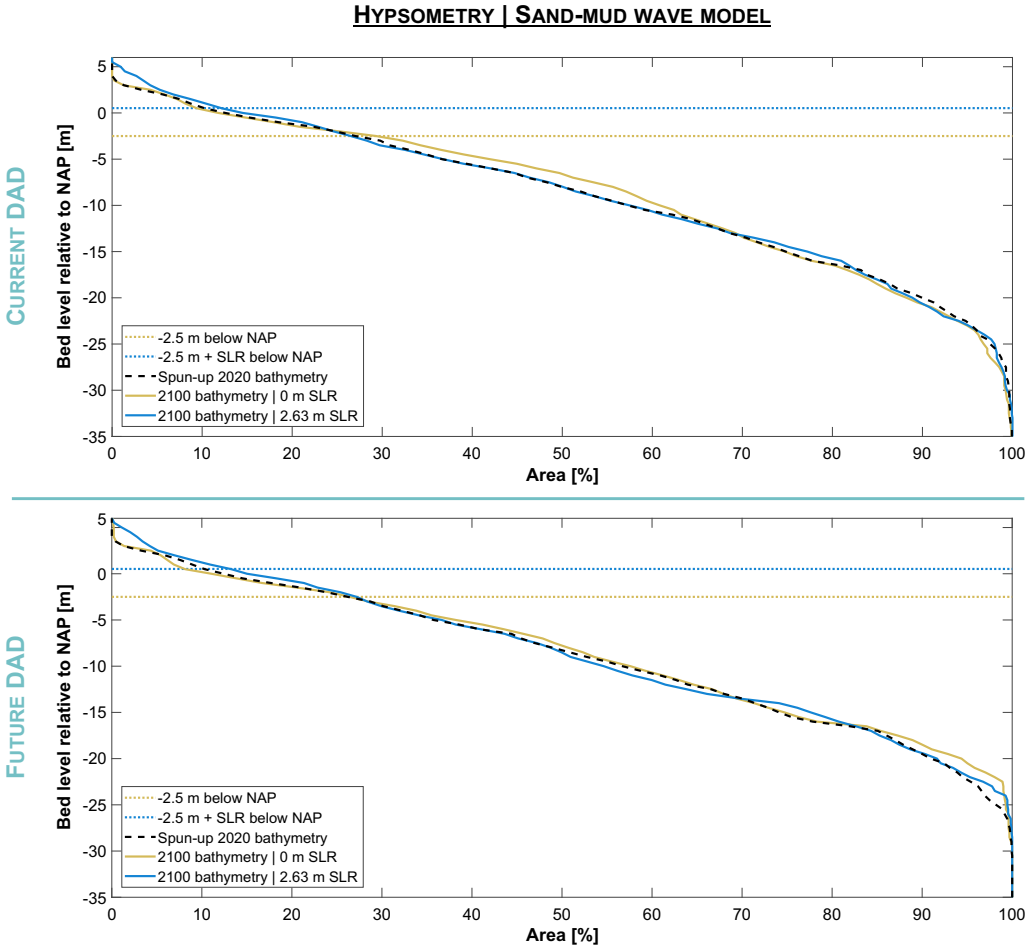

Figure 4.22 Hypsometric curves of the Western Scheldt estuary between Vlissingen-Breskens and the Dutch-Belgian border as simulated with the sand-mud wave model configuration of the Delft3D-Scheldt-SLR Model for the 0 m SLR (beige solid lines) and for the 2.63 m (blue solid lines) linear SLR scenarios based on the current (top) and future (bottom) DAD strategies (cf. Table 3.2). The black dashed lines show the hypsometries of the initial, spun-up 2020 model bathymetries. For reasons of comparability, the reference level of all displayed hypsometric curves is the current sea level (0 m NAP). The two -2.5 m NAP marks indicate the approximate lower limits of the intertidal area for a sea level of 0 m NAP (beige dotted lines) and for a future sea level of 2.63 m NAP (blue dotted lines).

rise of bed levels with SLR corresponding to the rising dredging level (see above).

The inclusions of beach nourishments and particularly of the wave forcing in the model results in clear differences in the 2100 bed levels of downstream part of the thalweg, especially in case of the future DAD strategy (Figs. A.25–A.27 in the Appendix). Nevertheless, most of the general observations made above for the case without nourishments and without wave forcing remain the same, also with regard to the effects of SLR. The 2100 thalweg bed levels predicted by the sand-mud wave model differ even more (Fig. A.28 in the Appendix): the bed levels are clearly smoothed (mainly related to the coarser grid resolution of this model), are generally higher and show smaller differences between the various SLR scenarios. At the same time, the rise of the thalweg bed levels with SLR is more pronounced and now also obvious in the western estuary. The impact of the DAD strategies is comparably small except for the westernmost part.

The hypsometric curves displayed in Fig. 4.22 give a summary view of the bed level changes of the Western Scheldt simulated for the period 2020–2100 based on the

sand-mud wave model (most appropriate to evaluate the mud driven dynamics in the intertidal area) with both DAD strategies. The results are only shown for the 0 m SLR and for the 2.63 m linear SLR scenarios in order to visualise the maximum effects of SLR on the hypsometry, while the effects are similar for the other SLR scenarios although less pronounced. The comparison of the beige and blue solid curves demonstrates that in case of both DAD strategies the intertidal area (circa above -2.5 m NAP) rises in the 2.63 m SLR scenario but rises less than the SLR. The rise of the intertidal area with SLR can particularly be observed in the area of Saeftinghe, while the intertidal shoals Platen van Valkenisse, Platen van Ossenisse, Middelplaat and Hooge Plaaten (for labels see Fig. 1.1) show comparably less accumulation in the 2.63 m SLR scenario (cf. Figs. A.22 and A.24 in the Appendix). Independent of the DAD strategy, the area of intermediate depths, i.e. between circa -2.5 m NAP and -17 m NAP, usually becomes lower with SLR. The depths of the deep channels (below circa -17 m NAP) are hardly affected by SLR in case of the current DAD strategy, while they clearly increase in case of the future DAD strategy, which is in line with the observations made above based on the thalweg depth profiles. Both the sand-only model and the sand-only wave model mostly indicate similar trends with regard to SLR as implied by the sand-mud wave model (cf. Figs. A.29 and A.30 in the Appendix), although the predicted rise of the intertidal area with SLR is clearly smaller in both sand-only cases due to the absence of mud.

5 Discussion and conclusions

As stated in Sec. 3 and in Sec. 4.2, the focus of the current study is to investigate particularly the relative impact (i.e. the trends) of SLR and sediment strategies on the hydrodynamics, sediment budget and morphodynamics of the Western Scheldt estuary, while the absolute simulation results are secondary. The scenario results presented in Sec. 4.2 indicate consistent trends for the different SLR scenarios and sediment strategies in the simulation period 2020–2100. In general, the following observations can be made, independent of the model configuration (i.e. sand-only model, sand-only wave model and sand-mud wave model):

- The mean high water levels in the Western Scheldt increase stronger with SLR than the mean low water levels, resulting in an increase of the tidal range in the whole estuary. This increase gets more pronounced in an upstream direction. The increase of the tidal range is related to resonance effects in the Scheldt river: with an average propagation velocity of the tide in the Scheldt river of about $13\,m\,s^{-1}$, the corresponding average water depth amounts to circa 18 m in the present situation. Based on this average water depth, the resonance length of the present Scheldt river amounts to 145 km, which is less than the length of the tidal limit at Gent, about 160 km distant from the mouth. However, with SLR, the resonance length comes closer to the inlet length of 160 km (e.g. 160 km in case of the 2.63 m SLR, corresponding to almost 3 m SLR in the study area), which results in an increase of the tidal amplitudes.

- SLR causes the estuary to become less flood dominant or even ebb dominant in the westernmost part in case of the extreme SLR scenarios. This is reflected by the observed changes of the maximum flood and ebb flow velocities in the channels of the estuary with SLR: as a result of the increasing water depth with SLR (larger cross-sectional area), both the maximum flood and ebb flow velocities in the channels decrease. The absolute decrease in velocity, however, is larger for the maximum flood than for the maximum ebb flow. Since the difference between maximum flood and ebb flow velocities is indicative of the residual sediment transport, a stronger decrease of the maximum flood flow velocities than of the maximum ebb flow velocities results in a decreasing/increasing landward/seaward residual sediment transport with SLR.

- The decreasing/increasing landward/seaward residual sediment transport with SLR is reflected by an increasing sediment export through cross-section Vlissingen-Breskens and the increasing seaward migration of the channel-shoal pattern at the entrance to the estuary with SLR. The decrease of the maximum flood flow velocities with SLR is particularly pronounced in the western part of the estuary (i.e. Cells 2 and 3 in Fig. 4.14), which is the same area indicating increasing sediment export with SLR. In summary, there is an increasing loss of sediment in the Western Scheldt estuary with increasing SLR, controlled by the increase of sediment export through the cross-section Vlissingen-Breskens with SLR due to the changes in the peak current asymmetry. At the same time a decreasing landward sediment transport with SLR in the central and eastern estuary can be observed.

- Most of the extra amount of sediment being exported from the estuary in case of SLR originates from the westernmost estuary near Vlissingen-Breskens (Cell 2 in Fig. 4.14) and accumulates in the mouth area (Cell 1).

- The intertidal area rises with SLR but it rises less than the sea level (see more details below).
- In the easternmost estuary, the bed levels of the main navigation channel rise with SLR because the dredging depths remain constant while the sea level rises.
- Altogether, the predicted bed levels of the thalweg as well as the predicted hypsometries imply that the dredging volumes may decrease with increasing SLR, especially in case of the current DAD strategy in which no sediment is dumped in the channels. The main reasons for this are the increasing water depths with SLR and the increasing export of sediment with SLR which partly originates from the channels.
- The DAD strategies have a significant impact on the bed levels and on the sediment budget of the estuary. The future DAD strategy results in considerably less sediment export at Vlissingen-Breskens compared to the case with the current DAD strategy. This is at least partly related to the fact that a larger portion of dredged material is dumped in the eastern estuary and by this further distant from the mouth.
- Beach nourishments result in reduced net sediment export at Vlissingen-Breskens, although the effect is much smaller than observed for the future DAD strategy. At the same time, there is a clear impact of beach nourishments on the micro- to meso-scale morphodynamic development of the western estuary.

While the absolute simulation results have to be further validated, the robustness of the above described trends/relative impact of SLR and sediment strategies is supported by the following:

- The results of the morphological hindcast presented in Sec. 4.1 imply a good reproduction particularly of the observed development of the sediment budget and of the bed levels in the Western Scheldt estuary in the period 1964–2012. The match is particularly good for the sand-mud wave model.
- All three model configurations, i.e. (i) the sand-only model, (ii) the sand-only wave model and the (iii) sand-mud wave model indicate the same trends with regard to SLR and the sediment strategies in the scenarios.
- While particularly the sediment volume changes and sediment budgets per cell predicted for the hindcast period 1964–2012 were highly sensitive to the various applied model settings (cf. Sec. 4.1.1), the above described trends in the scenarios were little sensitive to the different settings. The latter include different (i) values for the horizontal eddy diffusivity, (ii) bottom frictions, (iii) sediment transport formulations, (iv) values for the current- and wave related suspended and bedload transport factors for sand, (v) grain sizes and combinations of different grain sizes, (vi) values for the critical bed shear stress for erosion of mud, (vii) discharges of the Scheldt river and (viii) computational modes (2D versus 3D).
- Morphostatic simulations, i.e. simulations without updating the bed levels, show the same trends of sediment transport and budget in the scenarios as the morphodynamic simulations (i.e. with bed level updating). Consequently, the observed trends are probably not dependent on the bed level changes simulated for the period 2020–2100.

- The observed trends in the scenarios are little sensitive to the different applied SLR rates for the 80 year period: although the simulation results based on the non-linear SLR show a less advanced morphological development compared to the linear SLR in 2100 (because there is a shorter period with higher SLR in case of the non-linear compared to the linear SLR), both the constant and accelerating SLR rates result in the same trends with regard to SLR and the sediment strategies. This also implies that a constant, temporally averaged SLR rate as applied in the linear SLR scenarios are — although an unrealistic assumption — is not a limitation of the current study but instead shows that the findings hold true for the hole range (linear to non-linear) of SLR rates.

The increase of sediment export and the relative decrease of the intertidal area with SLR are observations made earlier for the Western Scheldt estuary by JEUKEN *et al.* (2002), which used a semi-empirical ESTMORF model by WANG and VAN HELVERT (2001) to study the effects of DAD and of SLR on the sand budget of the Western Scheldt. JEUKEN *et al.* (2002) found that in the estuary, the increased tidal prism with SLR causes a decrease of the SLR induced sediment demand due to a delayed response of the intertidal area to SLR and to the increasing tidal range with SLR. Consequently, an acceleration of the SLR causes relatively most sediment demand in the mouth area resulting in an increased sediment export from the estuary to the mouth area. Although the ESTMORF model does not make a distinction between sand and mud, the current study indicates the same trends with regard to SLR for both the sand-only (wave) model and the sand-mud wave model. In contrast to the findings by JEUKEN *et al.* (2002), the study by WANG (1997) based on the ASMITA model implies that accelerated SLR causes an increase of sediment import into the estuary through cross-section Vlissingen-Breskens due to an increased sediment demand. However, the increase in sediment import can not be observed before about 30 years after the start of the SLR and even then cannot compensate the effects of SLR resulting in a relative loss of sediment with SLR. Similar findings are implied by the studies by WANG and ROELFZEMA (2001) and WANG and JEUKEN (2004) for the Humber estuary in the UK.

While the observed impact of the different sediment strategies as well as the hydrodynamic effects of SLR in the Western Scheldt are intuitive and considered as robust findings, the response of the sediment budget to SLR, i.e. the increasing sediment loss of the estuary with SLR, is more complex and requires more research to be better understood. The current study demonstrates that SLR has a strong impact on the peak current asymmetry in the Western Scheldt, which, in turn, controls the residual sediment transport and, by this, the sediment budget of the estuary. Based on the observed changes in the peak current asymmetry, the Delft3D-Scheldt-SLR Model predicts increasing sediment loss of the estuary with SLR. At the same time, the model indicates that the intertidal area rises less than the sea level. Although the morphological hindcast demonstrates that the model is able to reproduce the approximate sediment budgets of the different cells in the period 1964–2012, it also shows that the model underestimates the rise of the intertidal area in this period, in which the SLR was minor. This raises the question (i) whether the model predictions on the behaviour of the intertidal area with SLR are reliable and (ii) whether a rise of the intertidal area of the order of SLR or larger may (over-)compensate for the increasing seaward residual sediment transport due to the changes in peak current asymmetry. Furthermore, a larger rise of the intertidal area with SLR would also affect the tidal prism and by this the general hydrodynamics in the estuary.

Although it will be difficult to quantitatively assess the role of the intertidal area, supplementary model simulations could bring more insight whether a rise of the intertidal

area of the order of SLR or larger is a relevant process with regard to the sediment budget of the Western Scheldt. Those simulations could be realised by, for instance, adding a finer sand fraction to the model that may help to let the intertidal area rise with SLR. Alternatively, simulations could be performed in which the SLR is implemented by subsiding the bed levels of the channels, while the bed levels of the intertidal area stay constant.

A Appendix

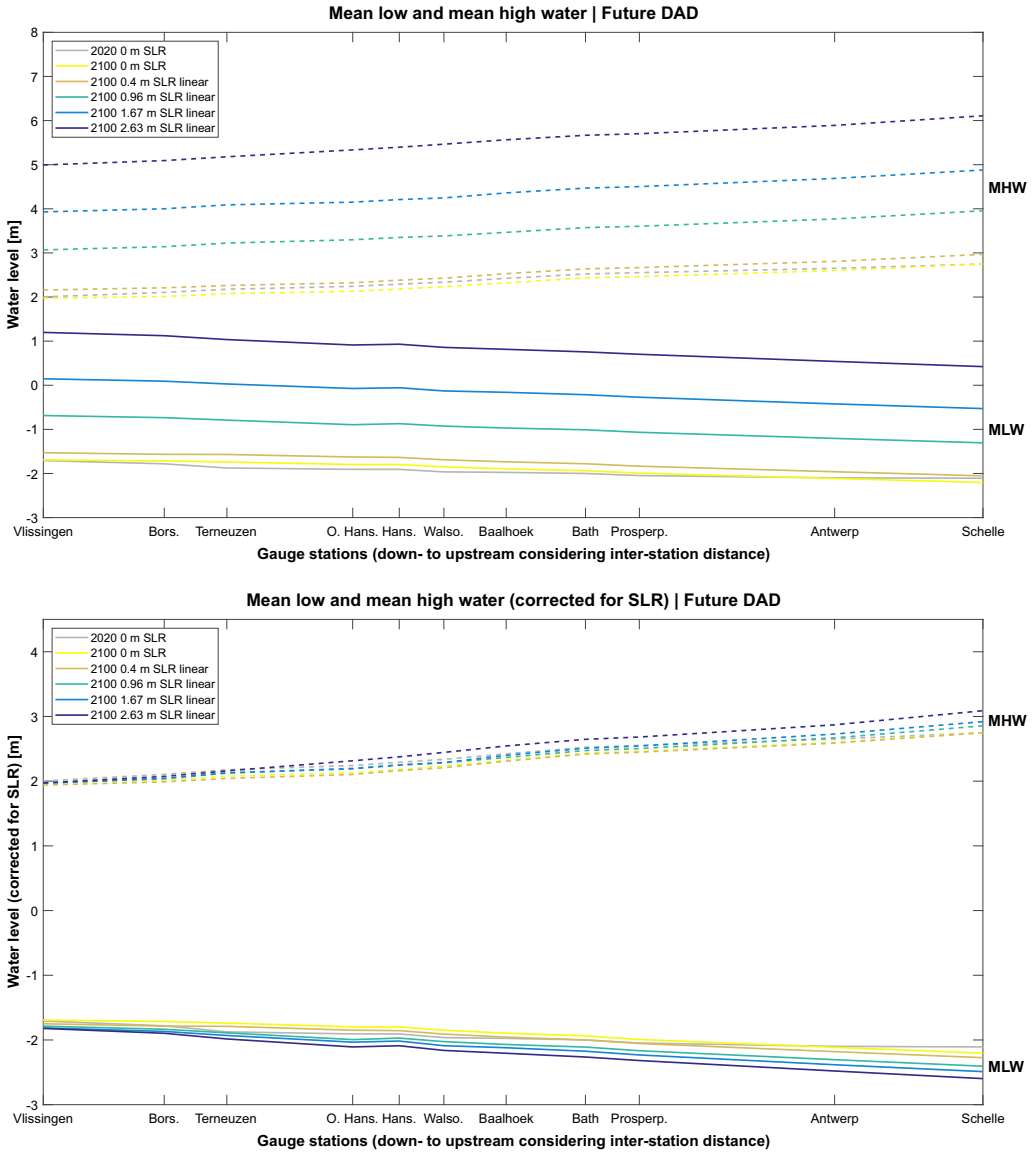

Figure A.1 Comparison of simulated mean low (MLW) and mean high water levels (MHW) without SLR correction (top) and with SLR correction (based on the local SLR listed in Table 3.1; bottom) at various stations in the Western Scheldt estuary for the year 2020 (no SLR) and the year 2100 for various linear SLR scenarios for the future DAD strategy based on the sand-only model (cf. Table 3.2). MLW and MHW were derived from hydrodynamic simulation runs based (i) on the 2020 initial model bathymetry and 0 m SLR boundary conditions for the 2020 curves and (ii) on the 2100 predicted bathymetries and 2100 SLR boundary conditions associated with each SLR scenario for the 2100 curves. Based on the applied correction for SLR, differences between the curves in the bottom panel can directly be ascribed (i) to SLR related effects on the tides (amplitudes and phases) and (ii) to changes of the bathymetries within the 80 year simulation period in each SLR scenario.

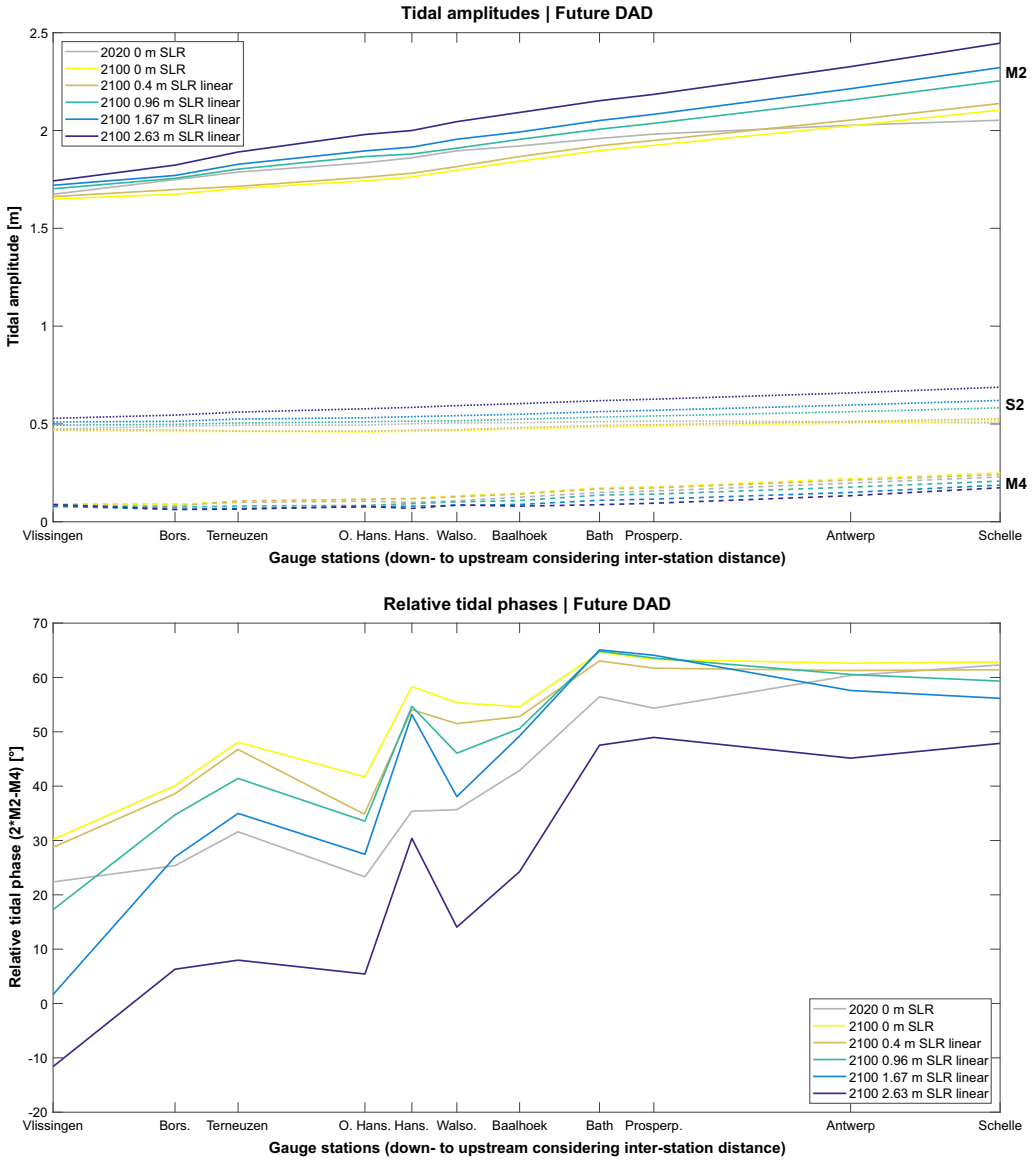

Figure A.2 Comparison of simulated M2, S2 and M4 tidal amplitudes (top) and simulated relative tidal phases $2*\varphi M2-\varphi M4$ (bottom) at various stations in the Western Scheldt estuary for the year 2020 (no SLR) and the year 2100 for various linear SLR scenarios for the future DAD strategy based on the sand-only model (cf. Table 3.2). All parameters are derived from hydrodynamic simulation runs based (i) on the 2020 initial model bathymetry and 0 m SLR boundary conditions for the 2020 curves and (ii) on the 2100 predicted bathymetries and 2100 SLR boundary conditions associated with each SLR scenario for the 2100 curves. Differences between the curves can directly be ascribed (i) to SLR related effects on the tides (amplitudes and phases) and (ii) to changes of the bathymetries within the 80 year simulation period in each SLR scenario.

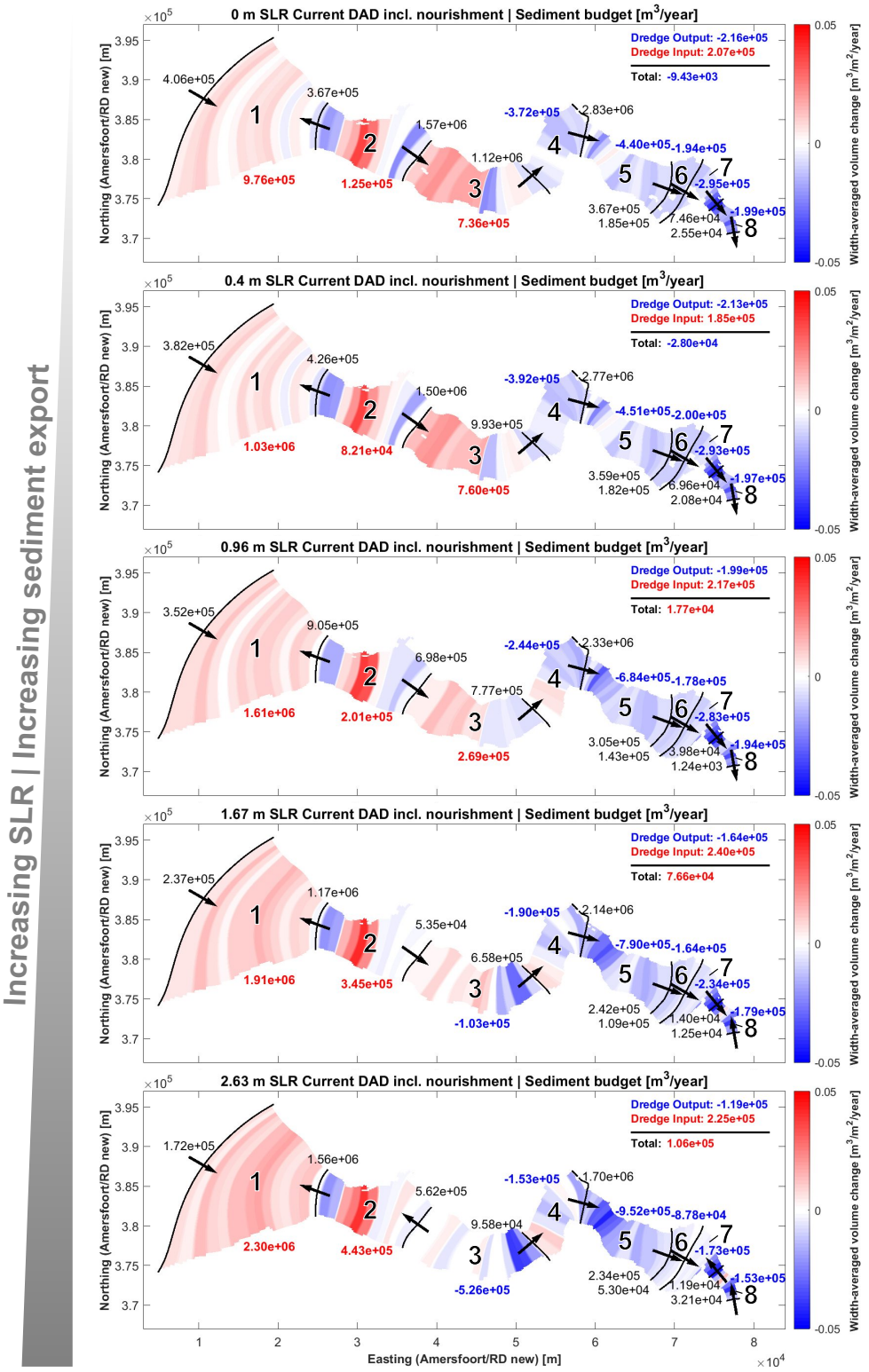

Figure A.3 Sediment (sand only) transport and budget for various defined cells (numbers 1 to 8) in the Western Scheldt estuary simulated with the sand-only model configuration of the Delft3D-Scheldt-SLR Model for five linear SLR scenarios for the current dredging and dumping (DAD) strategy including beach nourishments (cf. Table 3.2). Numbers in black indicate the yearly sediment transport through each cross-section in the direction of the arrows based on the average transport in the period 2020–2100. Dumping of sediment across the cross-sections is not accounted for in the sediment transport volumes. Numbers in blue/red indicate the averaged yearly negative/positive sediment budget per cell. Blue/red patches show areas of net negative/positive sediment volumes changes averaged over the width of the computational grid. *Dredge Output*/*Dredge Input* refer to the amount of dredged sediment that is dumped outside/inside the estuary from inside/outside the estuary. The *Total* gives the balance of both volumes. Generally, the sediment export through cross-section Vlissingen-Breskens increases with increasing SLR.

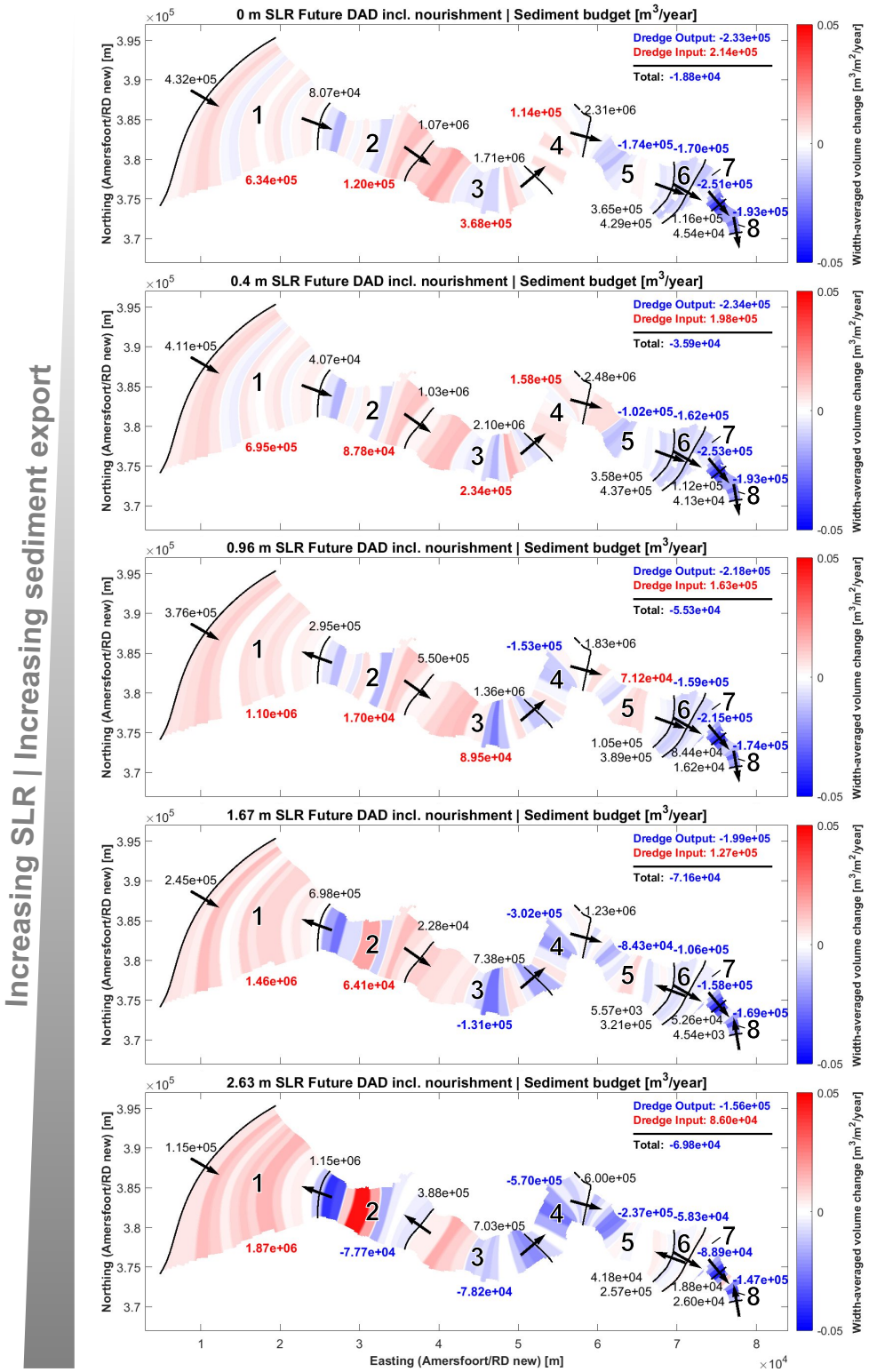

Figure A.4 Sediment (sand only) transport and budget for various defined cells (numbers 1 to 8) in the Western Scheldt estuary simulated with the sand-only model configuration of the Delft3D-Scheldt-SLR Model for five linear SLR scenarios for the future dredging and dumping (DAD) strategy including beach nourishments (cf. Table 3.2). Numbers in black indicate the yearly sediment transport through each cross-section in the direction of the arrows based on the average transport in the period 2020–2100. Dumping of sediment across the cross-sections is not accounted for in the sediment transport volumes. Numbers in blue/red indicate the averaged yearly negative/positive sediment budget per cell. Blue/red patches show areas of net negative/positive sediment volumes changes averaged over the width of the computational grid. *Dredge Output*/*Dredge Input* refer to the amount of dredged sediment that is dumped outside/inside the estuary from inside/outside the estuary. The *Total* gives the balance of both volumes. Generally, the sediment export through cross-section Vlissingen-Breskens increases with increasing SLR.

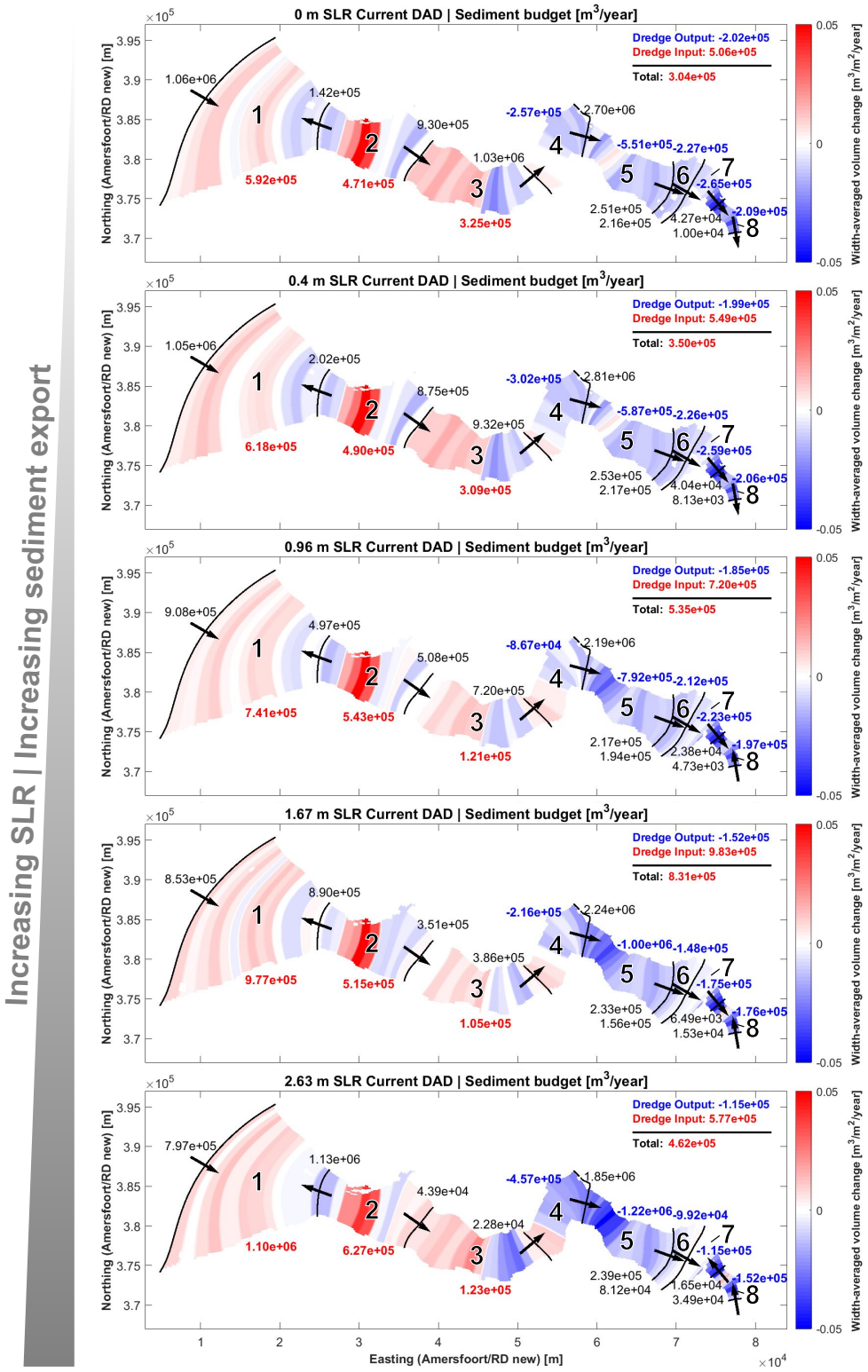

Figure A.5 Sediment (sand only) transport and budget for various defined cells (numbers 1 to 8) in the Western Scheldt estuary simulated with the sand-only wave model configuration of the Delft3D-Scheldt-SLR Model for five linear SLR scenarios for the current dredging and dumping (DAD) strategy (cf. Table 3.2). Numbers in black indicate the yearly sediment transport through each cross-section in the direction of the arrows based on the average transport in the period 2020–2100. Dumping of sediment across the cross-sections is not accounted for in the sediment transport volumes. Numbers in blue/red indicate the averaged yearly negative/positive sediment budget per cell. Blue/red patches show areas of net negative/positive sediment volumes changes averaged over the width of the computational grid. *Dredge Output*/*Dredge Input* refer to the amount of dredged sediment that is dumped outside/inside the estuary from inside/outside the estuary. The *Total* gives the balance of both volumes. Generally, the sediment export through cross-section Vlissingen-Breskens increases with increasing SLR.

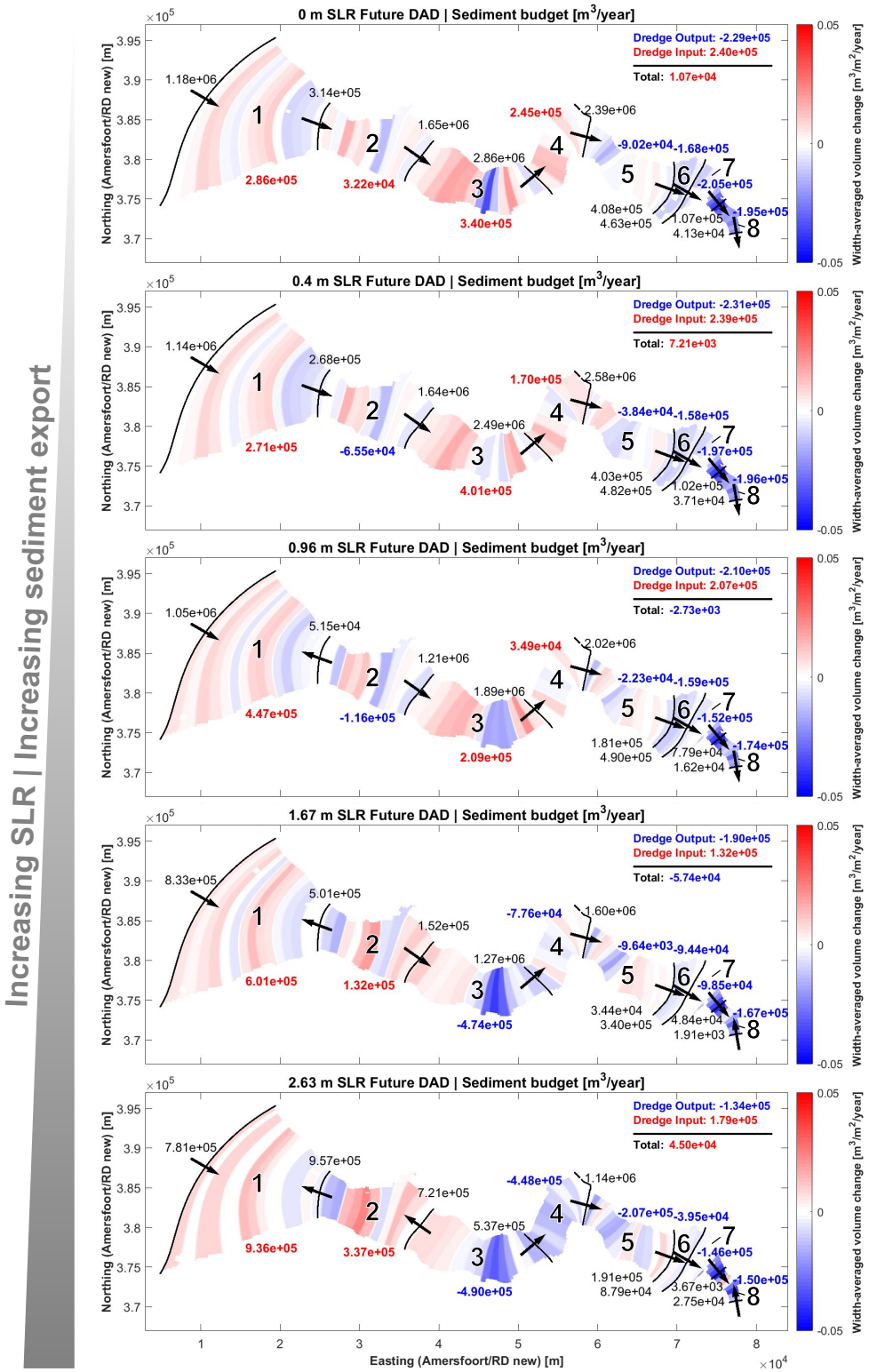

Figure A.6 Sediment (sand only) transport and budget for various defined cells (numbers 1 to 8) in the Western Scheldt estuary simulated with the sand-only wave model configuration of the Delft3D-Scheldt-SLR Model for five linear SLR scenarios for the future dredging and dumping (DAD) strategy (cf. Table 3.2). Numbers in black indicate the yearly sediment transport through each cross-section in the direction of the arrows based on the average transport in the period 2020–2100. Dumping of sediment across the cross-sections is not accounted for in the sediment transport volumes. Numbers in blue/red indicate the averaged yearly negative/positive sediment budget per cell. Blue/red patches show areas of net negative/positive sediment volumes changes averaged over the width of the computational grid. *Dredge Output*/*Dredge Input* refer to the amount of dredged sediment that is dumped outside/inside the estuary from inside/outside the estuary. The *Total* gives the balance of both volumes. Generally, the sediment export through cross-section Vlissingen-Breskens increases with increasing SLR.

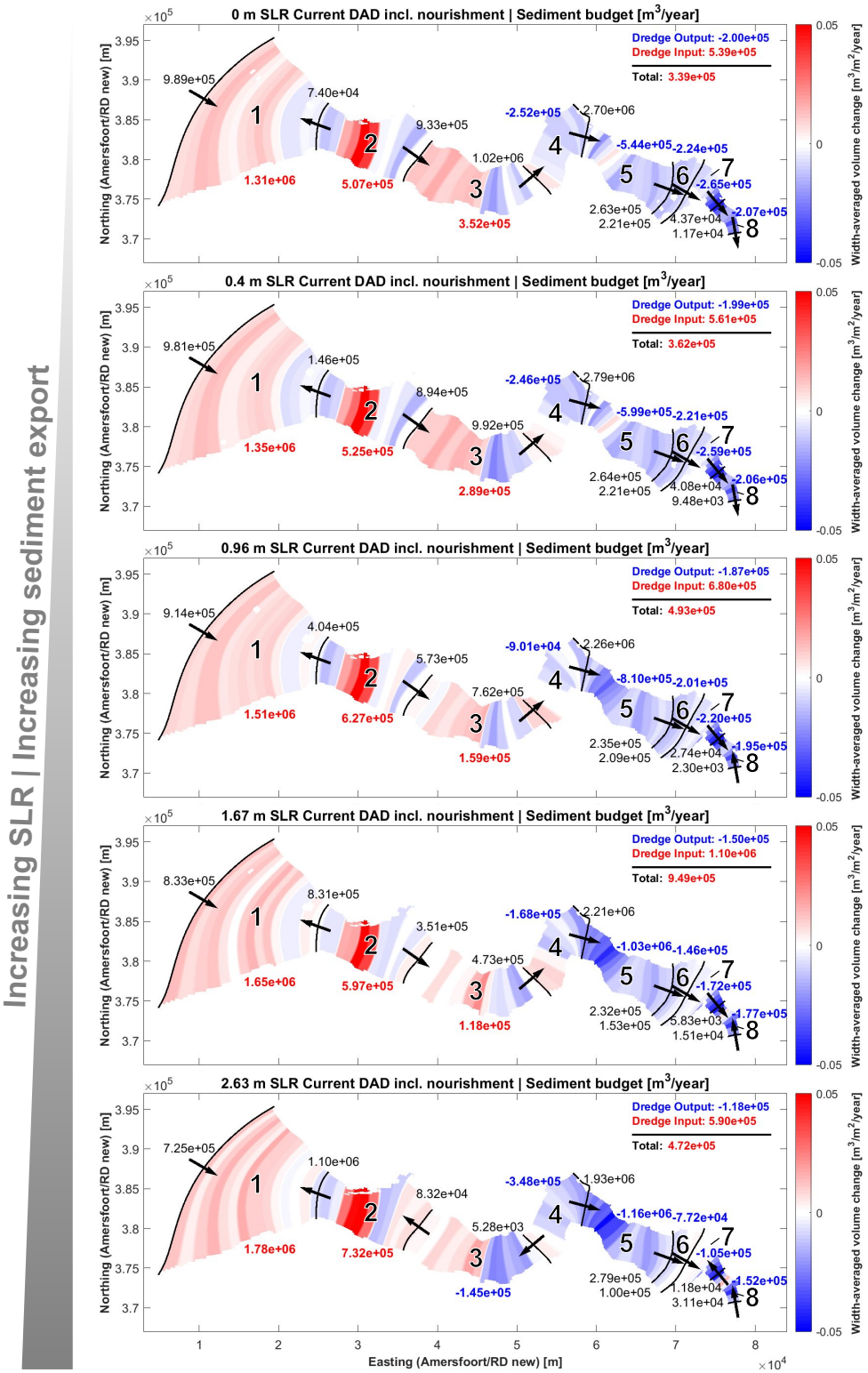

Figure A.7 Sediment (sand only) transport and budget for various defined cells (numbers 1 to 8) in the Western Scheldt estuary simulated with the sand-only wave model configuration of the Delft3D-Scheldt-SLR Model for five linear SLR scenarios for the current dredging and dumping (DAD) strategy including beach nourishments (cf. Table 3.2). Numbers in black indicate the yearly sediment transport through each cross-section in the direction of the arrows based on the average transport in the period 2020–2100. Dumping of sediment across the cross-sections is not accounted for in the sediment transport volumes. Numbers in blue/red indicate the averaged yearly negative/positive sediment budget per cell. Blue/red patches show areas of net negative/positive sediment volumes changes averaged over the width of the computational grid. *Dredge Output*/*Dredge Input* refer to the amount of dredged sediment that is dumped outside/inside the estuary from inside/outside the estuary. The *Total* gives the balance of both volumes. Generally, the sediment export through cross-section Vlissingen-Breskens increases with increasing SLR.

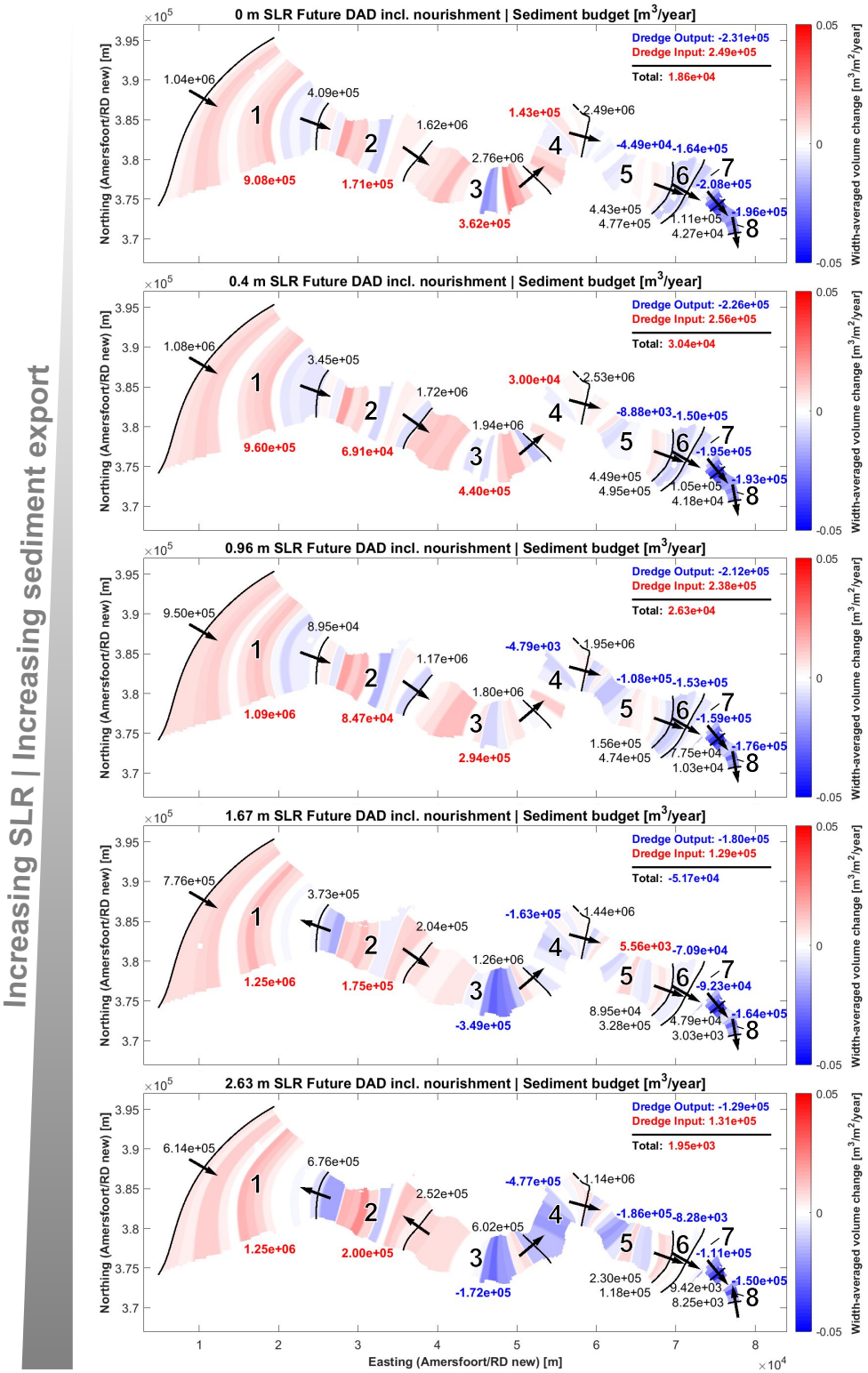

Figure A.8 Sediment (sand only) transport and budget for various defined cells (numbers 1 to 8) in the Western Scheldt estuary simulated with the sand-only wave model configuration of the Delft3D-Scheldt-SLR Model for five linear SLR scenarios for the future dredging and dumping (DAD) strategy including beach nourishments (cf. Table 3.2). Numbers in black indicate the yearly sediment transport through each cross-section in the direction of the arrows based on the average transport in the period 2020–2100. Dumping of sediment across the cross-sections is not accounted for in the sediment transport volumes. Numbers in blue/red indicate the averaged yearly negative/positive sediment budget per cell. Blue/red patches show areas of net negative/positive sediment volumes changes averaged over the width of the computational grid. *Dredge Output*/*Dredge Input* refer to the amount of dredged sediment that is dumped outside/inside the estuary from inside/outside the estuary. The *Total* gives the balance of both volumes. Generally, the sediment export through cross-section Vlissingen-Breskens increases with increasing SLR.

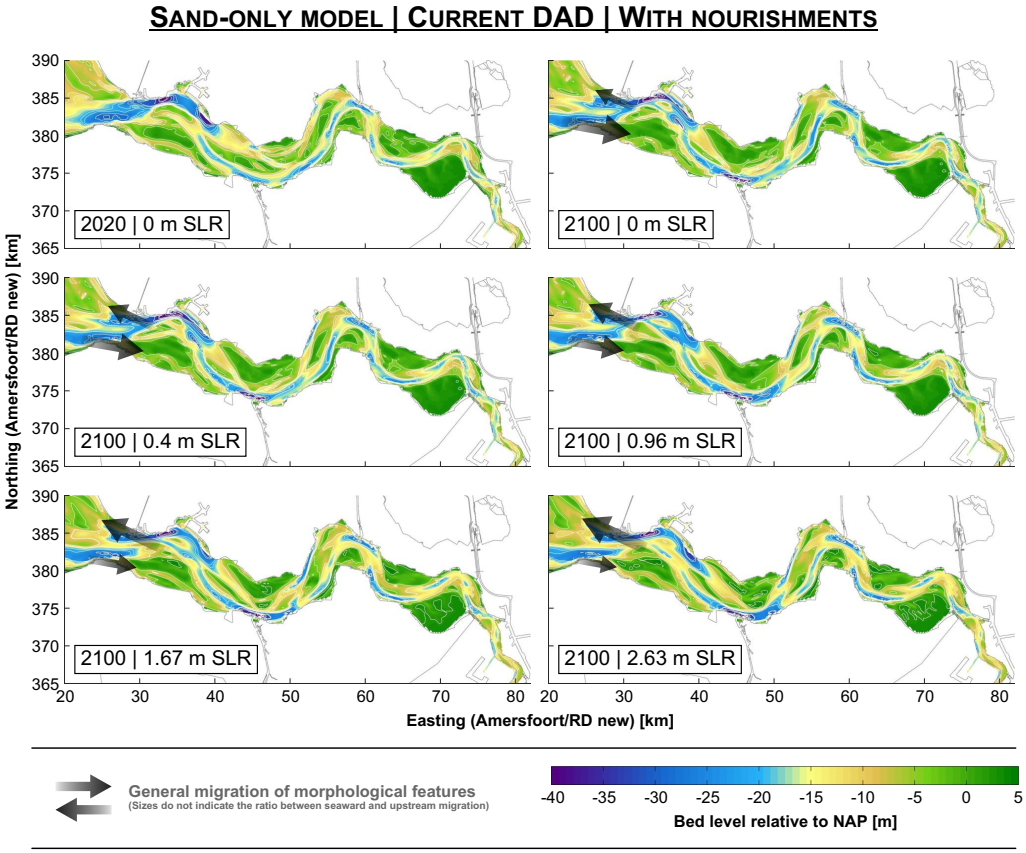

Figure A.9 Bed level of the Western Scheldt estuary in 2020 (including 25 years spin-up time based on the current DAD strategy) and 2100 as simulated with the sand-only model configuration of the Delft3D-Scheldt-SLR Model for five linear SLR scenarios for the current DAD (dredging and dumping) strategy including beach nourishments (cf. Table 3.2). For reasons of comparability, the reference level in all bed level plots is the current sea level (0 m NAP).

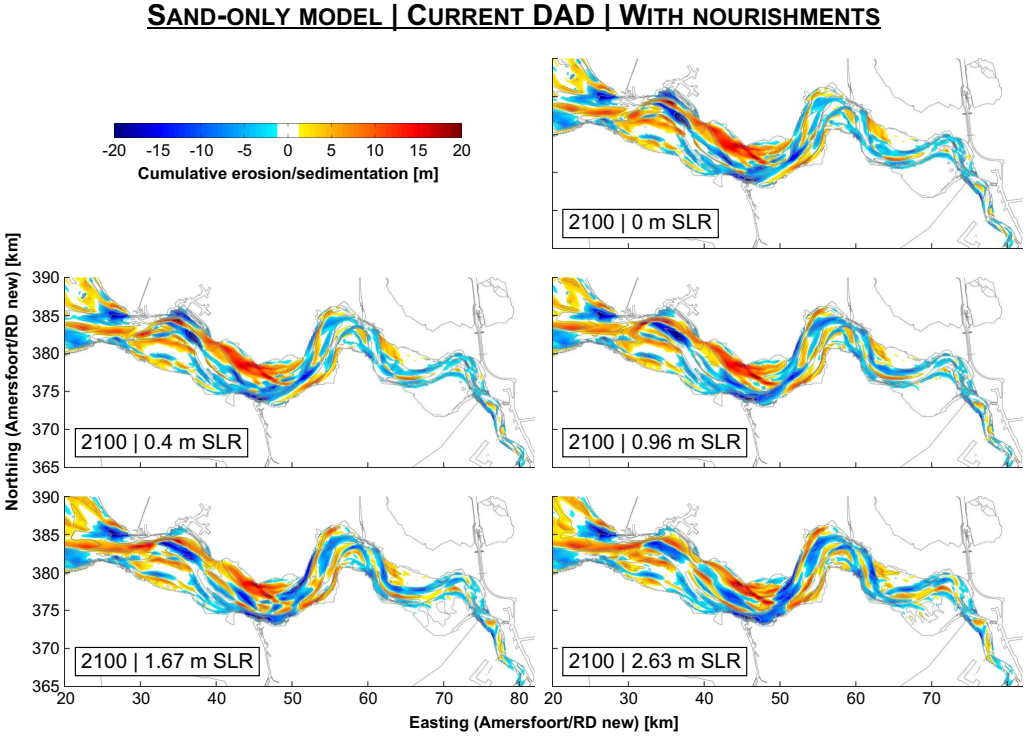

Figure A.10 Cumulative erosion and sedimentation in the period 2020 to 2100 in the Western Scheldt as simulated with the sand-only model configuration of the Delft3D-Scheldt-SLR Model for five linear SLR scenarios for the current DAD (dredging and dumping) strategy including beach nourishments (cf. Table 3.2).

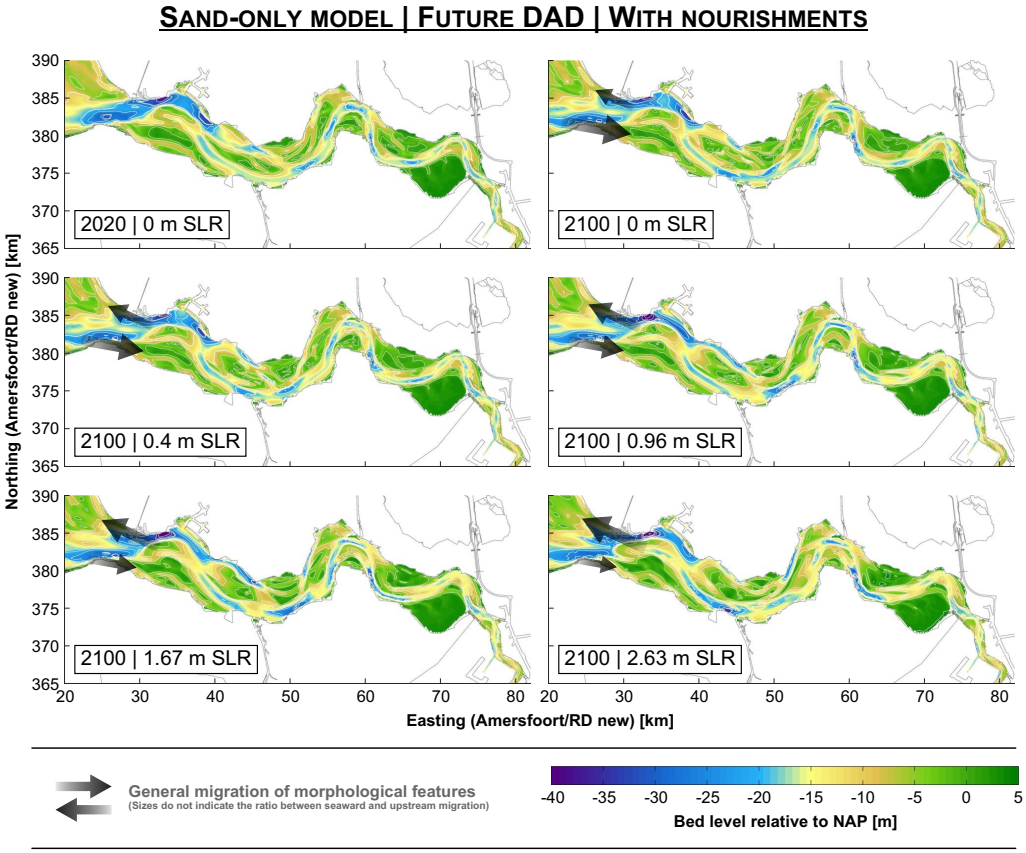

Figure A.11 Bed level of the Western Scheldt estuary in 2020 (including 25 years spin-up time based on the future DAD strategy) and 2100 as simulated with the sand-only model configuration of the Delft3D-Scheldt-SLR Model for five linear SLR scenarios for the future DAD (dredging and dumping) strategy including beach nourishments (cf. Table 3.2). For reasons of comparability, the reference level in all bed level plots is the current sea level (0 m NAP).

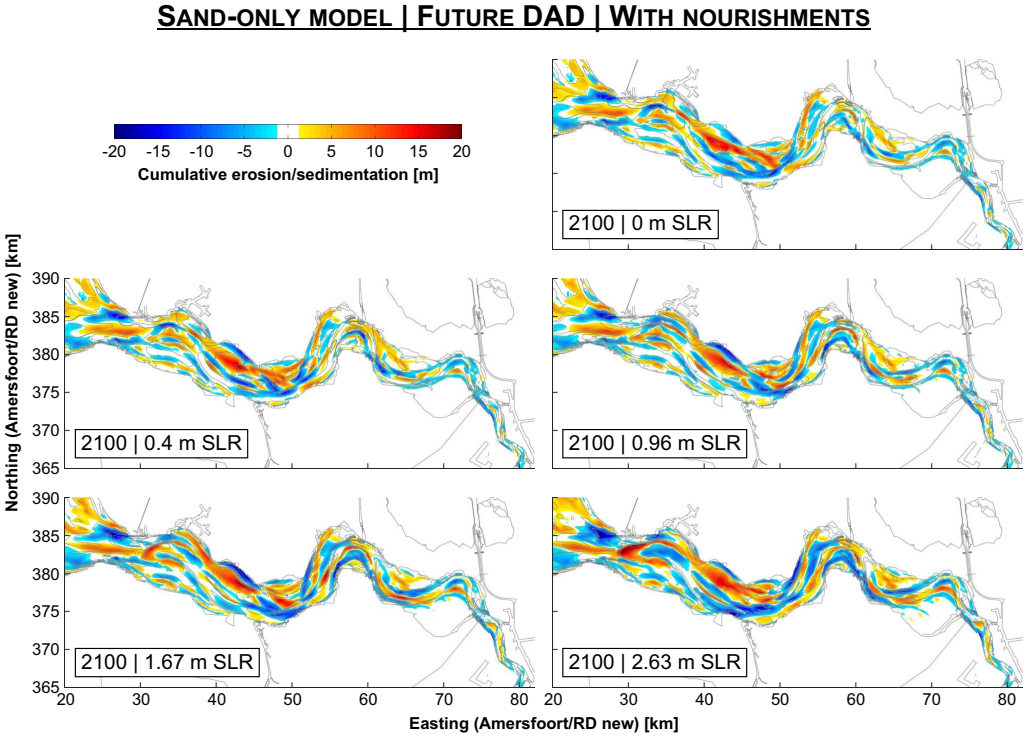

Figure A.12 Cumulative erosion and sedimentation in the period 2020 to 2100 in the Western Scheldt as simulated with the sand-only model configuration of the Delft3D-Scheldt-SLR Model for five linear SLR scenarios for the future DAD (dredging and dumping) strategy including beach nourishments (cf. Table 3.2).

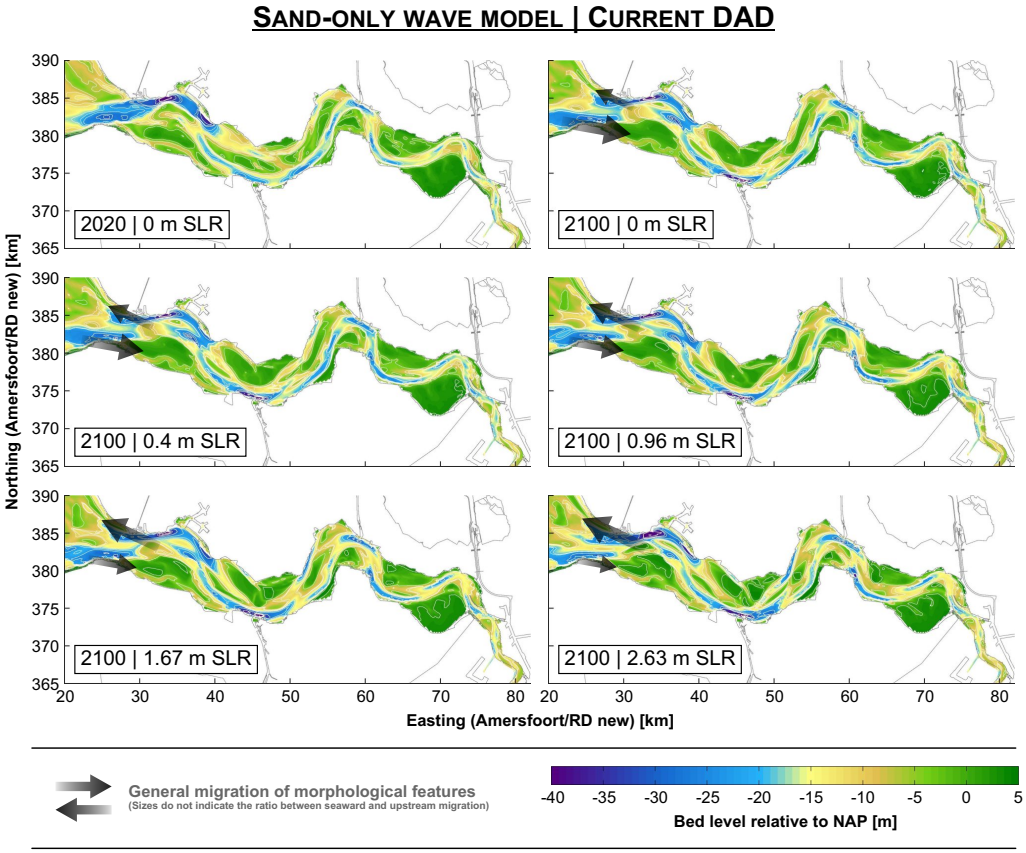

Figure A.13 Bed level of the Western Scheldt estuary in 2020 (including 25 years spin-up time based on the current DAD strategy) and 2100 as simulated with the sand-only wave model configuration of the Delft3D-Scheldt-SLR Model for five linear SLR scenarios for the current DAD (dredging and dumping) strategy (cf. Table 3.2). For reasons of comparability, the reference level in all bed level plots is the current sea level (0 m NAP).

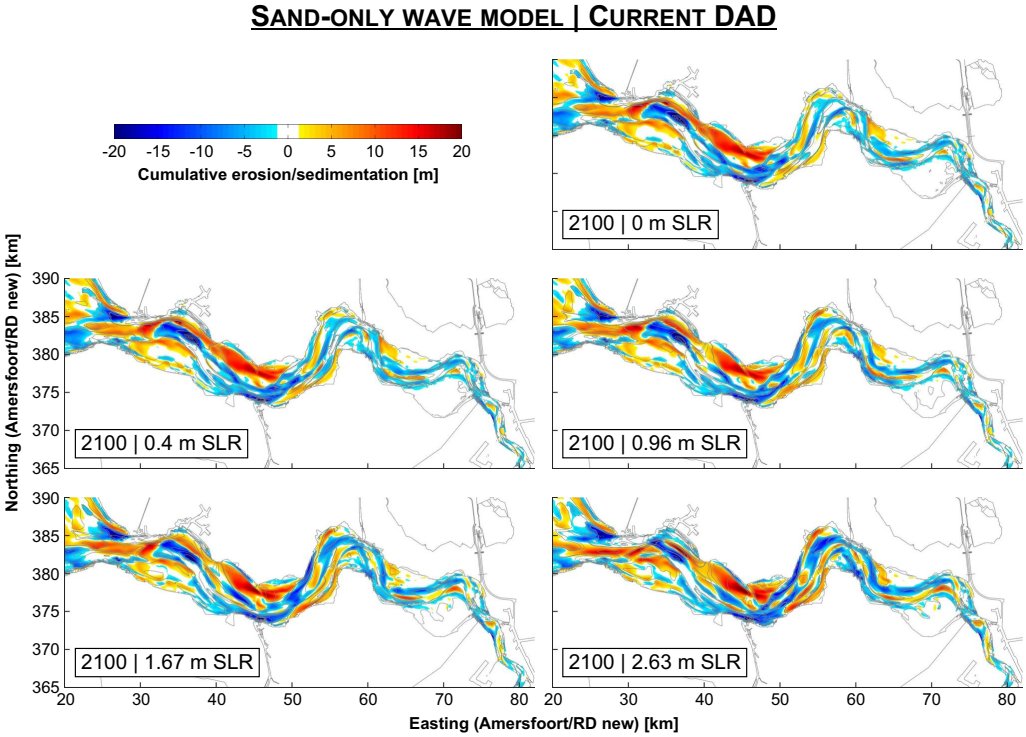

Figure A.14 Cumulative erosion and sedimentation in the period 2020 to 2100 in the Western Scheldt as simulated with the sand-only wave model configuration of the Delft3D-Scheldt-SLR Model for five linear SLR scenarios for the current DAD (dredging and dumping) strategy (cf. Table 3.2).

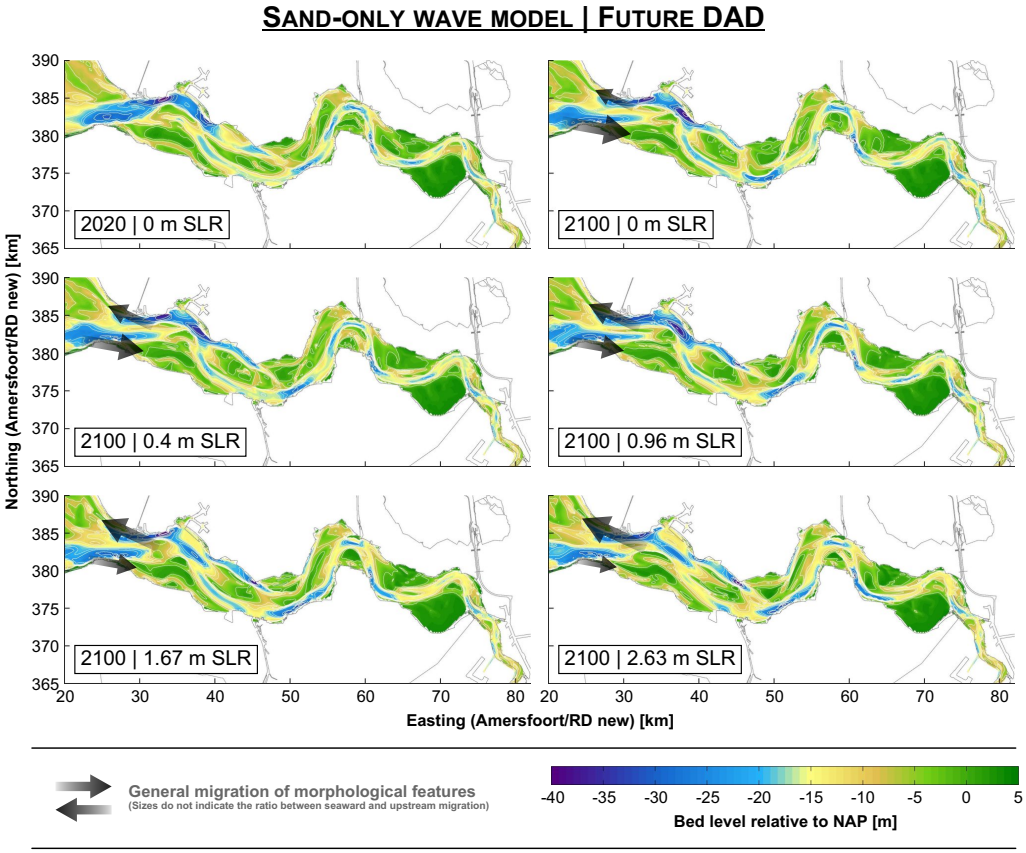

Figure A.15 Bed level of the Western Scheldt estuary in 2020 (including 25 years spin-up time based on the future DAD strategy) and 2100 as simulated with the sand-only wave model configuration of the Delft3D-Scheldt-SLR Model for five linear SLR scenarios for the future DAD (dredging and dumping) strategy (cf. Table 3.2). For reasons of comparability, the reference level in all bed level plots is the current sea level (0 m NAP).

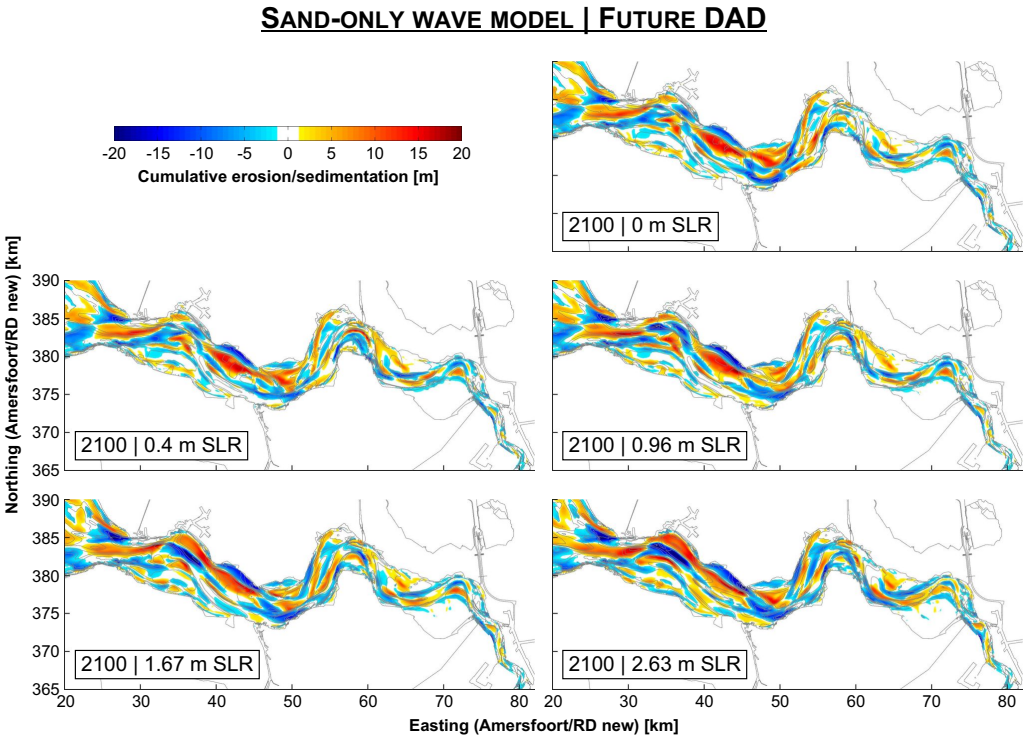

Figure A.16 Cumulative erosion and sedimentation in the period 2020 to 2100 in the Western Scheldt as simulated with the sand-only wave model configuration of the Delft3D-Scheldt-SLR Model for five linear SLR scenarios for the future DAD (dredging and dumping) strategy (cf. Table 3.2).

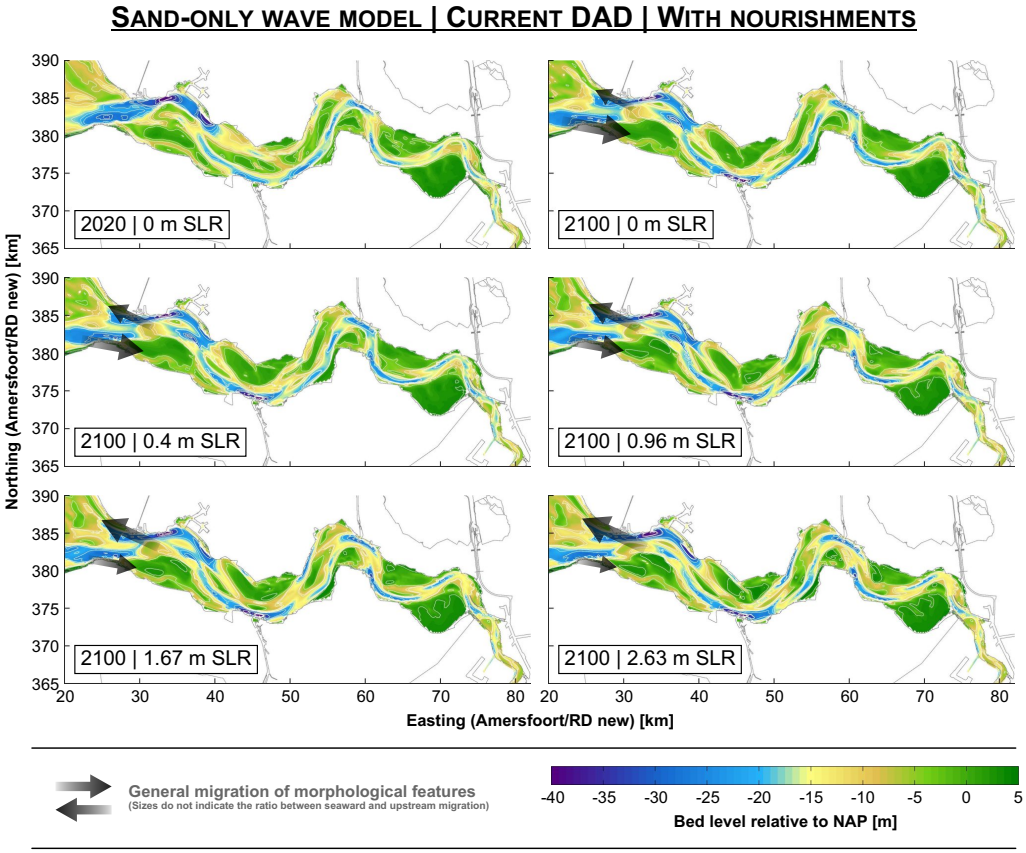

Figure A.17 Bed level of the Western Scheldt estuary in 2020 (including 25 years spin-up time based on the current DAD strategy) and 2100 as simulated with the sand-only wave model configuration of the Delft3D-Scheldt-SLR Model for five linear SLR scenarios for the current DAD (dredging and dumping) strategy including beach nourishments (cf. Table 3.2). For reasons of comparability, the reference level in all bed level plots is the current sea level (0 m NAP).

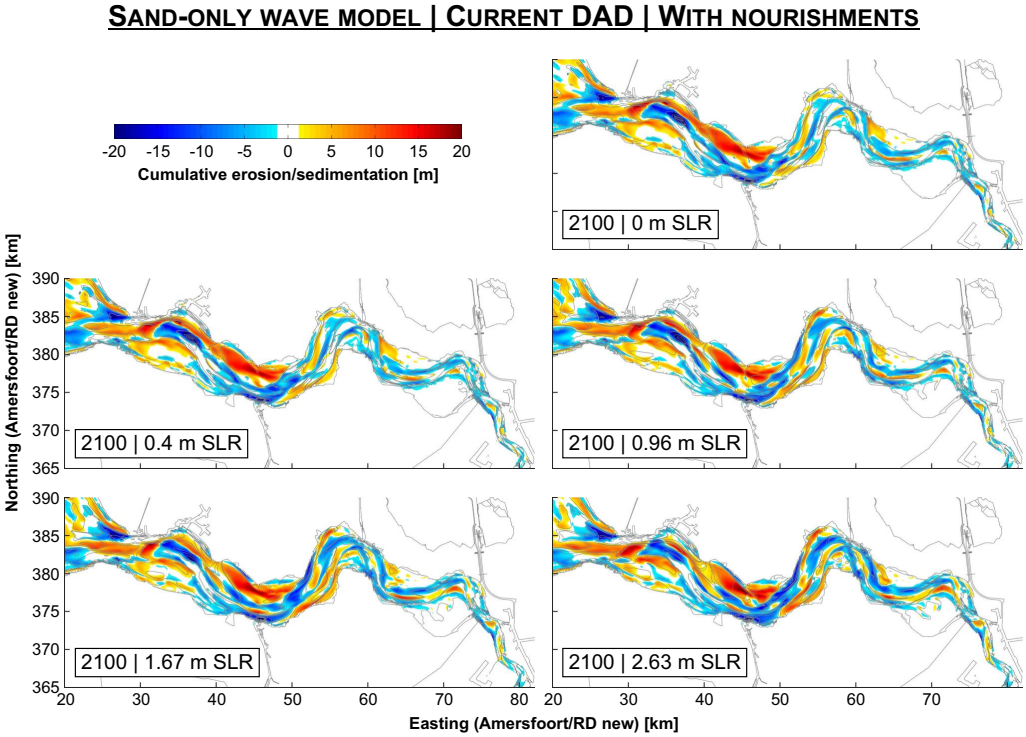

Figure A.18 Cumulative erosion and sedimentation in the period 2020 to 2100 in the Western Scheldt as simulated with the sand-only wave model configuration of the Delft3D-Scheldt-SLR Model for five linear SLR scenarios for the current DAD (dredging and dumping) strategy including beach nourishments (cf. Table 3.2).

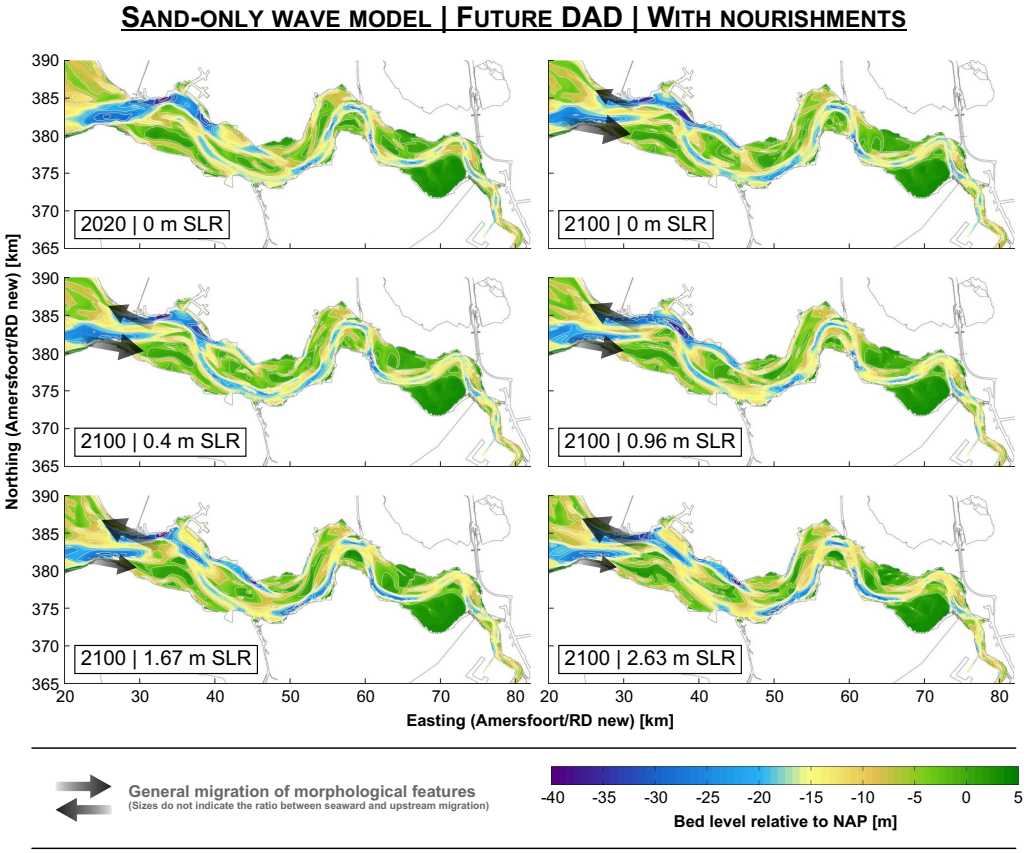

Figure A.19 Bed level of the Western Scheldt estuary in 2020 (including 25 years spin-up time based on the future DAD strategy) and 2100 as simulated with the sand-only wave model configuration of the Delft3D-Scheldt-SLR Model for five linear SLR scenarios for the future DAD (dredging and dumping) strategy including beach nourishments (cf. Table 3.2). For reasons of comparability, the reference level in all bed level plots is the current sea level (0 m NAP).

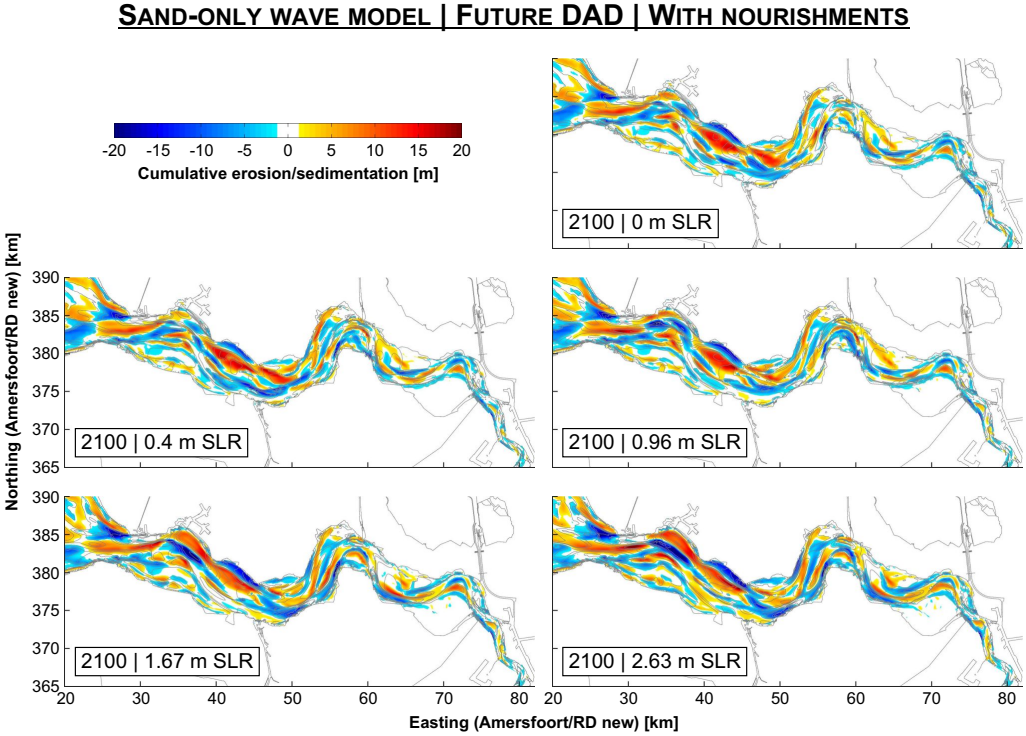

Figure A.20 Cumulative erosion and sedimentation in the period 2020 to 2100 in the Western Scheldt as simulated with the sand-only wave model configuration of the Delft3D-Scheldt-SLR Model for five linear SLR scenarios for the future DAD (dredging and dumping) strategy including beach nourishments (cf. Table 3.2).

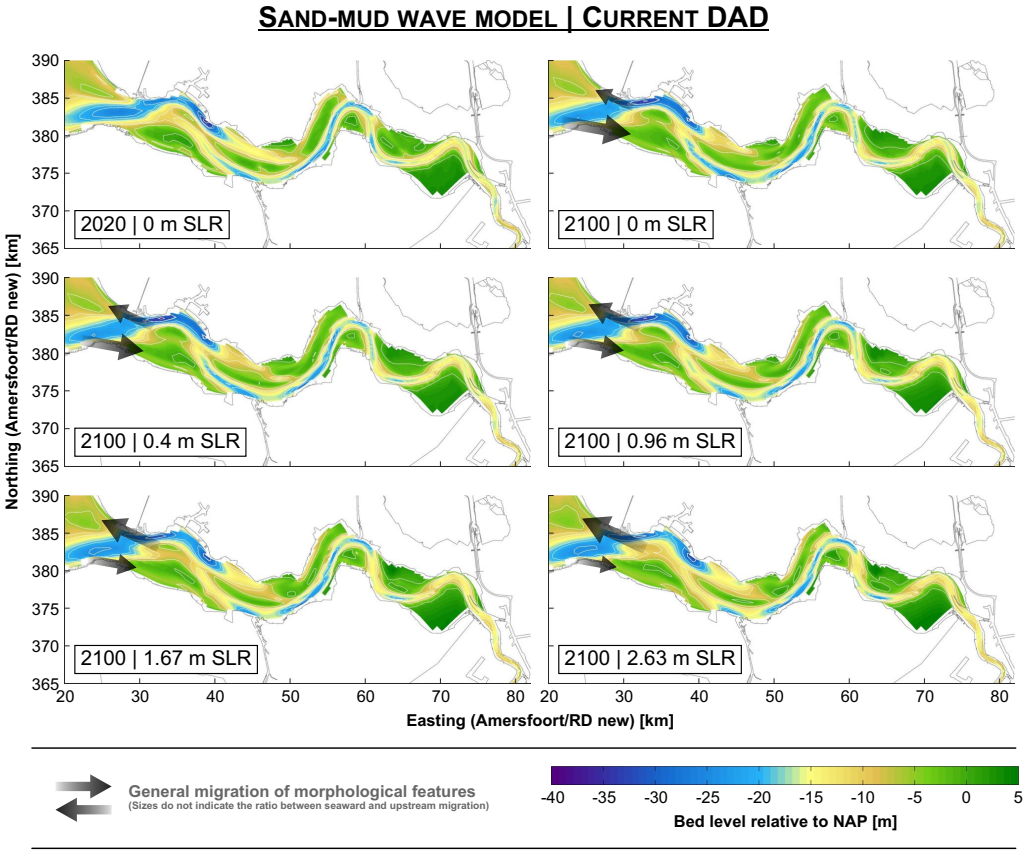

Figure A.21 Bed level of the Western Scheldt estuary in 2020 (including 25 years spin-up time based on the current DAD strategy) and 2100 as simulated with the sand-mud wave model configuration of the Delft3D-Scheldt-SLR Model for five linear SLR scenarios for the current DAD (dredging and dumping) strategy (cf. Table 3.2). For reasons of comparability, the reference level in all bed level plots is the current sea level (0 m NAP).

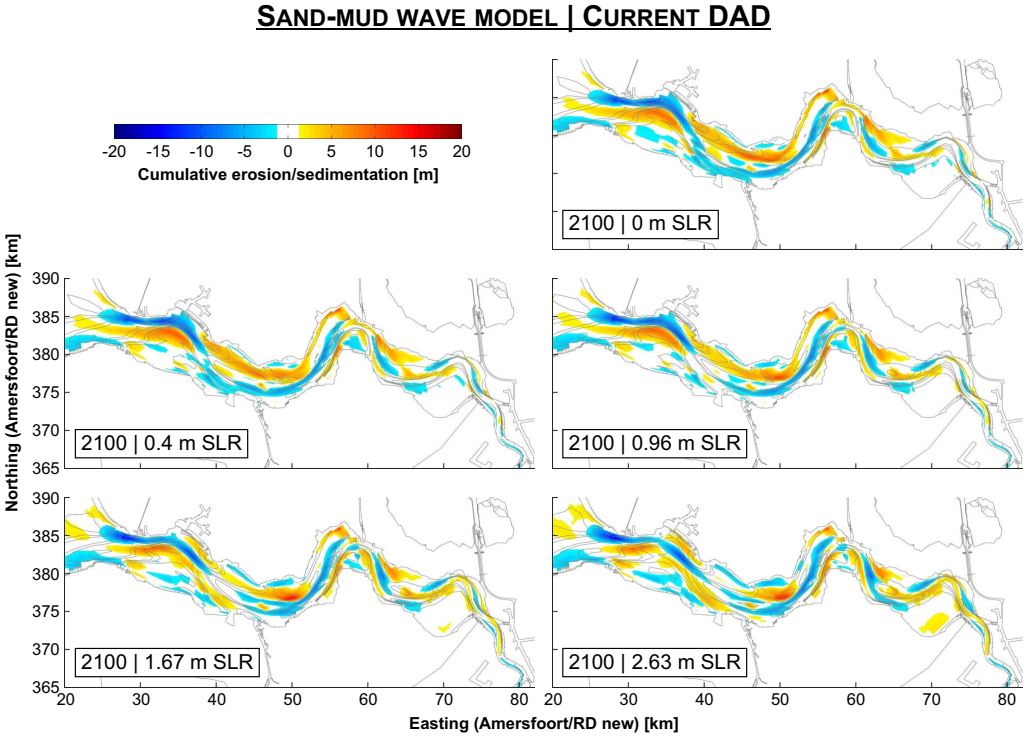

Figure A.22 Cumulative erosion and sedimentation in the period 2020 to 2100 in the Western Scheldt as simulated with the sand-mud wave model configuration of the Delft3D-Scheldt-SLR Model for five linear SLR scenarios for the current DAD (dredging and dumping) strategy (cf. Table 3.2).

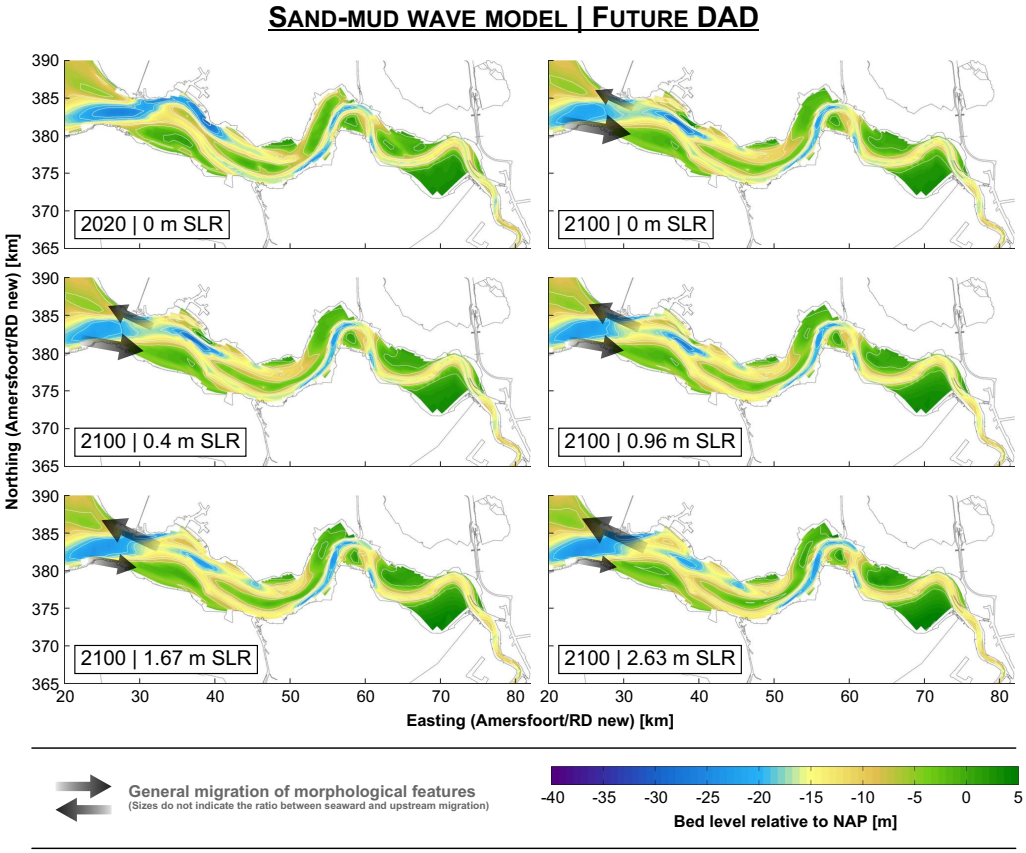

Figure A.23 Bed level of the Western Scheldt estuary in 2020 (including 25 years spin-up time based on the future DAD strategy) and 2100 as simulated with the sand-mud wave model configuration of the Delft3D-Scheldt-SLR Model for five linear SLR scenarios for the future DAD (dredging and dumping) strategy (cf. Table 3.2). For reasons of comparability, the reference level in all bed level plots is the current sea level (0 m NAP).

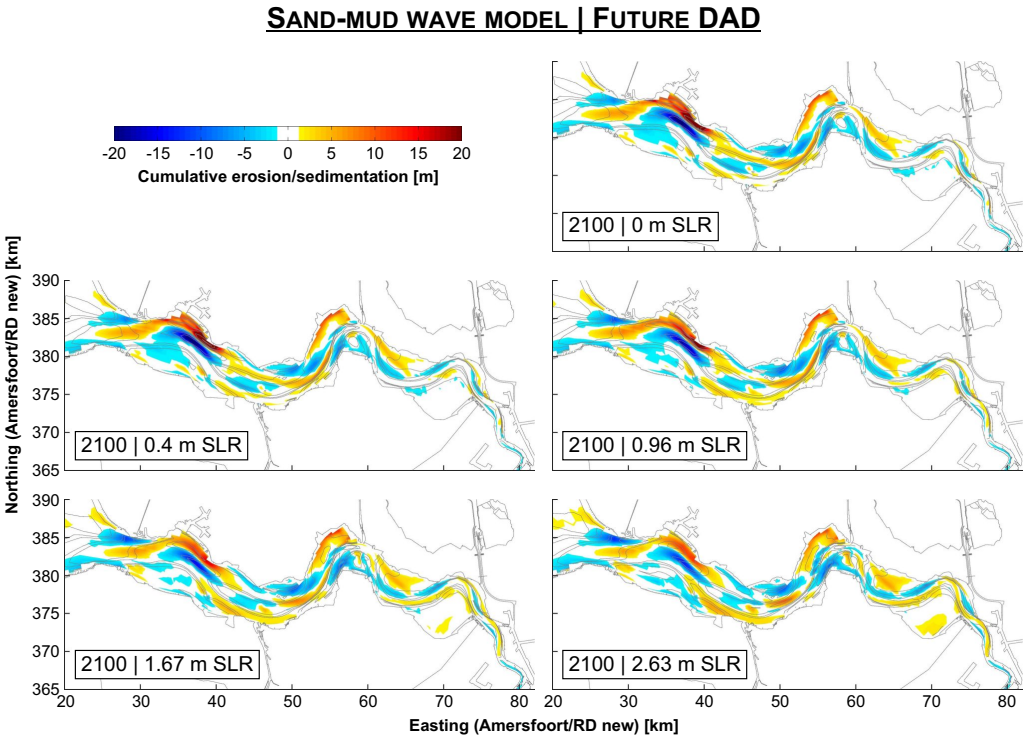

Figure A.24 Cumulative erosion and sedimentation in the period 2020 to 2100 in the Western Scheldt as simulated with the sand-mud wave model configuration of the Delft3D-Scheldt-SLR Model for five linear SLR scenarios for the future DAD (dredging and dumping) strategy (cf. Table 3.2).

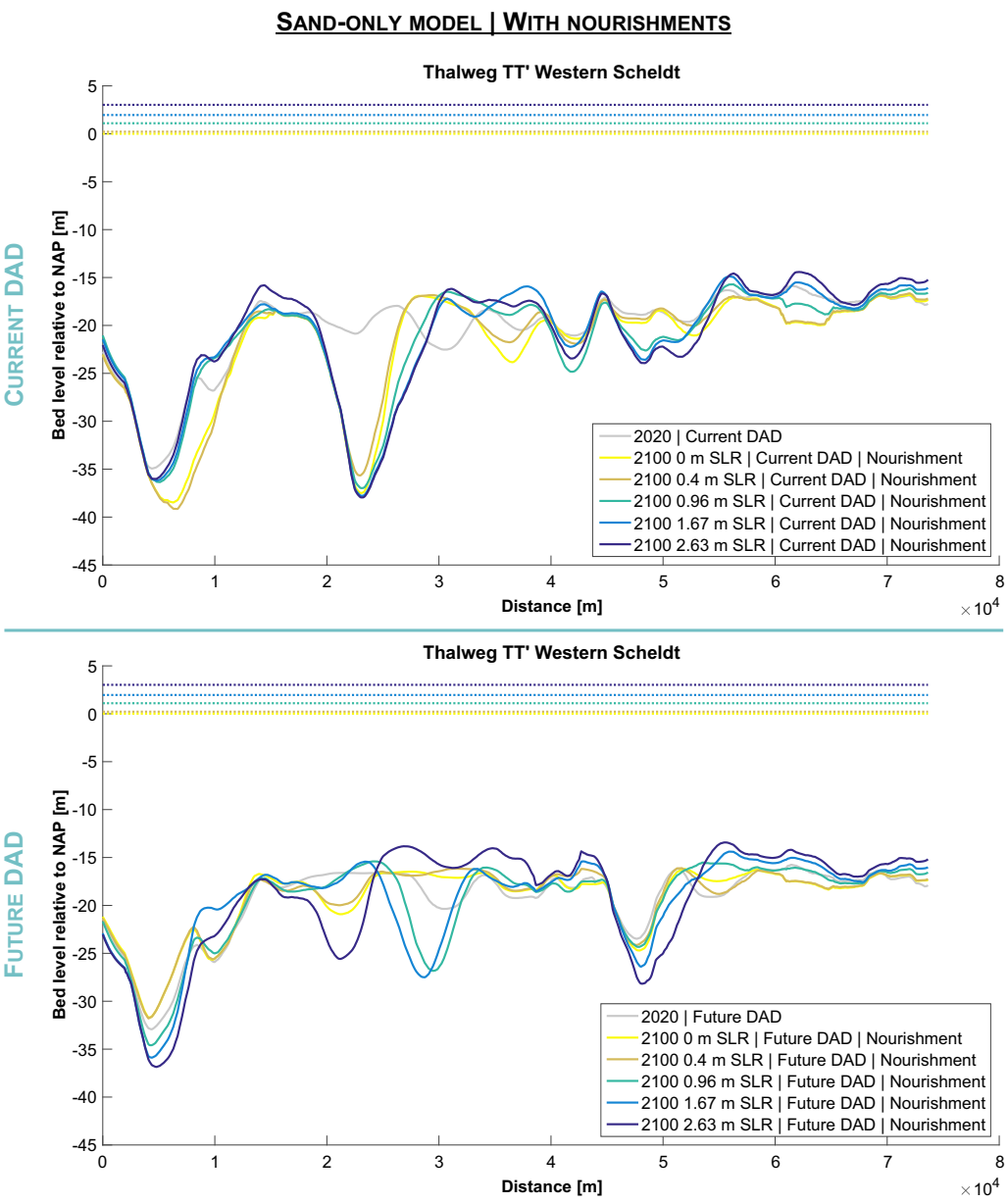

Figure A.25 Depth profiles of the thalweg (i.e. the line of lowest bed levels) of the main navigation channel in the Western Scheldt estuary as simulated with the sand-only model configuration of the Delft3D-Scheldt-SLR Model for various linear SLR scenarios based on the current (top) and future (bottom) DAD strategies including beach nourishments (cf. Table 3.2). For reasons of comparability, the same thalweg line is applied for all scenarios and the reference level of all depth profiles is the current sea level (0 m NAP). Dotted lines show the 2100 sea levels for all SLR scenarios. The course of the thalweg including distance marks is displayed in Fig. 4.20.

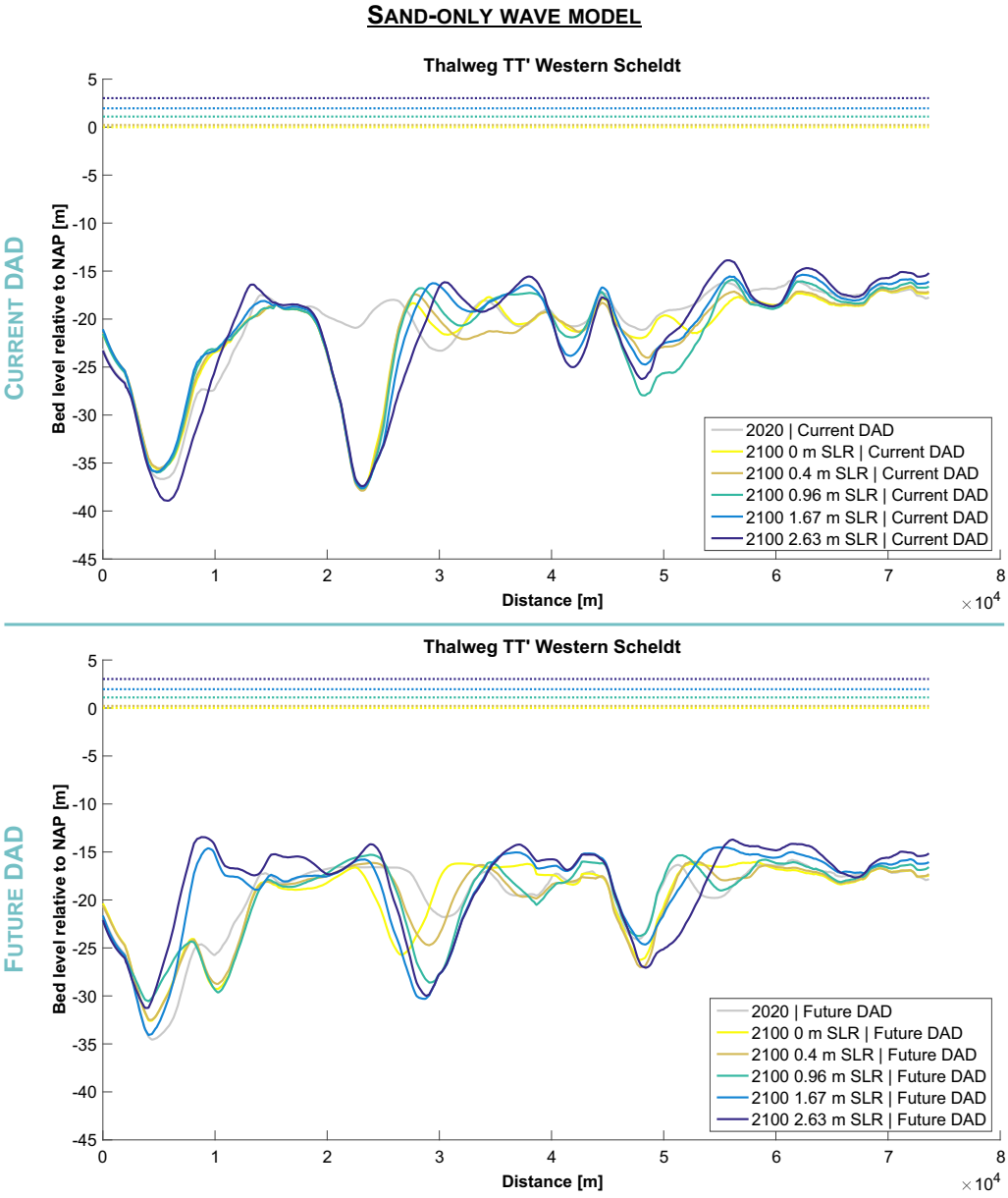

Figure A.26 Depth profiles of the thalweg (i.e. the line of lowest bed levels) of the main navigation channel in the Western Scheldt estuary as simulated with the sand-only wave model configuration of the Delft3D-Scheldt-SLR Model for various linear SLR scenarios based on the current (top) and future (bottom) DAD strategies (cf. Table 3.2). For reasons of comparability, the same thalweg line is applied for all scenarios and the reference level of all depth profiles is the current sea level (0 m NAP). Dotted lines show the 2100 sea levels for all SLR scenarios. The course of the thalweg including distance marks is displayed in Fig. 4.20.

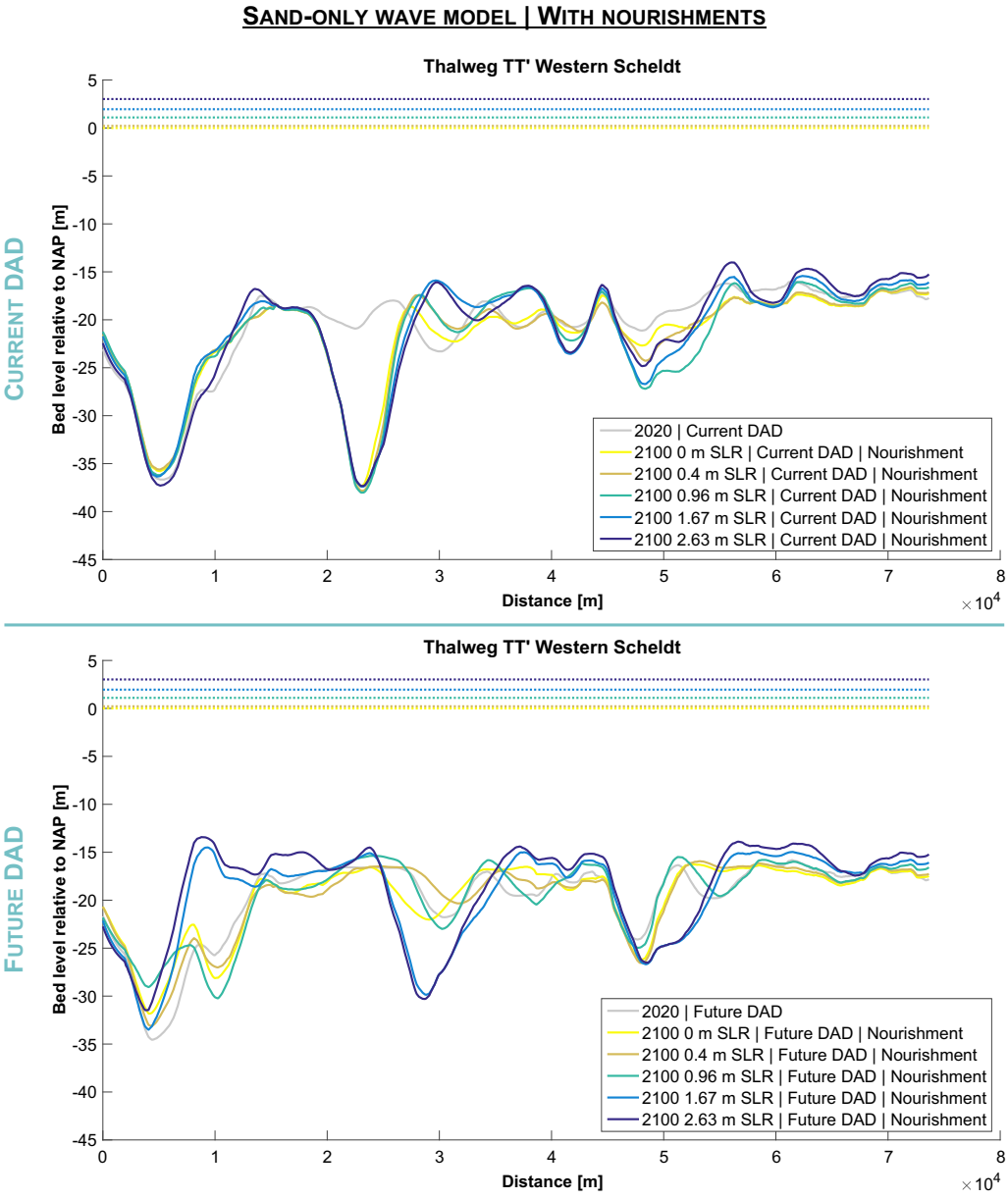

Figure A.27 Depth profiles of the thalweg (i.e. the line of lowest bed levels) of the main navigation channel in the Western Scheldt estuary as simulated with the sand-only wave model configuration of the Delft3D-Scheldt-SLR Model for various linear SLR scenarios based on the current (top) and future (bottom) DAD strategies including beach nourishments (cf. Table 3.2). For reasons of comparability, the same thalweg line is applied for all scenarios and the reference level of all depth profiles is the current sea level (0 m NAP). Dotted lines show the 2100 sea levels for all SLR scenarios. The course of the thalweg including distance marks is displayed in Fig. 4.20.

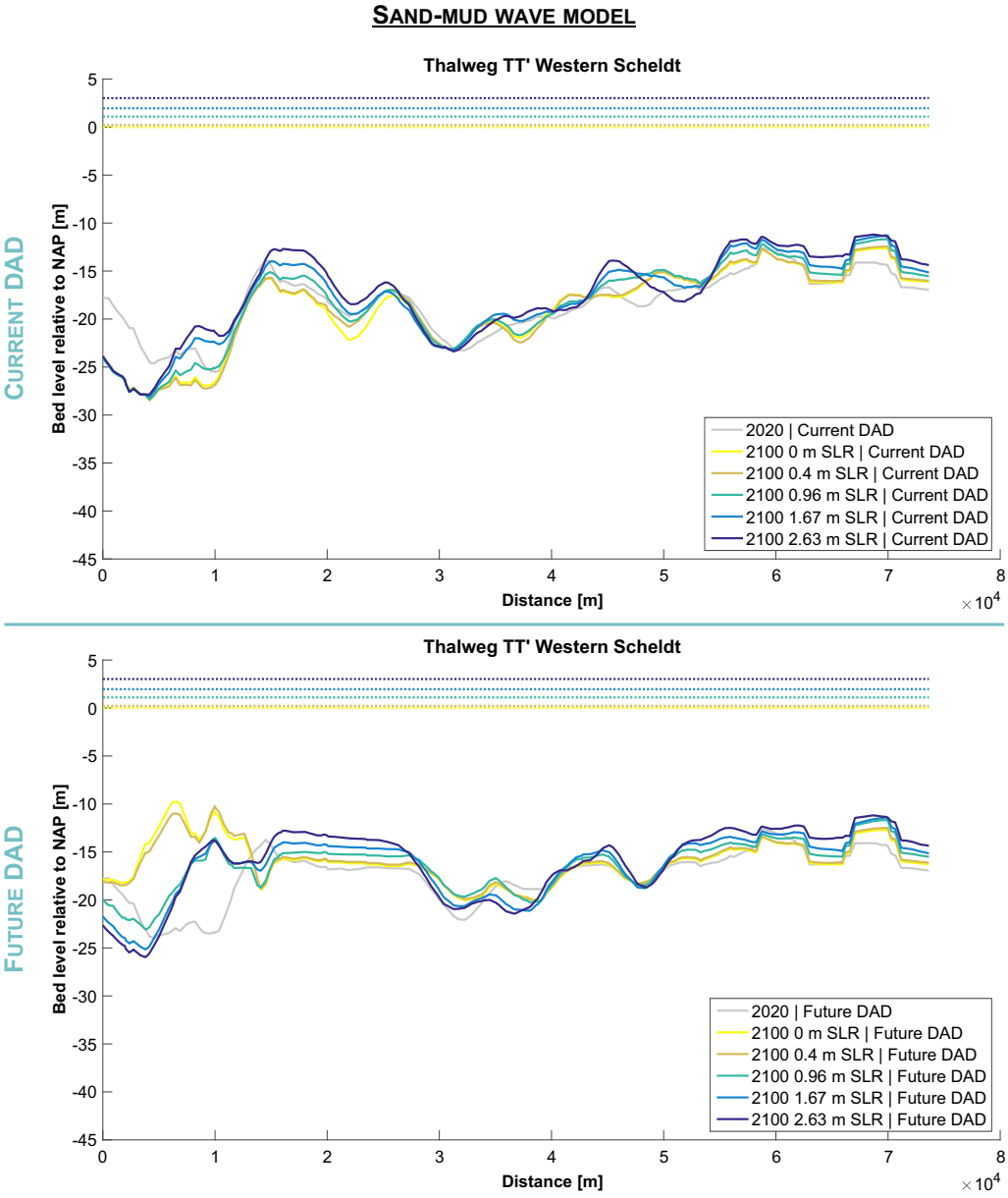

Figure A.28 Depth profiles of the thalweg (i.e. the line of lowest bed levels) of the main navigation channel in the Western Scheldt estuary as simulated with the sand-mud wave model configuration of the Delft3D-Scheldt-SLR Model for various linear SLR scenarios based on the current (top) and future (bottom) DAD strategies (cf. Table 3.2). For reasons of comparability, the same thalweg line is applied for all scenarios and the reference level of all depth profiles is the current sea level (0 m NAP). Dotted lines show the 2100 sea levels for all SLR scenarios. The course of the thalweg including distance marks is displayed in Fig. 4.20.

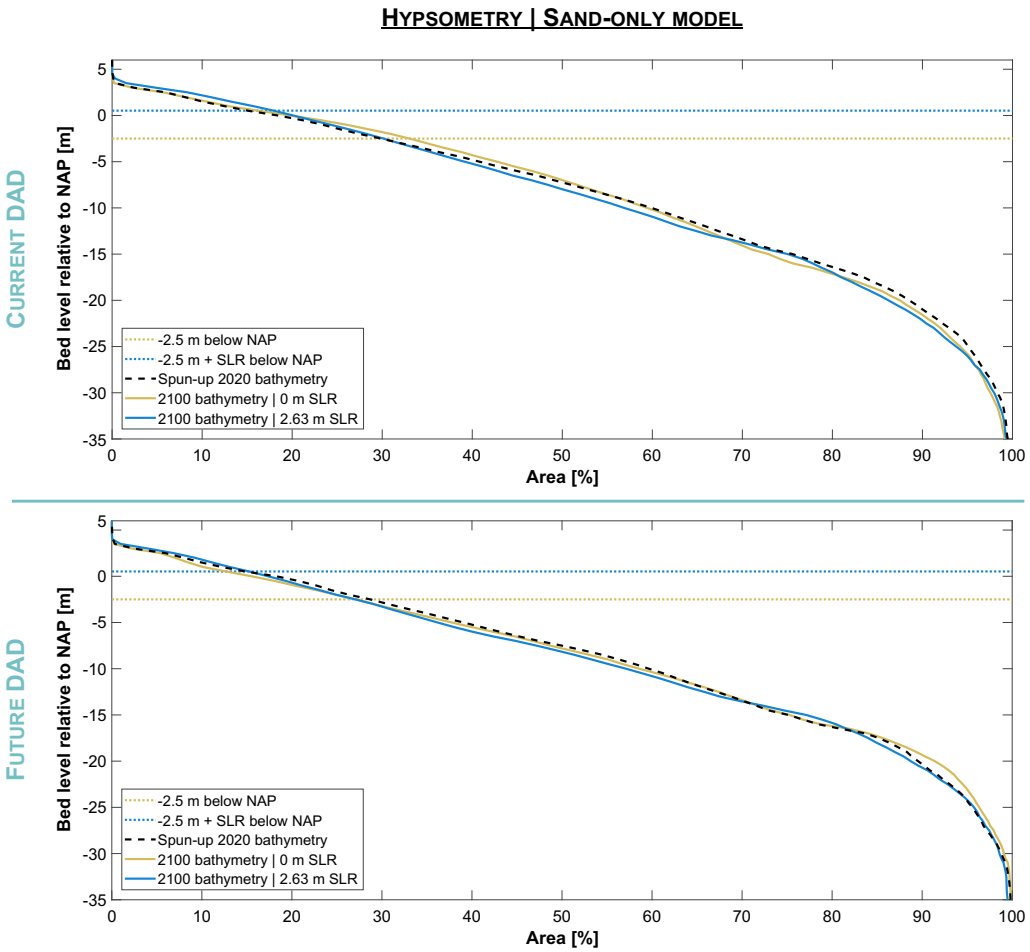

Figure A.29 Hypsometric curves of the Western Scheldt estuary between Vlissingen-Breskens and the Dutch-Belgian border as simulated with the sand-only model configuration of the Delft3D-Scheldt-SLR Model for the 0 m SLR (beige solid lines) and for the 2.63 m (blue solid lines) linear SLR scenarios based on the current (top) and future (bottom) DAD strategies (cf. Table 3.2). The black dashed lines show the hypsometries of the initial, spun-up 2020 model bathymetries. For reasons of comparability, the reference level of all displayed hypsometric curves is the current sea level (0 m NAP). The two -2.5 m NAP marks indicate the approximate lower limits of the intertidal area for a sea level of 0 m NAP (beige dotted lines) and for a future sea level of 2.63 m NAP (blue dotted lines).

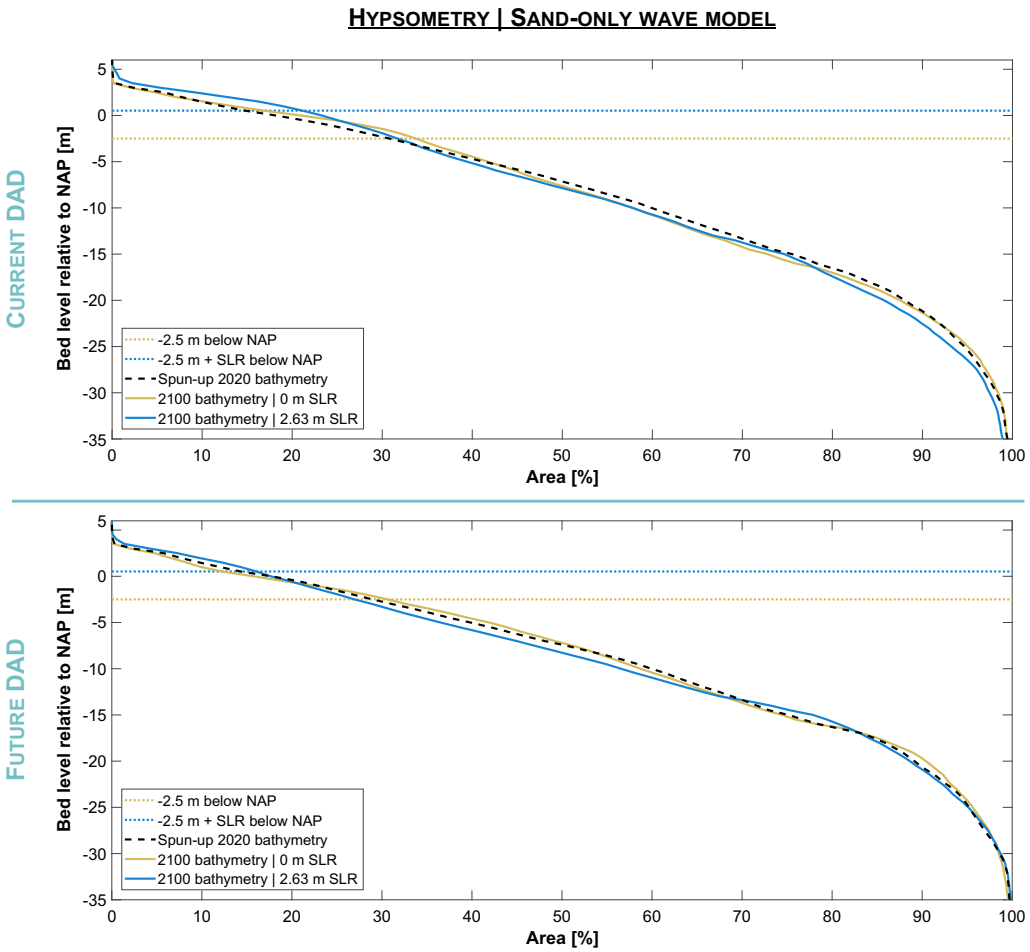

Figure A.30 Hypsometric curves of the Western Scheldt estuary between Vlissingen-Breskens and the Dutch-Belgian border as simulated with the sand-only wave model configuration of the Delft3D-Scheldt-SLR Model for the 0 m SLR (beige solid lines) and for the 2.63 m (blue solid lines) linear SLR scenarios based on the current (top) and future (bottom) DAD strategies (cf. Table 3.2). The black dashed lines show the hypsometries of the initial, spun-up 2020 model bathymetries. For reasons of comparability, the reference level of all displayed hypsometric curves is the current sea level (0 m NAP). The two -2.5 m NAP marks indicate the approximate lower limits of the intertidal area for a sea level of 0 m NAP (beige dotted lines) and for a future sea level of 2.63 m NAP (blue dotted lines).

References

BAEYE, M., M. FETTWEIS, G. VOULGARIS and V. VAN LANCKER, 2010. "Sediment mobility in response to tidal and wind-driven flows along the Belgian inner shelf, southern North Sea." *Ocean Dynamics* 61: pp. 611–622. doi:10.1007/s10236-010-0370-7.

BLIEK, B., A. DE GELDER, C. GAUTIER and B. LES, 1998. "De rol van het getij in de morfologische ontwikkeling van de Westerscheldemond. Een modelmatige onderbouwing. Eindrapport getijreconstructie Westerscheldemond." In Svasek, ed., *Svasek rapporten*, vol. K2000*KOP.

BOLLE, A., Z. WANG, C. AMOS and J. RONDE, 2010. "The influence of changes in tidal asymmetry on residual sediment transport in the Western Scheldt." *Continental Shelf Research* 30: pp. 871–882. doi:10.1016/j.csr.2010.03.001.

CHURCH, J. and P. CLARK, 2013. "Sea level change." In T. STOCKER, M. t. S. t. J. t. A. t. Y. t. V. t. D. QIN, G.-K. PLATTNER and P. MIDGLEY, eds., *Climate change 2013: the physical science basis. Contribution of working group I to the fifth assessment report of the Intergovernmental Panel on Climate Change*. Cambridge University Press, Cambridge. Pp. 1137–1216.

DAM, G., 2013a. "Harde lagen Westerschelde." In International Marine & Dredging Consultants, ed., *Achtergrondrapport*, vol. A-28.

DAM, G., 2013b. "Long-term modeling of the impact of dredging strategies on morpho- and hydrodynamic developments in the Western Scheldt." *Nature* 531: pp. 591–597. doi:10.1038/nature17145.

DECONTO, R. and D. POLLARD, 2016. "Contribution of Antartica to past and future sea-level rise." *Nature* 531: pp. 591–597. doi:10.1038/nature17145.

Deltares, 2019a. "D-Flow Flexible Mesh. D-Flow FM in Delta Shell. User manual, version 1.5.0." https://www.deltares.nl/app/uploads/2020/01/Documentation-Delft3D-FM-Suite-2020.02-1.6.1.zip. 2020-01-30.

Deltares, 2019b. "D-Waves. Simulation of short-crested waves with SWAN. User manual, version 1.2." https://www.deltares.nl/app/uploads/2020/01/Documentation-Delft3D-FM-Suite-2020.02-1.6.1.zip. 2020-01-30.

Deltares, 2020a. "Delft3D-FLOW. Simulation of multi-dimensional hydrodynamic flows and transport phenomena, including sediments. User manual, version 3.15.65593." https://content.oss.deltares.nl/delft3d/manuals/Delft3D-FLOW_User_Manual.pdf. 2020-07-01.

Deltares, 2020b. "Delft3D-WAVE. Simulation of short-crested waves with SWAN. User manual, version 3.05.62107." https://content.oss.deltares.nl/delft3d/manuals/Delft3D-WAVE_User_Manual.pdf. 2020-07-01.

EMODNET — European Marine Observation and Data Network, 2016. "EMODnet Digital Terrain Model (DTM) for European sea regions (version 2016)." https://www.emodnet-bathymetry.eu/data-products. 2019-06-26.

ENGELUND, F. and E. HANSEN, 1967. *A monograph on sediment transport in alluvial systems*. Teknisk Forlag, Copenhagen.

FETTWEIS, M., B. NECHAD and D. VAN DEN EYNDE, 2007. "An estimate of the suspended particulate matter (SPM) transport in the southern North Sea using SeaWiFS images, in situ measurements and numerical model results." *Continental Shelf Research* 27: pp. 1568–1583. doi:10.1016/j.csr.2007.01.017.

FETTWEIS, M. and D. VAN DEN EYNDE, 2003. "The mud deposits and the high turbidity in the Belgian-Dutch coastal zone, southern bight of the North Sea." *Continental Shelf Research* 23: pp. 669–691. doi:10.1016/S0278-4343(03)00027-X.

GUO, L., M. BRAND, B. SANDERS, E. FOUFOULA-GEORGIOU and E. STEIN, 2018. "Tidal asymmetry and residual sediment transport in a short tidal basin under sea level rise." *Advances in Water Resources* 121: pp. 1–8. doi:10.1016/j.advwatres.2018.07.012.

IOC — Intergovernmental Oceanographic Commission, IHO — International Hydrographic Organization and UNESCO — United Nations Educational, Scientific and Cultural Organization, 2015. "General Bathymetric Chart of the Oceans (GEBCO). GEBCO 2014 Grid. Liverpool." https://www.gebco.net/data_and_products/historical_data_sets/#gebco_2019/. 2019-06-26.

IRAZOQUI-APECECHEA, M., S. MUIS, D. LE BARS, M. HAASNOOT, R. DE WINTER and M. VERLAAN, 2020. "Changes in global tides in response to future sea-level rise." *Earth's Future* Under review.

JEUKEN, C., M. VAN HELVERT and Z. WANG, 2002. "ESTMORF berekeningen naar de invloed van ingrepen en natuurlijke forceringen op de zandhuishouding van Westerschelde en monding." In WL |Delft Hydraulics (Netherlands), ed., *Delft Hyraulics report*, vol. Z3246.

LE BARS, D., S. DRIJFHOUT and H. DE VRIES, 2017. "A high-end sea level rise probabilistic projection including rapid Antarctic ice sheet mass loss." *Environmental Research Letters* 12: pp. 1–9. doi:10.1088/1748-9326/aa6512.

MUIS, S., M. VERLAAN, H. WINSEMIUS, J. AERTS and P. WARD, 2016. "A global reanalysis of storm surges and extreme sea levels." *Nature Communications* 7: pp. 1–11. doi:10.1038/ncomms11969.

PARTHENIADES, E., 1965. "Erosion and deposition of cohesive soils." *Journal of the Hydraulics Division* 91: pp. 105–139.

PAWLOWICZ, R., B. BEARDSLEY and S. LENTZ, 2002. "Classical tidal harmonic analysis including error estimates in MATLAB using T_TIDE." *Computers & Geosciences* 28: pp. 929–937. doi:10.1016/S0098-3004(02)00013-4.

RWS — Rijkswaterstaat Ministerie van Infrastructuur en Milieu, 1963. "Vaklodingen 1963." https://waterinfo-extra.rws.nl/monitoring/morfologie/#h53b817e6-e5cd-49d1-873c-9a0f85d8e416. 2019-06-23.

RWS — Rijkswaterstaat Ministerie van Infrastructuur en Milieu, 1964. "Vaklodingen 1964." https://waterinfo-extra.rws.nl/monitoring/morfologie/#h53b817e6-e5cd-49d1-873c-9a0f85d8e416. 2019-06-23.

RWS — Rijkswaterstaat Ministerie van Infrastructuur en Milieu, 1969. "Vaklodingen 1969." https://waterinfo-extra.rws.nl/monitoring/morfologie/#h53b817e6-e5cd-49d1-873c-9a0f85d8e416. 2019-06-23.

RWS — Rijkswaterstaat Ministerie van Infrastructuur en Milieu, 2011a. "Vaklodingen 2011." https://waterinfo-extra.rws.nl/monitoring/morfologie/#h53b817e6-e5cd-49d1-873c-9a0f85d8e416. 2012-09-14.

RWS — Rijkswaterstaat Ministerie van Infrastructuur en Milieu, 2011b. “JARKUS 2011.” https://ihm-open-data-viewer-waterinfo.infoprojects.nl/index.htm?opendatalayer=JARKUS+2014&opendatafolder=Morfologie. 2012-09-20.

RWS — Rijkswaterstaat Ministerie van Infrastructuur en Milieu, 2012a. “Vaklodingen 2012.” https://waterinfo-extra.rws.nl/monitoring/morfologie/#h53b817e6-e5cd-49d1-873c-9a0f85d8e416. 2012-09-14.

RWS — Rijkswaterstaat Ministerie van Infrastructuur en Milieu, 2012b. “JARKUS 2012.” https://ihm-open-data-viewer-waterinfo.infoprojects.nl/index.htm?opendatalayer=JARKUS+2014&opendatafolder=Morfologie. 2012-09-20.

RWS — Rijkswaterstaat Ministerie van Infrastructuur en Milieu, 2012c. “Zandbalans per macrocel tot 1-1-2013.” http://publicaties.minienm.nl/jaaroverzichten. 2020-07-20.

RWS — Rijkswaterstaat Ministerie van Infrastructuur en Milieu, 2017. “Rijkswaterstaat Matroos NOOS_E.” http://noos.matroos.rws.nl/index.php. 2017-08-30.

Spencer, T., S. Brooks, B. Evans, J. Tempest and I. Möller, 2015. “Southern North Sea storm surge event of 5 December 2013: water levels, waves and coastal impacts.” *Earth-Science Reviews* 146: pp. 120–145. doi:10.1016/j.earscirev.2015.04.002.

Trouw, K., N. Zimmermann, L. Wang, B. De Maerschalck, R. Delgado, T. Verwaest and F. Mostaert, 2015. “Scientific support regarding hydrodynamics and sand transport in the coastal zone: literature and data review coastal zone Zeebrugge–Zwin.” In Waterboukundig Laboratorium Antwerpen (Belgium), ed., *WL Rapporten*, vol. 12_107.

van der Wegen, M., A. Dastgheib, B. Jaffe and D. Roelvink, 2011. “Bed composition generation for morphodynamic modeling: case study of San Pablo Bay in California, USA.” *Ocean Dynamics* 61: pp. 173–186. doi:10.1007/s10236-010-0314-2.

van der Wegen, M., J. van der Werf, P. de Vet and B. Röbke, 2017. “Hindcasting Westerschelde mouth morphodynamics (1963–2011).” In Deltares Delft (Netherlands), ed., *Deltares report*, vol. 1210301-001-ZKS-0006.

van der Werf, J. and C. Brière, 2013. “The influence of morphology on tidal dynamics and sand transport in the Scheldt estuary.” In Deltares Delft (Netherlands), ed., *Deltares report*, vol. 1207720-000.

Van Lancker, V., M. Baeye, I. Du Four, R. Janssens, S. Degraer, M. Fettweis, F. Francken, J. Houziaux, P. Luyten, D. Van den Eynde, M. Devolder, K. De Cauwer, J. Monbaliu, E. Toorman, J. Portilla, A. Ullman, M. Liste Muñoz, L. Fernandez, H. Komijani, T. Verwaest, R. Delgado, J. De Schutter, J. Janssens, Y. Levy, J. Vanlede, M. Vincx, M. Rabaut, H. Vandenberghe, E. Zeelmaekers and A. Goffin, 2012. “Quantification of erosionsedimentation patterns to trace the natural versus anthropogenic sediment dynamics “QUEST4D”.” In Belgian Science Policy, ed., *Science for Sustainable Development*, vol. SDNS06B.

van Maren, D., J. Vroom, M. Fettweis and J. Vanlede, 2020. “Formation of the Zeebrugge coastal turbidity maximum: the role of uncertainty in near-bed exchange processes.” *Marine Geology* 425: pp. 1–18. doi:10.1016/j.margeo.2020.106186.

van Rijn, L., 1993. *Principles of sediment transport in rivers, estuaries and coastal seas*. Aqua Publications, Amsterdam.

VAN RIJN, L., 2007. "Unified view of sediment transport by currents and waves. I: Initiation of motion, bed roughness, and bed-load transport." *Journal of Hydraulic Engineering* 133: pp. 649–667. doi:10.1061/(ASCE)0733-9429(2007)133:6(649).

VERLAAN, P., 1998. *Mixing of marine and fluvial particles in the Scheldt estuary*. Ph.D. thesis, Delft University of Technology, Delft (Netherlands).

VROOM, J. and R. SCHRIJVERSHOF, 2015. "Overzicht van menselijke ingrepen in de Westerschelde en haar mondingsgebied in de periode 1985–2014." In Deltares Delft (Netherlands), ed., *Deltares memo*, vol. 1210301-001-ZKS-0005.

WANG, Z., 1997. "Morfologische interactie Westerschelde en het Mondingsgebied, ASMITA-Westerschelde — een gedragsgeoriënteerde modellering." In WL |Delft Hydraulics (Netherlands), ed., *Delft Hyraulics report*, vol. Z2253.

WANG, Z. and M. JEUKEN, 2004. "Long-term morphologic modeling of the Humber estuary with ESTMORPH. The future morphologic evolution and the impact of set backs." In WL |Delft Hydraulics (Netherlands), ed., *Delft Hyraulics report*, vol. Z3451/Z3521.

WANG, Z., M. JEUKEN, H. GERRITSEN, H. DE VRIEND and B. KORNMAN, 2002. "Morphology and asymmetry of the vertical tide in the Westerschelde estuary." *Continental Shelf Research* 22: pp. 2599–2609. doi:10.1016/S0278-4343(02)00134-6.

WANG, Z. and A. ROELFZEMA, 2001. "Long-term morphologic modeling for Humber estuary with ESTMORF." In Tsinghua University Press, ed., *IAHR congress proceedings, hydraulics for maritime engineering*. Pp. 229–234.

WANG, Z. and M. VAN HELVERT, 2001. "ESTMORF, a model for long term morphological development of estuaries and tidal lagoons." In WL |Delft Hydraulics (Netherlands), ed., *Delft Hyraulics report*, vol. Z3105.

Vlaamse Hydrografie, 2011. *Overzicht van de tijwaarnemingen langs de Belgische kust. Periode 2001–2010 voor Nieuwpoort, Oostende en Zeebrugge*. Ministrie van de Vlaamse Gemeenschap, Oostende (Belgium).